Journal of Medicinal Chemistry

pubs.acs.org/jmc

Article

Abolishing Dopamine D_{2long}/D_3 Receptor Affinity of Subtype-Selective Carbamoylguanidine-Type Histamine H_2 Receptor Agonists

Katharina Tropmann, Merlin Bresinsky, Lisa Forster, Denise Mönnich, Armin Buschauer, Hans-Joachim Wittmann, Harald Hübner, Peter Gmeiner, Steffen Pockes,* and Andrea Strasser*

Cite This: *J. Med. Chem.* 2021, 64, 8684–8709

Read Online

ACCESS | Metrics & More | Article Recommendations | Supporting Information

ABSTRACT: 3-(2-Amino-4-methylthiazol-5-yl)propyl-substituted carbamoylguanidines are potent, subtype-selective histamine H_2 receptor (H_2R) agonists, but their applicability as pharmacological tools to elucidate the largely unknown H_2R functions in the central nervous system (CNS) is compromised by their concomitant high affinity toward dopamine D_2-like receptors (especially to the D_3R). To improve the selectivity, a series of novel carbamoylguanidine-type ligands containing various heterocycles, spacers, and side residues were rationally designed, synthesized, and tested in binding and/or functional assays at H_{1-4} and $D_{2long/3}$ receptors. This study revealed a couple of selective candidates (among others **31** and **47**), and the most promising ones were screened at several off-target receptors, showing good selectivities. Docking studies suggest that the amino acid residues (3.28, 3.32, E2.49, E2.51, 5.42, and 7.35) are responsible for the different affinities at the H_2- and $D_{2long/3}$-receptors. These results provide a solid base for the exploration of the H_2R functions in the brain in further studies.

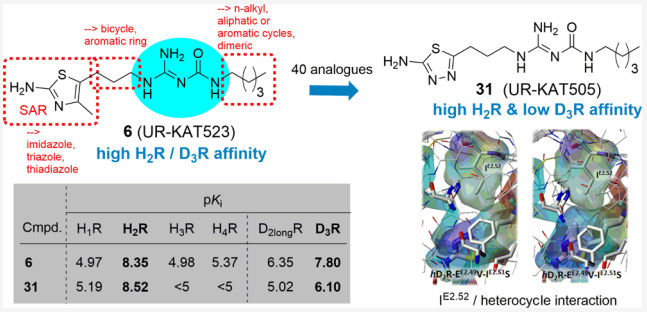

Cmpd.	pKi H_1R	H_2R	H_3R	H_4R	$D_{2long}R$	D_3R
6	4.97	**8.35**	4.98	5.37	6.35	**7.80**
31	5.19	**8.52**	<5	<5	5.02	**6.10**

INTRODUCTION

The histamine H_2 receptor (H_2R) has been the subject of many research studies due to its versatile physiological properties.[1,2] The H_2R belongs to the class A G protein-coupled receptors (GPCRs) and is expressed throughout the whole human body, most importantly in the stomach, heart, and central nervous system (CNS).[1−4] Activation of the H_2R by its endogenous ligand histamine (**1**, Figure 1A) leads to adenylyl cyclase activation by coupling to the Gs protein.[2] The central role of the H_2R in the stimulation of gastric acid secretion[2,5] is the basis for the therapeutic use of H_2R antagonists to treat the gastro-esophageal reflux disease and gastroduodenal ulcers.[1,6] The function of the H_2R in the CNS is largely unknown but includes, e.g., modulation of cognitive processes and circadian rhythm.[7] Furthermore, positive effects of the H_2-antagonist famotidine (**2**, Figure 1A) in schizophrenia and an improvement in L-3,4-dihydroxyphenylalanine (L-DOPA)-induced dyskinesia are reported in the literature.[7−15] In addition, there are studies reporting that the stimulation of the postsynaptic H_2R has positive effects on learning and memory.[16] So far, these effects have only been shown with dual-acting acetylcholinesterase inhibitors and H_3R antagonists as these molecules initiate this process through the inhibition of presynaptic H_3-autoreceptors.[16−18] Therefore, the use of CNS-penetrating H_2R agonists is of great interest.

Starting from the H_2R agonists of the arpromidine (**3**, Figure 1A) series, several highly potent (up to 3000 times the potency of histamine) monomeric and dimeric H_2R agonists with the acylguanidine or carbamoylguanidine partial structure were developed (**4**−**6**, Figure 1A).[19−24] In contrast to acylguanidines, the carbamoylguanidines are chemically stable and possess an excellent selectivity over the other three histamine receptors ($H_{1,3,4}$) if a 2-aminothiazole ring is used for the bioisosteric replacement of the imidazole ring (**5**, **6**, Figure 1A).[22,23,25] Based on the existing knowledge about the physicochemical and/or pharmacokinetic properties of acyl- and carbamoylguanidines, we assume that carbamoylguanidines are also able to overcome the blood−brain barrier (BBB).[19,20,23,26] This advantage over previously reported H_2R agonists (cf. guanidines, e.g., **3**, Figure 1A) should enable access to the H_2R in the CNS.[19,20] On the other hand, the direct injection of the ligand into the brain is also possible as a means of application in the case of insufficient bioavailability and/or BBB penetration.[27]

Received: April 16, 2021
Published: June 10, 2021

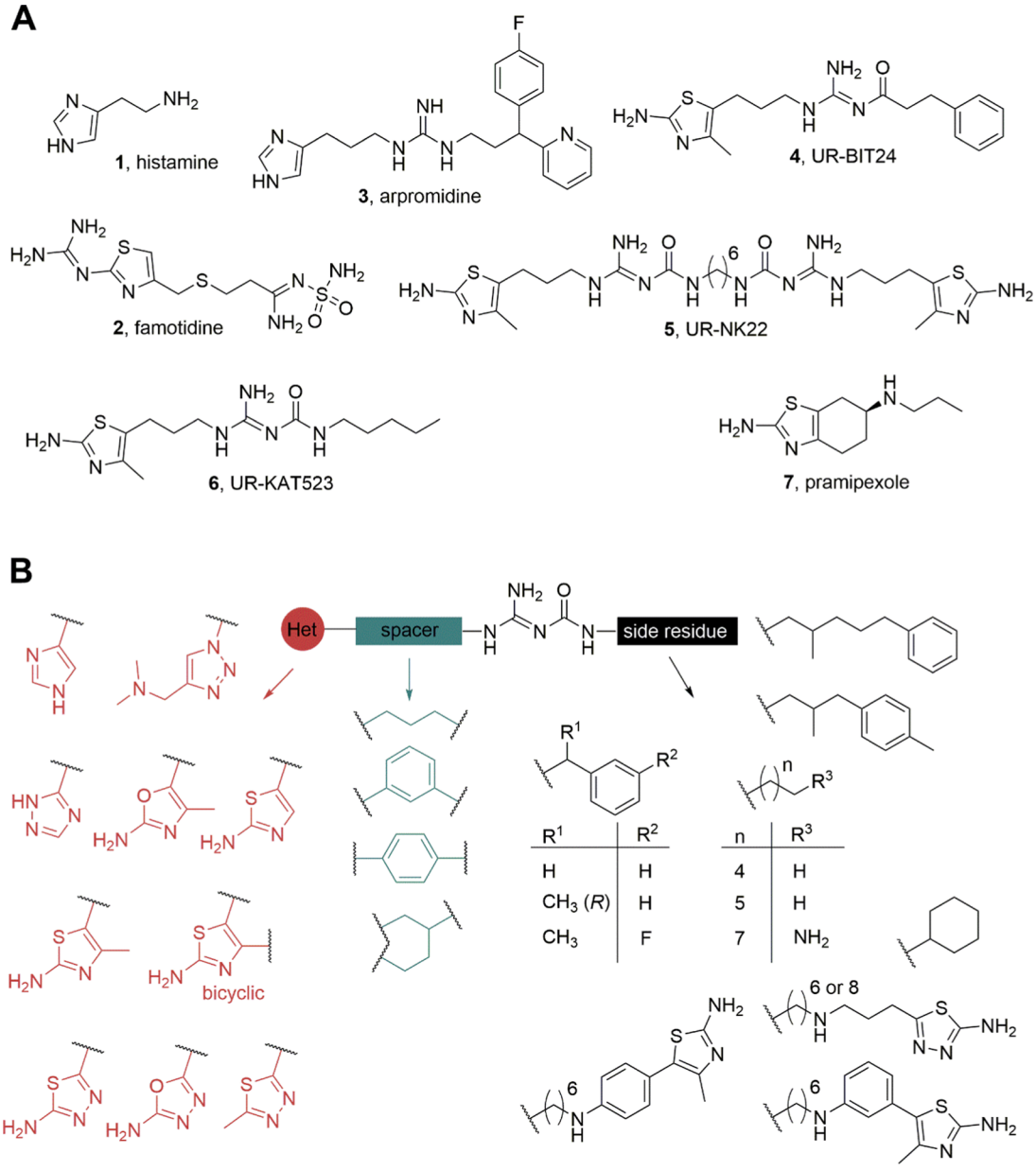

Figure 1. (A) Structures of histamine (**1**), famotidine (**2**), arpromidine (**3**), and related prototypical acylguanidine-type (**4**) and carbamoylguanidine-type (**5**, **6**) H_2R agonists, as well as the D_2-like receptor agonist pramipexole (**7**). (B) Structural modifications of N^G-carbamoylated guanidines resulting in the title compounds. Het: heterocycle.

However, the 2-aminothiazole structural motif is also part of the dopamine receptor agonist pramipexole (**7**, Figure 1A), which is used as a drug for the treatment of Parkinson's disease.[28,29] Due to these similarities, we assumed that H_2R agonists containing the 2-aminothiazole motif might also bind to dopamine receptors. Indeed, we could prove this assumption during previous studies with radioligand binding experiments and found that such H_2R agonists revealed a considerable affinity to dopamine receptors of the D_2-like family, in particular to the D_3 receptor.[23,24]

To enable the use of carbamoylguanidines as pharmacological tools to elucidate the H_2R functions in the CNS, we addressed the need to develop improved molecules that bind exclusively selective to the H_2 receptor. Thus, we herein report the synthesis and pharmacological characterization of these novel, subtype-selective H_2R ligands by variation of the carbamoylguanidine-based scaffold with different heterocycles, spacers, and side residues (Figure 1B).

The synthesized compounds were investigated for their functional activity at the H_2R and/or $D_{2long/3}R$ in minimal G (mini-G) protein- and/or β-arrestin2-recruitment assays as well as on the isolated spontaneously beating guinea pig (*gp*) right atrium in a more complex but well-established standard model for the characterization of H_2R ligands.[1,30] The selectivity for the human (*h*) H_2R over $hH_{1/3/4}R$ and $hD_{2long/3}R$ was evaluated in radioligand competition binding experiments. To support our investigations in silico, molecular docking studies were performed. We compared the binding of the selected (4-methyl)thiazolyl- or thiadiazolyl-containing carbamoylguanidines to identify the amino acid (aa) residues that might be responsible for the different binding affinities of these ligands at the H_2- and $D_{2long/3}$-receptors. Finally, an affinity screening of

https://doi.org/10.1021/acs.jmedchem.1c00692
J. Med. Chem. 2021, 64, 8684−8709

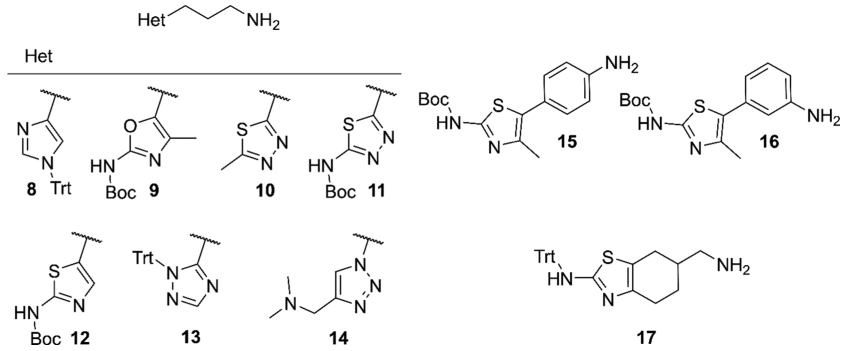

Figure 2. Structures of amines **8**−**17** used for the synthesis of monomeric (**30**−**36**, **38**−**57**, and **59**−**66**) and dimeric (**67**−**70**) carbamoylguanidines. Het: heterocycle. For more details regarding **8**−**17**, see the SI.

Scheme 1. Synthesis of Monomeric Carbamoylguanidines 30−66[a]

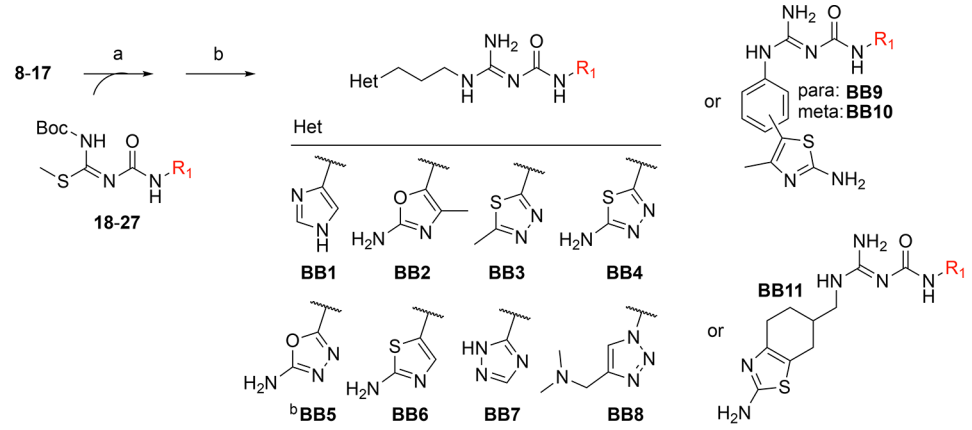

R_1:

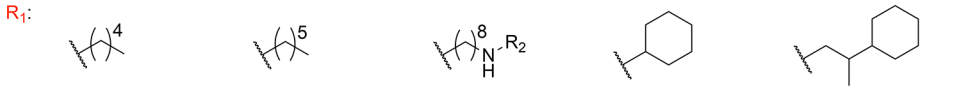

- : **18**
BB3: **30** (34%)
BB4: **31** (19%)
BB6: **32** (26%)
BB9: **33** (45%)
BB10: **34** (48%)
BB11: **35** (22%)

- : **19**
BB4: **36** (18%)
BB5: **37** (6%)[b]

- , R_2 = Boc: **20**
BB3, R_2 = H: **38** (37%)
BB4, R_2 = H: **39** (26%)

- : **21**
BB9: **40** (53%)

- : **22**
BB2: **41** (24%)
BB3: **42** (19%)
BB4: **43** (17%)
BB9: **44** (64%)

- : **23**
BB2: **45** (27%)
BB3: **46** (20%)
BB4: **47** (23%)
BB6: **48** (30%)
BB9: **49** (48%)
BB10: **50** (44%)
BB11: **51** (38%)

- : **24**
BB1: **52** (37%)
BB4: **53** (8%)
BB7: **54** (47%)
BB8: **55** (5%)

- : **25**
BB4: **56** (32%)

- : **26**
BB4: **57** (18%)
BB5: **58** (61%)[b]
BB6: **59** (23%)
BB9: **60** (55%)
BB10: **61** (34%)
BB11: **62** (16%)

- : **27**
BB4: **63** (12%)
BB9: **64** (41%)
BB10: **65** (38%)
BB11: **66** (14%)

[a]Reagents and conditions: (a) NEt_3, $HgCl_2$, CH_2Cl_2, room temperature (rt), 4−48 h and (b) TFA, CH_2Cl_2, rt, 7−18 h, 4−64% over two steps. Isolated yields over two steps are given in brackets. For more details regarding **8**−**27**, see the SI. [b]Modified synthetic procedure (see the Experimental Section and Scheme S8). BB: building block and Het: heterocycle. Amines **8**−**17**: all compounds were used as free bases; and guanidinylating reagents **18**−**27**: all compounds were used as mono-Boc-protected (or di-Boc-protected if applicable) intermediates. The target compounds **30**−**52**, **55**, and **57**−**66** were obtained as TFA and **53**, **54**, and **56** as HCl salts.

the best compounds at common off-target GPCRs was performed and the gastrointestinal (GI) absorption and BBB penetration of these ligands were estimated by the SwissADME online tool.[31]

RESULTS AND DISCUSSION

Chemistry. The amines **8**−**17**[19,20,32−34] (Figure 2) and the guanidinylating reagents **18**−**29**[22−24,26] (Schemes 1 and 2) were synthesized as reported in the SI or in the literature. We chose several different side residues for the guanidinylating reagents

https://doi.org/10.1021/acs.jmedchem.1c00692
J. Med. Chem. 2021, 64, 8684−8709

Scheme 2. Synthesis of the Dimeric N^G-Carbamoylated Guanidines 67−70[a]

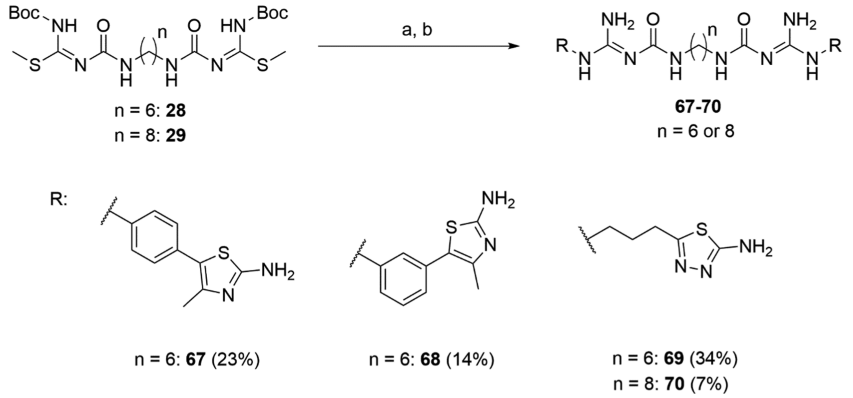

[a]Reagents and conditions: (a) **11**, **15**, or **16**, NEt_3, $HgCl_2$, CH_2Cl_2, rt, 8 h and (b) TFA, CH_2Cl_2, rt, 6−16 h, 7−23% over two steps. Isolated yields over two steps are given in brackets. For more details regarding **11**, **15**, **16**, **28**, and **29**, see the SI. Amines **11**, **15**, and **17**: all compounds were used as free bases; and guanidinylating reagents **28** and **29**: all compounds were used as di-Boc-protected intermediates. The target compounds **67**−**70** were obtained as TFA salts.

18−**29**, which performed well in our recent studies about 2-aminothiazoles.[19−24,26] The monomeric (Scheme 1) or dimeric (Scheme 2) carbamoylguanidine-type ligands were prepared by reacting the amines **8**−**17** with the guanidinylating reagents **18**−**29** in the presence of $HgCl_2$ and triethylamine (NEt_3).[35] Finally, the protected carbamoylguanidine-type intermediates were treated with trifluoroacetic acid (TFA), giving compounds **30**−**36**, **38**−**57**, and **59**−**70** (Schemes 1 and 2), which were purified by preparative high-performance liquid chromatography (HPLC) (acetonitrile (MeCN)/0.1% TFA in H_2O) or column chromatography (CH_2Cl_2/7 N NH_3 in MeOH) and subsequent recrystallization into the corresponding HCl salts. **37** and **58** were synthesized using a modified synthetic procedure (for details, see the Experimental Section and Scheme S8 in the SI).

Chemical Stability of Carbamoylguanidines. The chemical stability of the selected compounds (**30**−**35**, **37**, **41**, and **57**) was investigated in binding buffer[22] (pH 7.4) at room temperature (rt) over a time period of 2 weeks. Under these conditions, the investigated N^G-carbamoylated guanidines proved to be stable (for graphs, see Figures S123−S131 in the SI, for details, see the SI).

Pharmacology. *H_2R Affinity and Receptor Subtype Selectivity.* The pK_i values of all target compounds were determined in competition binding studies on membrane preparations of Sf9 cells expressing the *h*H_2R-$G_{s\alpha S}$ fusion protein using the radioligand [^{3}H]UR-DE257[36] (Table 1). At first, we investigated the influence of the linker on the binding affinity. The conformationally restricted compounds (e.g., **33** (para, pK_i = 6.34), **34** (meta, pK_i = 6.72), and **35** (bicyclic, pK_i = 6.81), Table 1) bind well to the *h*H_2R albeit with lower affinities compared to their flexible (propyl linker) counterparts (e.g., **6**[23] (pK_i = 8.32[23]), Table 1).

Next, we investigated the influence of the heterocycle. The replacement of the sulfur atom in the 2-amino-4-methylthiazole by an oxygen atom resulted in a decreased *h*H_2R affinity (e.g., oxazole: **45** (pK_i = 6.41, Table 1) vs thiazole UR-CH22[23,24] (pK_i = 7.16,[23,24] see Figure S135 and Table S1 in the SI)). The omission of the methyl group in position 4 of the heterocyclic ring did not cause a significant change in the *h*H_2R affinity (**32**, **48**, and **59** vs **6**[23] (Table 1), UR-CH22[23,24] and UR-SB257,[23,24] see Figure S135 and Table S1 in the SI). However, the replacement of the amino(methyl)thiazole by a 2-amino-1,3,4-thiadiazole was favorable: the K_i-values of compounds **31** (pK_i = 8.52), **36** (pK_i = 8.29), **47** (pK_i = 8.30), **56** (pK_i = 8.09), and **57** (pK_i = 8.19) were in the single-digit nanomolar range (cf. Table 1). Also, in the case of the diazoles, the substitution of the sulfur atom by an oxygen atom resulted in a decreased *h*H_2R affinity (e.g., oxadiazole: **58** (pK_i = 6.17) vs thiadiazole **57** (pK_i = 8.19), Table 1). The replacement of the free amine group in the 2-amino-1,3,4-thiadiazole by a methyl group (**30**, **38**, **42**, and **46**) resulted in a dramatic decrease of the *h*H_2R affinity (cf. Table 1), indicating that the heteroaromatic amine group is extremely important for high affinity. This observation was also supported by docking experiments (see the Molecular Docking Studies section). Finally, using the reported 1*H*-1,2,4-triazole[34] or a more explorative 4-(dimethylamino)methyl-1,2,3-triazole instead of the 2-amino-4-methylthiazole resulted in decreased *h*H_2R affinities (1,2,4-triazole **54** (pK_i = 7.27, Table 1) and 1,2,3-triazole **55** (pK_i = 5.35, Table 1) vs thiazole UR-Po563[23] (pK_i = 7.75,[23] see Figure S135 and Table S1 in the SI)).

It is literature known that dimeric ligands possess a significantly increased H_2R affinity (human or guinea pig).[22,25] Therefore, we also synthesized several dimeric compounds, e.g., the 2-amino-1,3,4-thiadiazole heterocycle containing ligands **69** (hexyl-spacer, pK_i = 8.28, Table 1) and **70** (octyl-spacer, pK_i = 8.32, Table 1). However, no further increase in affinity could be achieved compared to the monomeric compounds **31** (pentyl, pK_i = 8.52, Table 1) and **36** (hexyl, pK_i = 8.29, Table 1).

The pK_i values of all synthesized compounds were also determined at the *h*H_1, *h*H_3, and *h*H_4 receptors on membranes of Sf9 cells expressing the respective histamine receptor using the radioligands [^{3}H]mepyramine (*h*H_1R), [^{3}H]N^α-methylhistamine, or [^{3}H]UR-PI294[37] (*h*H_3R) and [^{3}H]**1** (*h*H_4R, cf. Table 1). The imidazole-containing ligand **52** was synthesized as a control compound to showcase that the subtype selectivity is largely influenced by the heterocycle. Unsurprisingly, despite a high affinity at the H_2R, it bound similarly well or even better to the H_3R and H_4R. In contrast, neither of the 2-amino-1,3,4-thiadiazoles (**31**, **36**, **43**, **47**, **53**, **56**, **57**, **63**, **69**, and **70**) displayed remarkable affinity to the *h*H_1, *h*H_3, or *h*H_4 receptors leading to at least 100-fold selectivity for the *h*H_2R (cf. Table 1). The only exception among the thiadiazoles was observed for compound **39**, which contains the 8-aminooctyl side chain. Within the synthesized series, compound **31** showed the highest affinity

https://doi.org/10.1021/acs.jmedchem.1c00692
J. Med. Chem. 2021, 64, 8684−8709

Table 1. Binding Data of the Compounds 30−70 on Human Histamine Receptor Subtypes[a]

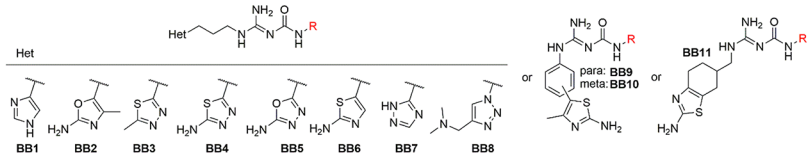

Cmpd.	structure		pKi								H2R selectivity Ki(HxR)/Ki(H2R), x=1,3,4		
	BB	R	*h*H1R[b]	*N*	*h*H2R[c]	*N*	*h*H3R[d,e]	*N*	*h*H4R[f]	*N*	H1	H3	H4
1	-	-	5.62 ± 0.03[37]	4	6.58 ± 0.04[38]	48	7.59 ± 0.01[37]	42	7.60 ± 0.01[37]	45	9	0.1	0.1
5[22]	-	-	6.06 ± 0.05[22]	-	8.07 ± 0.05[22]	-	5.94 ± 0.16[22]	-	5.69 ± 0.07[22]	-	102	135	240
7	-	-	n.d.[h]	-	4.86 ± 0.07[23]	-	n.d.[h]	-	n.d.[h]	-	-	-	-
6[23]	-		4.97 ± 0.10[23]	3	8.35 ± 0.08[23]	3	4.98 ± 0.17[23]	3	5.37 ± 0.09[23]	3	2399	2344	955
30	3		< 5	3	5.66 ± 0.15	3	< 5[e]	3	< 5	3	> 5	> 5	> 5
31 (UR-KAT505)	4		5.19 ± 0.05	3	8.52 ± 0.16	3	< 5[e]	3	< 5	3	2138	>3311	>3311
32 (UR-KAT583)	6		5.02 ± 0.03	3	7.64 ± 0.07	3	< 5[e]	3	< 5	3	417	> 437	> 437
33	9		5.43 ± 0.09	3	6.34 ± 0.06	3	4.94 ± 0.06[d,e]	3	5.11 ± 0.04	3	8	25	17
34	10		5.18 ± 0.09	3	6.72 ± 0.03	3	5.02 ± 0.07[e]	3	5.13 ± 0.05	3	35	50	39
35	11		5.28 ± 0.10	3	6.81 ± 0.07	3	5.18 ± 0.15[d,e]	3	5.23 ± 0.04	3	34	43	38
36	4		5.30 ± 0.09	3	8.29 ± 0.20	3	< 5[e]	3	< 5	3	977	> 1950	> 1950
37	5		5.05 ± 0.06	3	6.41 ± 0.01	3	< 5[e]	3	< 5	3	23	> 26	> 26
38	3		6.51 ± 0.19	3	5.74 ± 0.14	3	4.93 ± 0.18[e]	3	< 5	3	0.2	7	> 5
39	4		6.28 ± 0.09	3	7.48 ± 0.14	3	< 5[e]	3	< 5	3	16	> 302	> 302
40	9		5.26 ± 0.17	3	6.26 ± 0.14	3	4.91 ± 0.09[d,e]	3	5.16 ± 0.07	3	10	22	13
41	2		5.22 ± 0.04	3	6.61 ± 0.08	3	5.08 ± 0.11[e]	3	5.12 ± 0.07	3	25	34	31
42	3		5.15 ± 0.01	3	5.98 ± 0.12	3	4.94 ± 0.06	3	< 5	3	7	11	> 10
43	4		5.13 ± 0.06	3	7.71 ± 0.14	4	5.56 ± 0.10[e]	3	4.90 ± 0.12	3	380	141	646
44	9		5.54 ± 0.13	3	6.51 ± 0.10	3	5.25 ± 0.05[e]	3	5.11 ± 0.04	3	9	18	25

https://doi.org/10.1021/acs.jmedchem.1c00692
J. Med. Chem. 2021, 64, 8684−8709

Table 1. continued

Cmpd.	structure		pKi								H2R selectivity Ki(HxR)/Ki(H2R), x=1,3,4		
	BB	R	*h*H1R[b]	*N*	*h*H2R[e]	*N*	*h*H3R[d,e]	*N*	*h*H4R[f]	*N*	H1	H3	H4
45	2		5.05 ± 0.06	3	6.41 ± 0.11	3	< 5[e]	3	< 5	3	23	> 26	> 26
46	3		4.97 ± 0.08	3	5.25 ± 0.15	3	< 5[e]	3	< 5	3	2	> 2	> 2
47 (UR-KAT533)	4		5.27 ± 0.12	3	8.30 ± 0.07	3	< 5[e]	3	< 5	3	1072	> 1995	> 1995
48	6		5.25 ± 0.01	3	7.57 ± 0.07	3	< 5[e]	3	< 5	3	209	> 372	> 372
49	9		5.89 ± 0.03	3	6.67 ± 0.05	3	5.07 ± 0.10[d,e]	3	4.92 ± 0.14	3	6	40	56
50	10		5.14 ± 0.14	3	6.52 ± 0.13	3	< 5[e]	3	< 5	3	24	> 33	> 33
51	11		5.41 ± 0.12	3	6.52 ± 0.02	3	4.95 ± 0.06[d]	3	5.23 ± 0.02	3	13	37	19
52	1		5.40 ± 0.04	3	8.21 ± 0.09	3	8.77 ± 0.02[e]	3	8.07 ± 0.06	3	646	0.3	1
53[g]	4		< 5	3	7.89 ± 0.06	3	< 5[e]	3	< 5	3	> 776	> 776	> 776
54[g]	7		5.10 ± 0.05	3	7.27 ± 0.07	3	< 5[e]	3	< 5	3	148	> 186	> 186
55	8		< 5	3	5.35 ± 0.02	3	4.99 ± 0.02[e]	3	< 5	3	> 2	2	> 2
56[g] (UR-MB-165)	4		4.98 ± 0.02	3	8.09 ± 0.03	3	< 5[e]	3	< 5	3	1288	> 1230	> 1230
57	4		5.87 ± 0.12	3	8.19 ± 0.11	3	5.63 ± 0.11[e]	3	5.16 ± 0.11	3	209	363	1072
58	5		5.57 ± 0.09	3	6.17 ± 0.08	3	5.04 ± 0.03[e]	3	< 5	3	4	13	> 15
59	6		5.60 ± 0.05	3	7.19 ± 0.14	3	5.32 ± 0.11[e]	3	5.35 ± 0.11	3	39	74	69
60	9		5.74 ± 0.14	4	6.48 ± 0.04	3	5.08 ± 0.07[d,e]	3	5.20 ± 0.03	3	5	25	19
61	10		5.28 ± 0.18	3	6.63 ± 0.06	3	4.89 ± 0.13[e]	3	5.13 ± 0.06	3	22	45	32
62	11		6.74 ± 0.12	3	6.97 ± 0.03	3	5.71 ± 0.10[d]	3	5.47 ± 0.10	3	2	18	32
63	4		5.29 ± 0.08	3	7.82 ± 0.11	3	5.40 ± 0.13[e]	3	5.31 ± 0.16	3	339	263	324
64	9		5.12 ± 0.11	3	6.50 ± 0.05	3	5.10 ± 0.11[d,e]	3	5.22 ± 0.03	3	24	25	19
65	10		4.88 ± 0.15	3	6.63 ± 0.07	3	4.97 ± 0.10[e]	3	5.15 ± 0.03	3	56	46	30

https://doi.org/10.1021/acs.jmedchem.1c00692
J. Med. Chem. 2021, 64, 8684−8709

Table 1. continued

Cmpd.	structure		pK$_i$								H$_2$R selectivity K$_i$(H$_x$R)/K$_i$(H$_2$R), x=1,3,4		
	BB	R	*h*H$_1$R[b]	N	*h*H$_2$R[c]	N	*h*H$_3$R[d,e]	N	*h*H$_4$R[f]	N	H$_1$	H$_3$	H$_4$
66	11		5.41 ± 0.08	3	6.96 ± 0.19	3	5.76 ± 0.13[d,e]	3	5.39 ± 0.11	3	35	16	37
67	9	dimeric 	5.67 ± 0.14	3	6.46 ± 0.18	3	5.71 ± 0.09[e]	3	5.67 ± 0.10	3	6	6	6
68	10		5.84 ± 0.03	3	6.42 ± 0.02	3	6.15 ± 0.04[e]	3	5.63 ± 0.04	3	4	2	6
69	4		5.45 ± 0.08	3	8.28 ± 0.13	3	5.00 ± 0.06[e]	3	< 5	3	676	1905	> 1905
70	4	dimeric 	5.74 ± 0.08	3	8.32 ± 0.11	3	5.16 ± 0.06[e]	3	5.05 ± 0.07	3	380	1445	1862

[a]Radioligand competition binding assay using membrane preparations of Sf9 cells expressing the *h*H$_1$R + RGS4, *h*H$_2$R-G$_{s\alpha S}$, *h*H$_3$R + G$_{\alpha i2}$ + G$_{\beta 1\gamma 2}$, or *h*H$_4$R + G$_{\alpha i2}$ + G$_{\beta 1\gamma 2}$. All compounds were tested as TFA salts unless otherwise noted. Data represent mean values ± standard error of the mean (SEM) of *N* independent experiments, each performed in triplicate. The displacement curves of compounds **31**, **32**, **36**, **43**, **47**, **53**, **54**, **56**, **57**, **59**, **63**, and **69** are presented in Figures S133 and 134 in the SI. [b]Displacement of 5 nM [^{3}H]mepyramine (K$_d$ = 4.5 nM). [c]Displacement of 20 nM [^{3}H]UR-DE257[36] (K$_d$ = 12.2 nM). [d]Displacement of 8.6 nM [^{3}H]*N*$^\alpha$-methylhistamine (K$_d$ = 3 nM). [e]Displacement of 2 nM [^{3}H]UR-PI294[37] (K$_d$ = 3 nM). [f]Displacement of 15 nM [^{3}H]**1** (K$_d$ = 16 nM). [g]Tested as the HCl salt instead of the TFA salt. [h]n.d.: not determined.

(pK$_i$ = 8.52, Table 1) and subtype selectivity (ratio of K$_i$ H$_1$R/H$_3$R/H$_4$R of 2138:>3311:>3311, Table 1).

D$_{2long}$R and D$_3$R Affinities of N^G-Carbamoylated Guanidines. N^G-Carbamoylated guanidines with a pK$_i$ value >7.0 at the *h*H$_2$R were investigated for their affinities to the *h*D$_{2long}$ and *h*D$_3$ receptors in radioligand binding assays on homogenates of HEK293T-CRE-Luc cells coexpressing the respective receptor (Table 2). Ligands with pK$_i$ values <7.0 were not tested, as they are not suitable as pharmacological tools to study the H$_2$R function in the brain due to their low affinity. Compounds containing the 2-aminothiazole heterocycle without a methyl group in position 4 (**32**, **48**, and **59**) still showed high to moderate affinities to the *h*D$_{2long/3}$ receptors, especially to the *h*D$_3$R (cf. Table 2). The determined *h*D$_{2long/3}$ receptor affinities were comparable to affinities published for 2-amino(4-methyl)-thiazoles.[23] Fortunately, compounds containing the 2-amino-1,3,4-thiadiazole or the 1*H*-1,2,4-triazole heterocycle displayed only low affinity to the *h*D$_{2long}$ and *h*D$_3$ receptors. We observed that some of them (**31**, **36**, **47**, **53**, **54**, and **57**) showed even more than 100-fold selectivity for the *h*H$_2$R over the *h*D$_{2long}$ and *h*D$_3$ receptors (cf. Table 2). This trend indicates that the nitrogen in position 4 might be responsible for the lower affinity to the *h*D$_3$R (for more details, see docking results; Figure 3D). In addition to the effect of the heterocycle, the side residue played an important role in the dopamine *h*D$_{2long/3}$ receptor affinities. For example, thiadiazoles **43** (2-cyclohexylpropyl side residue) and **63** (2-methyl-5-phenylpentyl side residue) still had a moderate affinity for the *h*D$_{2long/3}$ receptors, which might indicate an additional (hydrophobic) interaction in the binding pocket of the D$_{2long/3}$ receptors (not further investigated). Finally, the dimeric ligand **69** also possessed high *h*D$_{2long}$ and *h*D$_3$ receptor affinities compared to the corresponding monomeric ligands **31** and **36** (cf. Table 2). Therefore, **70**, also being a dimeric ligand, was not further investigated. **39** and **52** were, despite their high H$_2$R affinity, also excluded from additional experiments due to their low subtype selectivity (cf. Table 1).

In summary, although many ligands (**31**, **36**, **47**, **53**, **54**, and **57**) showed a decent selectivity for the *h*H$_2$R over the *h*D$_{2long}$ and *h*D$_3$ receptors (ratios of K$_i$ > 100), **31** and **47** turned out to be the most promising candidates due to their excellent selectivity profiles.

Functional Studies at the Human H$_2$R. To gain further insights into the general structure−activity relationship of the N^G-carbamoylated guanidines, all target compounds **30**−**70** were investigated for *h*H$_2$R agonism and antagonism in the β-arrestin2- and mini-G protein recruitment assays using genetically engineered HEK293T cells, respectively. Only the functional data of the most interesting molecules (**31**, **32**, **36**, **43**, **47**, **48**, **53**, **54**, **56**, **57**, **59**, **63**, and **69**) are shown in Table 3 (for functional data of the remaining and reference compounds, see Table S2 in the SI). The responses in both assays were normalized to the maximum effect induced by 100 μM histamine (**1**, E$_{max}$ = 1.00) and buffer control (E$_{max}$ = 0). Thus, **1** is defined as a full, unbiased agonist in either readout. **1** exhibits a significantly lower potency in the β-arrestin2 recruitment assay compared to the mini-G protein recruitment assay (pEC$_{50}$ (β-arrestin2) = 5.42;[41] pEC$_{50}$ (mGs (minimal G$_{\alpha s}$ protein)) = 6.94;[42] cf. Table 3). Similarly, the potencies of the investigated N^G-carbamoylated guanidines were also lower in the β-arrestin2 recruitment assay (cf. Table 3). A possible explanation for this trend could be the use of the mGs protein since it is known that mG proteins stabilize active states of GPCRs, which favors the binding of agonists.[42−45]

The compounds shown in Table 3 proved to be strong partial agonists (E$_{max}$ = 0.83−0.95, cf. Table 3) in the mini-G protein recruitment assay with pEC$_{50}$ values >7.0. The determined pEC$_{50}$ values in most cases agree very well with the pK$_i$ values from the radioligand binding assay. Compound **47**, containing the benzyl side residue, showed the highest *h*H$_2$R potency with a pEC$_{50}$ of 8.48, and also **31** (pentyl side residue, pEC$_{50}$ = 8.22) showed an excellent potency in the single-digit nanomolar range (cf. Table 3). The incorporation of a ring system (cf. Scheme 1, BB9−11) in the spacer resulted in either antagonists or partial

https://doi.org/10.1021/acs.jmedchem.1c00692
J. Med. Chem. 2021, 64, 8684−8709

Table 2. Binding Data of the Selected N^G-Carbamoylated Guanidines on Human Dopamine D_{2long} and D_3 Receptors[a]

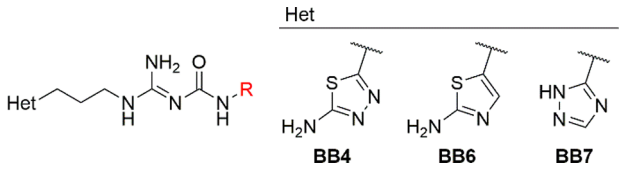

Cmpd.	structure		pKi				H_2R selectivity $K_i(D_xR)/K_i(H_2R)$ x = 2long, 3	
	BB	R	$hD_{2long}R$[b]	N	hD_3R[c]	N	$D_{2long}R$	D_3R
pramipexole (7)	-	-	hi 7.59 ± 0.12[39] low 6.00 ± 0.03[39]	3	9.18 ± 0.06[39]	3	0.002[e]	0.00005
5[22]	-	-	7.09 ± 0.07	3	8.70 ± 0.04	3	10	0.2
6[23]	-		6.35 ± 0.01[23]	3	7.80 ± 0.09[23]	3	100	4
31	4		5.02 ± 0.15	3	6.10 ± 0.05	4	3162	263
32	6		5.46 ± 0.07	3	7.50 ± 0.02	3	151	1
36	4		< 5	3	6.23 ± 0.02	3	> 1950	115
43	4		5.79 ± 0.01	3	6.63 ± 0.08	3	83	12
47	4		5.20 ± 0.04	3	5.58 ± 0.17	3	1259	525
48	6		5.34 ± 0.07	3	7.13 ± 0.04	3	170	3
53[d]	4		< 5	3	5.49 ± 0.10	3	> 776	251
54[d]	7		< 5	3	< 5	3	> 186	> 186
56[d]	4		< 5	3	6.18 ± 0.10	3	> 1230	81
57	4		5.97 ± 0.07	3	5.69 ± 0.11	4	166	316
59	6		6.31 ± 0.07	3	6.64 ± 0.01	3	8	4
63	4		6.35 ± 0.06	3	6.49 ± 0.02	3	30	21
69	4	dimeric 	6.02 ± 0.10	3	7.22 ± 0.07	3	182	12

[a]Data represent mean values ± SEM from *N* independent experiments, each performed in triplicate. All compounds were tested as TFA salts unless otherwise noted. [b]The radioligand competition binding assay with [^{3}H]*N*-methylspiperone ($hD_{2long}R$: K_d = 0.0149 nM, *c* = 0.05 nM) using homogenates of HEK293T-CRE-Luc-$hD_{2long}R$ cells.[40] [c]The radioligand competition binding assay with [^{3}H]*N*-methylspiperone (hD_3R: K_d = 0.0258 nM, *c* = 0.05 nM) using homogenates of HEK293T-CRE-Luc-hD_3R cells.[40] [d]Tested as the HCl salt instead of the TFA salt. The displacement curves are presented in Figures S136 and S137 in the SI. [e]Calculated using the high pK_i value.

agonists depending on the side residue (for details, see Table S2 in the SI). Surprisingly, some of the tested compounds revealed a completely different functional profile in the β-arrestin2 recruitment assay (cf. Tables 3 and S2). Almost all tested 2-aminothiazoles **6**,[23] UR-CH20,[23,24] UR-CH22,[23,24] UR-Po563,[23] UR-MB-69,[23] UR-SB257,[23,24] UR-KAT527,[23] **32**, **48**, and **59** and the thiadiazoles **57** and **63**, containing a propyl spacer, as well as triazole **54**, exhibited a certain degree of efficacy bias toward G protein activation. The compounds acted as strong partial agonists (E_{max} = 0.73−0.94, cf. Tables 3 and S2) in the mini-G protein recruitment assay but were only partial agonists in the β-arrestin2 recruitment assay (E_{max} = 0.10−0.73,

https://doi.org/10.1021/acs.jmedchem.1c00692
J. Med. Chem. 2021, 64, 8684−8709

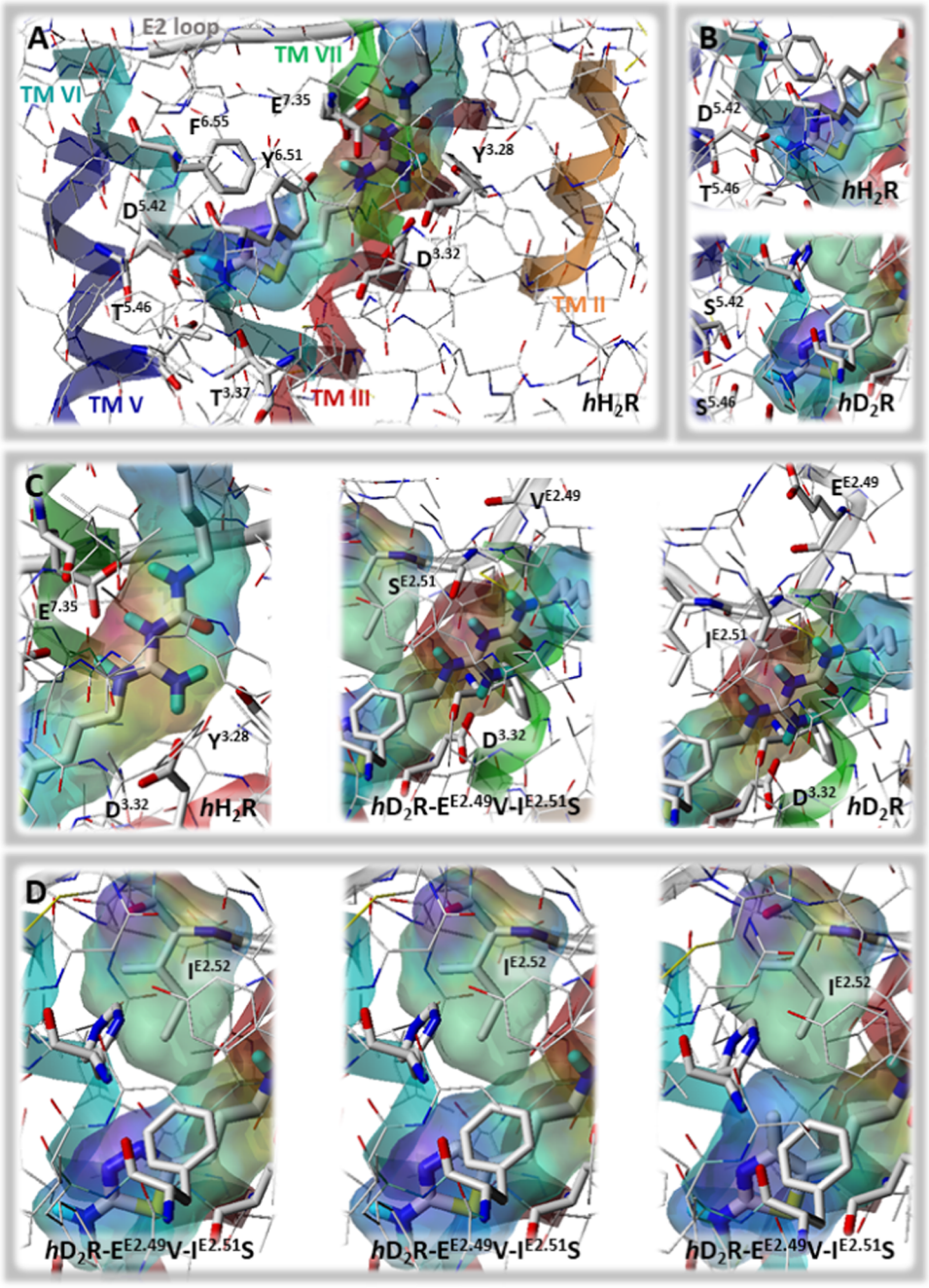

Figure 3. (A) Active-state model of the hH$_2$R with **31** in the binding pocket. The most important amino acids interacting with **31** are highlighted. (B) Differences between the interaction sites of the aminothiadiazole moiety of **31** and the hH$_2$R or the hD$_2$R, respectively. (C) The most important amino acids of hH$_2$R (left), hD$_2$R-E$^{E2.49}$V-I$^{E2.51}$S (center), and hD$_2$R (right) interacting with the carbamoylguanidine moiety of **31**. (D) The influence of the isoleucine at position E2.52 of the E2 loop onto the interaction with the heterocycle of **31** (left), **32** (center), and **6** (right). The active-state β_2-adrenergic receptor−Gs protein complex crystal structure (PDB ID: 3SN6[50]) was used as a starting point for the homology model of the hH$_2$R. In the case of the hD$_2$R, the PDB code is 6VMS.[51]

cf. Tables 3 and S2). The efficacy bias was confirmed by the determination of efficacy bias factors (eBF, for details, see Section S10 in the SI). By contrast, since most of the thiadiazoles (including the most promising candidates **31** and **47**) exhibited no significant bias, they behave in a way similar to the endogenous ligand histamine (**1**). This advantage should enable an authentic examination of the function of the H$_2$R in the CNS with these ligands. Finally, the dimeric ligands (e.g., thiazole: **5**,[22] thiadiazole: **69**) exhibited similar characteristics as their monomeric counterparts and all compounds containing a rigidized spacer (cf. Scheme 1, BB9−11) acted as antagonists in the β-arrestin2 recruitment assay (see Table S2 in the SI).

Functional Studies at the Guinea Pig H$_2$R. Furthermore, a selection of compounds (with a pK_i > 7.0 at the hH$_2$R and a selectivity over the hD$_{2long/3}$ receptors) was investigated on the isolated spontaneously beating guinea pig right atrium as a more complex, well-established standard model for the characterization of H$_2$R ligands (Table 4).[1,30] All compounds turned out to be full agonists in this assay (E_{max} = 0.98−1.15, cf. Table 4). The obtained data are generally comparable with the results

https://doi.org/10.1021/acs.jmedchem.1c00692
J. Med. Chem. 2021, 64, 8684−8709

Table 3. Potencies and Efficacies of the Selected N^G-Carbamoylated Guanidines in the β-Arrestin2 and Mini-G Protein Recruitment Assays at the hH_2R[a]

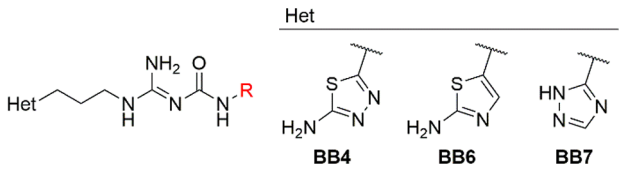

Cmpd.	structure		β-arrestin2 recruitment[b]			mGs recruitment[c]		
	BB	R	pEC_{50}	E_{max}[d]	N	pEC_{50}	E_{max}[d]	N
1	-	-	5.42 ± 0.02[40]	1.00[40]	3	6.94 ± 0.06[41]	1.00[41]	9
5[22]	-	-	6.80 ± 0.14	0.30 ± 0.04	6	7.62 ± 0.02	0.89 ± 0.01	3
7	-	-	4.40 ± 0.10[23]	0.35 ± 0.03[23]	3	6.78 ± 0.01	0.95 ± 0.01	
6[23]	-		6.75 ± 0.12[23]	0.15 ± 0.02[23]	4	8.34 ± 0.05	0.88 ± 0.01	3
31[f]	4		6.63 ± 0.08	0.94 ± 0.06	6	8.24 ± 0.22	0.93 ± 0.01	3
32	6		7.25 ± 0.04	0.64 ± 0.04	4	8.22 ± 0.04	0.89 ± 0.01	3
36	4		5.97 ± 0.04	1.16 ± 0.05	5	8.22 ± 0.06	0.95 ± 0.02	3
43[f]	4		6.87 ± 0.09	0.90 ± 0.04	6	7.97 ± 0.03	0.88 ± 0.03	3
47	4		6.86 ± 0.13	0.94 ± 0.06	5	8.48 ± 0.07	0.92 ± 0.01	4
48	6		7.31 ± 0.05	0.73 ± 0.03	4	8.31 ± 0.14	0.94 ± 0.03	4
53[e]	4		6.55 ± 0.09	0.87 ± 0.02	5	7.70 ± 0.04	0.91 ± 0.02	3
54[e]	7		6.49 ± 0.10	0.37 ± 0.02	4	7.59 ± 0.04	0.90 ± 0.02	3
56[e]	4		7.12 ± 0.05	1.04 ± 0.03	6	8.09 ± 0.04	0.95 ± 0.01	3
57[f]	4		6.89 ± 0.17	0.53 ± 0.04	5	7.21 ± 0.09	0.91 ± 0.01	4
59	6		6.63 ± 0.08	0.16 ± 0.01	4	7.11 ± 0.04	0.83 ± 0.01	4
63	4		6.54 ± 0.17	0.38 ± 0.04	5	7.62 ± 0.09	0.84 ± 0.02	4
69[f]	4	dimeric 	6.39 ± 0.07	0.82 ± 0.06	4	7.70 ± 0.12	0.94 ± 0.01	3

[a]Data represent mean values ± SEM from *N* independent experiments, each performed in triplicate. All compounds were tested as TFA salts unless otherwise noted. [b]The β-arrestin2 recruitment assay was performed using HEK293T-ARRB2-H_2R cells.[41,46] [c]The mini-G protein recruitment assay was performed using HEK293T NlucN-mGs/hH_2R-NlucC cells.[42] [d]The response in both assays was normalized to the maximal effect induced by 100 μM **1** (E_{max} = 1.00) and buffer control (E_{max} = 0.00). The concentration−response curves are presented in Figures S138 and S140 in the SI. [e]Tested as the HCl salt instead of the TFA salt. [f]Selected compounds were investigated for functional activity in the [^{35}S]GTPγS binding assay at the hH_2R-$G_{s\alpha S}$ fusion protein:[22] **31**: pEC_{50} = 7.59 ± 0.11, E_{max} = 0.84 ± 0.04 (*N* = 3); **43**: pEC_{50} = 7.88 ± 0.09, E_{max} = 0.78 ± 0.07 (*N* = 3); **57**: pEC_{50} = 7.89 ± 0.11, E_{max} = 0.88 ± 0.06 (*N* = 4); and **69**: pEC_{50} = 7.46 ± 0.09, E_{max} = 0.71 ± 0.06 (*N* = 3). The obtained results were in good agreement with the results from the mini-G protein recruitment assay.

from the gpH_2R mini-G protein recruitment assay in terms of potency and efficacy (Table 4). Noteworthily, **53**, **56**, and **57** showed the highest discrepancies regarding the potency in both assays. However, **53** and **56** showed higher potencies by about one logarithmic unit on the guinea pig right atrium, and **57** behaved exactly the opposite (Table 4). The thiadiazole **56** (pEC_{50} = 9.04) showed the highest potency on the guinea pig right atrium, whereas **47** was the most potent compound in the mini-G protein recruitment assay (pEC_{50} = 8.66). In general, a comparison of the mini-G protein recruitment assay data at the guinea pig and human H_2Rs showed that the potencies at the gpH_2R were slightly better for all substances tested, while the efficacies were pretty much the same. A similar observation was already published for the [^{35}S]GTPγS assay and the steady-state GTPase assay.[20,25,47,48]

Functional Studies at the Human $D_{2long/3}$ Receptors. Although the relevant N^G-carbamoylated guanidines (**31**, **32**, **36**, **47**, **53**, **54**, **56**, and **57**) bind to the $hD_{2long/3}$ receptors only with low affinity (pK_i < 6.5 (only **32** has a pK_i > 6.5 at the D_3R), see Table 2), we decided to characterize these ligands in the β-

https://doi.org/10.1021/acs.jmedchem.1c00692
J. Med. Chem. 2021, 64, 8684−8709

Table 4. Potencies and Efficacies of the Tested N^G-Carbamoylated Guanidines Determined in the Mini-G Protein Recruitment Assay at the *gp*H_2R or by Organ Bath Studies at the Spontaneously Beating Guinea Pig Right Atrium[a]

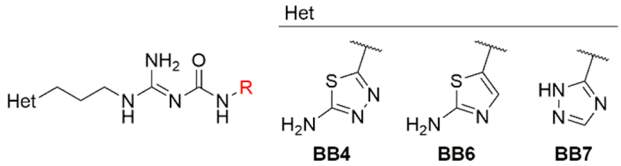

Cmpd.	structure		mGs recruitment[b]			atrium[d]		
	BB	R	pEC_{50}	E_{max}[c]	N	pEC_{50}[e]	E_{max}[f]	N
1	-	-	$6.60 \pm 0.07^{2}_{6}$	1.00^{26}	3	$6.16 \pm 0.01^{3}_{7}$	1.00^{37}	225
6[23]	-		n.d.[h]	n.d.[h]	-	$8.24 \pm 0.03^{2}_{3}$	$0.78 \pm 0.03^{2}_{3}$	3
31	4		8.36 ± 0.07	0.94 ± 0.01	3	8.25 ± 0.11	1.09 ± 0.02	3
36	4		8.64 ± 0.05	0.96 ± 0.01	3	8.32 ± 0.06	1.06 ± 0.05	3
47	4		8.66 ± 0.04	0.94 ± 0.01	3	8.88 ± 0.03	1.05 ± 0.01	3
53[g]	4		7.60 ± 0.03	0.90 ± 0.02	3	8.54 ± 0.09	0.98 ± 0.04	3
54[g]	7		7.79 ± 0.02	0.86 ± 0.03	3	7.42 ± 0.10	1.15 ± 0.11	3
56[g]	4		8.16 ± 0.03	0.93 ± 0.02	3	9.04 ± 0.10	1.10 ± 0.05	3
57	4		7.83 ± 0.09	0.92 ± 0.01	3	7.02 ± 0.08	1.02 ± 0.10	3

[a]Data represent mean values ± SEM from *N* independent experiments, each performed in triplicate. All compounds were tested as TFA salts unless otherwise noted. [b]The mini-G protein recruitment assay was performed using HEK293T NlucN-mGs/*gp*H_2R-NlucC cells.[26] [c]The response was normalized to the maximal effect induced by 100 μM **1** (E_{max} = 1.00) and buffer control (E_{max} = 0.00). The concentration−response curves are presented in Figure S139 in the SI. [d]Organ bath studies using the isolated, spontaneously beating guinea pig right atrium.[38] [e]The pEC_{50} value was calculated from the mean corrected shift ΔEC_{50} of the agonist curve relative to the histamine reference curve by the following equation: pEC_{50} = 6.16 + ΔpEC_{50}. [f]E_{max}: maximal response relative to the maximal increase in the heart rate induced by 30 μM **1** (E_{max} = 1.00). [g]Tested as the HCl salt instead of the TFA salt. [h]n.d.: not determined.

arrestin2 assay, which is already established in our lab.[40] In addition, the data of **5**,[22] **43**, **48**, **59**, **63**, and **69** were collected for a broader comparison of the compounds. The measured potencies and efficacies are presented in Table 5. All tested compounds showed agonistic activities in the β-arrestin2 recruitment assay at the *h*D_3R. In the β-arrestin2 recruitment assay at the *h*D_{2long}R, **47** and **54** were inactive (up to a tested concentration of 10 μM, cf. Table 5). The remaining compounds (**5**,[22] **31**, **32**, **36**, **43**, **48**, **53**, **56**, **59**, and **69**) acted as agonists with the exception of **57** and **63**, which were antagonists. Some compounds (**31**, **36**, **43**, **53**, and **56** at the *h*D_{2long}R and **54** and **57** at the *h*D_3R) showed only very weak partial agonism at the highest tested concentration of 10 μM, which could not be fitted. In general, thiadiazoles showed lower potencies and efficacies at the *h*$D_{2long/3}$ receptors than their thiazole counterparts (cf. Table 5).

Molecular Docking Studies. To shed light on the binding modes of the amino(methyl)thiazole- and the aminothiadiazole-containing carbamoylguanidines and to gain insight into the specific molecular interactions leading to the differences in the *h*H_2R, *h*D_2R, and *h*D_3R affinities, we performed molecular docking studies (Figure 3). We chose to investigate compounds **6** (2-amino-4-methylthiazole), **31** (2-aminothiadiazole) and, **32** (2-aminothiazole) on the active-state receptor models of the *h*H_2R (homology model based on the β_2-adrenergic receptor−Gs protein complex crystal structure 3SN6;[50] sequence identity of about 37%[19]) and the *h*D_2R (based on the D_2R-G protein complex crystal structure 6VMS[51]). Since **6**, **31**, and **32** act as agonists at the *h*D_3-receptor (β-arrestin2 assay, Table 5), they should be docked into its active-state receptor model. However, to the best of our knowledge, an active-state model of the D_3R has not been reported yet. To investigate the binding mode at the *h*D_3R despite this drawback, we decided to create mutants of

https://doi.org/10.1021/acs.jmedchem.1c00692
J. Med. Chem. 2021, 64, 8684−8709

Table 5. Potencies and Efficacies of Selected N^G-Carbamoylated Guanidines Determined in the β-Arrestin2 Recruitment Assay at the $hD_{2long}R$ or hD_3R[a]

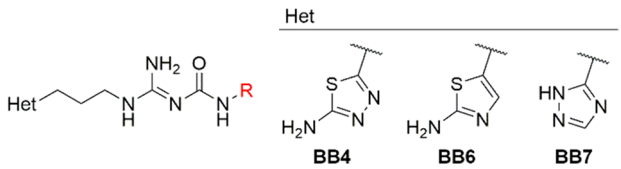

Cmpd.	structure		$hD_{2long}R$[b]			hD_3R[c]		
	BB	R	$pEC_{50}/(pK_b)$[d]	E_{max}[e]	N	pEC_{50}	E_{max}[e]	N
quinpirole	-	-	7.55 ± 0.07[39]	1.00[39]	5	8.75 ± 0.07[39]	1.00[39]	6
pramipexole	-	-	8.19 ± 0.05[39]	0.86 ± 0.04[39]	4	9.09 ± 0.06[39]	0.99 ± 0.04[39]	4
5[22]	-	-	6.67 ± 0.09	0.88 ± 0.07	4	7.70 ± 0.08	1.01 ± 0.06	6
6[23]	-		5.98 ± 0.02[23]	0.41 ± 0.05[23]	4	7.80 ± 0.05[23]	0.96 ± 0.05[23]	3
31	4		< 5	0.11 ± 0.01[g]	3	5.55 ± 0.18	0.74 ± 0.08	3
32	6		5.85 ± 0.07	0.56 ± 0.05	4	7.40 ± 0.01	0.87 ± 0.01	3
36	4		< 5	0.15 ± 0.01[g]	3	6.09 ± 0.09	0.73 ± 0.07	4
43	4		< 5	0.17 ± 0.05[g]	3	5.87 ± 0.10	0.26 ± 0.05	3
47	4		< 5	n.a.	5	5.92 ± 0.14	0.43 ± 0.02	4
48	6		5.47 ± 0.08	0.23 ± 0.04	3	7.17 ± 0.03	0.87 ± 0.04	3
53[f]	4		< 5	0.06 ± 0.01[g]	3	5.97 ± 0.16	0.71 ± 0.04	3
54[f]	7		< 5	n.a.	3	< 5	0.18 ± 0.05[g]	3
56[f]	4		< 5	0.07 ± 0.01[g]	3	5.72 ± 0.07	0.73 ± 0.11	3
57	4		(5.69 ± 0.01)	n.a.[h]	3	< 5	0.12 ± 0.01[g]	3
59	6		5.35 ± 0.06	0.31 ± 0.04	3	5.98 ± 0.02	0.71 ± 0.02	4
63	4		(5.42 ± 0.01)	n.a.[h]	4	6.33 ± 0.07	0.56 ± 0.05	3
69	4	dimeric 	5.95 ± 0.05	0.32 ± 0.05	3	6.53 ± 0.12	0.80 ± 0.03	3

[a]Data represent mean values ± SEM from *N* independent experiments, each performed in triplicate. All compounds were tested as TFA salts unless otherwise noted. [b]The β-Arrestin2 recruitment assay was performed using HEK293T ElucN-βarr2 $hD_{2long}R$-ElucC cells. [c]The β-Arrestin2 recruitment assay was performed using HEK293T ElucN-βarr2 hD_3R-ElucC cells. [d]$pK_b = -\log K_b$. K_b values were calculated according to the Cheng–Prusoff equation.[49] The IC_{50} values of antagonists were determined in the antagonist mode vs quinpirole (50 nM, $D_{2long}R$). [e]The response in both assays was normalized to the maximal effect induced by 10 μM quinpirole (E_{max} = 1.00) and buffer control (E_{max} = 0.00). [f]Tested as the HCl salt instead of the TFA salt.[40] [g]E_{max} at c = 10 μM. [h]Silent antagonist. n.a. = not active. The concentration–response curves are presented in Figures S141–S143 in the SI.

the active-state hD_2R model, containing amino acid(s) (aa(s)) of the hD_3R.

First of all, we studied and analyzed literature data regarding mutagenesis studies at aminergic GPCRs (primarily histamine and dopamine receptors), focusing on the different amino acids of the orthosteric binding pocket at the hH_2R, hD_2R, and hD_3R. The results are summarized in Table 6.

The docking studies of **31** and **32** suggest that the heterocyclic five-membered ring (BB4 or BB6, respectively), particularly if surrounded by the amino acids $C^{3.36}$, $T^{3.37}$, $D^{5.42}$, $T^{5.46}$, and $F^{6.55}$, fits well into the orthosteric binding pocket of the hH_2R (Figure 3A, shown for **31**). However, both heterocycles are suggested to bind in a conformation, with the sulfur being located near $C^{3.36}$ and $T^{3.37}$. Additionally, **31** and **32** are stabilized by an electrostatic interaction between the aspartate of the $D^{5.42}$-$T^{5.46}$ motif and the NH_2-group of the heterocycle (Figure 3A, shown for **31**). The carbamoylguanidine moiety of both **31** and **32** forms an electrostatic interaction network with the amino acids $Y^{3.28}$, $D^{3.32}$, and $E^{7.35}$ (Figure 3A, shown for **31**). **31** and **32** could also be docked into the analogue binding pocket of the hD_2R. In contrast to the hH_2R, there is a serine instead of an aspartate at position 5.42, which results in a reduced electrostatic interaction of the hD_2R and the NH_2 moiety of the heterocycle (BB4 or BB6, respectively) (Figure 3B, shown for **31**). As

https://doi.org/10.1021/acs.jmedchem.1c00692
J. Med. Chem. 2021, 64, 8684–8709

Table 6. Overview of the Literature Known Mutagenesis Studies at Aminergic GPCRs (Primarily Histamine and Dopamine Receptors), Focusing on Different Amino Acids of the Orthosteric Binding Pocket[a]

position	receptor	mutation	most important new finding	references
2.61	hD_2R	$V^{2.61}F$	•approx. 50-fold decrease in K_i of clozapine, leading to a comparable affinity like at the wt D_4R	52
			•aa in position 2.61 is part of microdomain (including the amino acids at 3.28, 3.29, 7.35), which is partially accountable for the selectivity between the hD_2R and the hD_4R	
	hH_1R	$N^{2.61}S$ ($hH_1R \rightarrow gpH_1R$)	•no or only a small influence on the binding affinities of small molecules (e.g., mepyramine, cetirizine, histamine)	53 and 54
			•pK_i of more voluminous partial agonists (e.g., suprahistaprodifen and dimeric histaprodifen) increased, resulting in an affinity like at the gpH_1R	
			•$N^{2.61}$ is not the only responsible aa for the observed species difference between the hH_1R and the gpH_1R	
E2.49, E2.51 and E2.52 of E2 loop	hD_2R/hD_3R	exemplarily: hD_3R-$I183^{E2.52}F$, hD_2R-$I184^{E2.52}A$, hD_2R-$E181^{E2.49}V$	•amino acids in these positions have influence on the binding affinity	55−58
5.42	several GPCRs, e.g., hD_1R, mD_2R, hD_2R, hD_3R	$S^{5.42}A$	•highly important for ligand binding (≥10-fold alteration of affinity of different ligands)	59−62
5.46	several GPCRs, e.g., hD_1R, gpH_1R, hH_4R	hD_1R-$S^{5.46}A$, gpH_1R-$N^{5.46}A$, hH_4R-$E^{5.46}D$, hH_4R-$E^{5.46}Q$	•≥10-fold alteration of affinity for selected ligands	59 and 63−69
			•in the case of the hD_1R, aa in position 5.46 is suggested to influence the subtype selectivity	
	$r\alpha_1AR$	single mutations: $S^{5.42}A$ and $S^{5.46}A$	•no significant reduction of the binding affinity for e.g., (−)-epinephrine	70
		double mutation $S^{5.42}A$/$S^{5.46}A$	•approx. 100-fold reduced affinity compared to the wt receptor	
6.51	hD_2R	$F^{6.51}A$, $F^{6.51}L$, $F^{6.51}Y$	•may affect the affinity up to 1000-fold	71
6.53	hH_1R	$I^{6.53}V$	•K_d of [^{3}H]mepyramine increased by approx. 10-fold; however, in another study slightly decreased	53 and 72
6.55	gpH_1R, rD_2R, hD_3R	gpH_1R-$F^{6.55}A$, rD_2R-$H^{6.55}L$, hD_3R-$H^{6.55}L$, rD_2R-$H^{6.55}N$	•up to 25-fold alteration of the binding affinity	73−76
			•may affect the binding affinity not only by a direct interaction with the ligand but also by changing the interaction network within the receptor	
7.35	hM_1R	$W^{7.35}A$, $W^{7.35}F$	•described to affect the ligand affinity	77

[a] *m*: mouse; *r*: rat; hM_1R: human muscarinic receptor M_1; and α_1AR: α_1 adrenergic receptor.

roughly estimated by calculating the docking energy between the hH_2R or the hH_2R-$D^{5.42}S$ mutant and **31** or **32**, respectively, the interaction energy is considerably reduced for the hH_2R-$D^{5.42}S$ mutant. Thus, this missing interaction is probably one reason for the reduced affinity of **31** or **32** at the hD_2R and the hD_3R, compared to the hH_2R. For the hD_2R, no compensating interaction between the heterocycle (BB4 or BB6, respectively) and the receptor could be identified.

Next, we performed further investigations to elucidate why the compounds **31** and **32** have a higher affinity to the hD_3R than to the hD_2R. Concerning the 5.42−5.46 motif, the situation at the hD_3R is identical compared to the hD_2R. Although a comparison of the amino acid sequence between the hD_2R and the hD_3R revealed two differences at the positions 4.53 and 4.56 (hD_2R: $S^{4.53}$, $I^{4.56}$; hD_3R: $A^{4.53}$, $V^{4.56}$), which are in close proximity to the 5.42−5.46 motif, subsequent docking studies at the hD_2R-$S^{4.53}A$-$I^{4.56}V$ mutant suggested that these amino acids are not responsible for the subtype selectivity between the hD_2R and the hD_3R. Therefore, we performed an analysis of the interaction between the carbamoylguanidine moiety and the hD_2R or hD_3R. We observed that at position 7.35, the glutamate (hH_2R) is exchanged into a tyrosine, which is not able to establish an as strong electrostatic interaction as the glutamate. Furthermore, the $Y^{3.28}$, which also interacts at the hH_2R with the carbamoylguanidine by an electrostatic interaction, is a phenylalanine at the hD_2R and hD_3R, resulting in a deficit in the electrostatic interaction. These two reduced interactions between the hD_2R and the carbamoylguanidine constitute probably another reason for the reduced affinity of **31** or **32** at the hD_2R or hD_3R compared to the hH_2R. An advanced comparison of the amino acid sequence between the hD_2R and the hD_3R revealed another two differences in the E2 loop in the neighborhood to the highly conserved cysteine (hD_2R: $E^{E2.49}C^{E2.50}I^{E2.51}$; hD_3R: $V^{E2.49}C^{E2.50}S^{E2.51}$) (for amino acid alignment, see Figure S146). In the case of the hD_2R, the $E^{E2.49}$ is too far from the carbamoylguanidine moiety of the ligand and is not able to establish an electrostatic interaction (Figure 3C, right). In contrast, at the hD_3R, the $S^{E2.51}$ is able to form a hydrogen bond with the carbamoylguanidine (cf. hD_2R-$E^{2.49}V$-$I^{E2.51}S$, Figure 3C, center). Thus, the reduced interaction between the receptor and the carbamoylguanidine moiety in the series $hH_2R \rightarrow hD_3R \rightarrow hD_2R$ will explain the reduced affinity, obtained by competition binding studies, within the same sequence. However, this effect could only be observed for the double mutant hD_2R-$E^{E2.49}V$-$I^{E2.51}S$, not for the single mutant hD_2R-$I^{E2.51}S$. As suggested by the modeling studies, in the case of the single mutant, the $S^{E2.51}$ interacts with $E^{E2.49}$ and not with the carbamoylguanidine moiety of the ligand. Thus, the double mutation is suggested to be essential for the reduced affinity of the compounds at the hD_2R compared to the hD_3R. Furthermore, the experimental studies show a decrease in affinity to the hD_3R in the series **6** → **32** → **31**. Here, the docking studies suggest that an isoleucine of the E2 loop ($I^{E2.52}$) is responsible for that trend (Figure 3D). This isoleucine is in close contact with the methyl group of the heterocycle of compound **6**, establishing an additional van der Waals interaction between **6**

https://doi.org/10.1021/acs.jmedchem.1c00692
J. Med. Chem. 2021, 64, 8684−8709

Table 7. Receptor Selectivity Studies of 6, 31, 47, and 54

	pK$_i$							
receptor	**6**	*N*	**31**	*N*	**47**	*N*	**54**	*N*
dopamine D$_1$ [a]	6.59 ± 0.05	3	5.61 ± 0.05	3	5.86 ± 0.12	3	5.66 ± 0.05	3
dopamine D$_{4.4}$ [b]	6.96 ± 0.01	3	5.65 ± 0.04	3	6.17 ± 0.10	3	5.18 ± 0.03	3
dopamine D$_5$ [c]	5.40 ± 0.04	3	4.46 ± 0.05	3	4.95 ± 0.07	3	4.62 ± 0.05	3
muscarinic acetylcholine M$_1$ [d]	<5	3	<5	3	<5	3	<5	3
muscarinic acetylcholine M$_2$ [e]	<5	3	<5	3	5.88 ± 0.03	3	<5	3
muscarinic acetylcholine M$_3$ [f]	<5	3	<5	3	<5	3	<5	3
muscarinic acetylcholine M$_4$ [g]	<5	3	<5	3	<5.5	3	<5	3
muscarinic acetylcholine M$_5$ [h]	<5	3	<5	3	<5	3	<5	3
α_{1A} adrenergic [i]	5.69 ± 0.08	3	5.45 ± 0.11	3	6.07 ± 0.02	3	5.72 ± 0.07	3
α_{2A} adrenergic [j]	6.05 ± 0.05	3	5.31 ± 0.02	3	5.90 ± 0.12	3	6.07 ± 0.11	3
β_1 adrenergic [k]	4.66 ± 0.04	3	<4	3	<4	3	4.31 ± 0.05	3
β_2 adrenergic [l]	4.93 ± 0.04	3	4.20 ± 0.06	3	4.40 ± 0.02	3	4.45 ± 0.03	3
μ-opioid [m]	5.99 ± 0.01	3	5.47 ± 0.03	3	5.40 ± 0.02	3	4.76 ± 0.03	3
serotonin 5-HT$_{1A}$ [n]	5.18 ± 0.05	3	4.49 ± 0.07	3	4.56 ± 0.05	4	4.29 ± 0.08	3

[a]Determined by competition binding with [^{3}H]SCH23390 (K_d/applied conc: D$_1$, 0.23/0.4 nM) using homogenates from HEK293T-CRE-Luc-*h*D$_1$R cells.[40] [b]Determined by competition binding with [^{3}H]*N*-methylspiperone (K_d/applied conc: D$_{4.4}$, 0.078/0.1 nM) using homogenates from HEK293T ElucN-βarr2 *h*D$_{4.4}$R-ELuc cells.[40] [c]Determined by competition binding with [^{3}H]SCH23390 (K_d/applied conc: D$_5$, 0.24/0.4 nM) using homogenates from HEK293T-CRE-Luc-*h*D$_5$R cells.[40] [d]Determined by competition binding with [^{3}H]*N*-methylscopolamine (K_d/applied conc: M$_1$, 0.17/0.2 nM) using the whole CHO-hM$_1$R cells.[78] [e]Determined by competition binding with [^{3}H]*N*-methylscopolamine (K_d/applied conc: M$_2$, 0.10/0.2 nM) using the whole CHO-hM$_2$R cells.[78] [f]Determined by competition binding with [^{3}H]*N*-methylscopolamine (K_d/applied conc: M$_3$, 0.12/0.2 nM) using the whole CHO-hM$_3$R cells.[78] [g]Determined by competition binding with [^{3}H]*N*-methylscopolamine (K_d/applied conc: M$_4$, 0.052/0.1 nM) using the whole CHO-hM$_4$R cells.[78] [h]Determined by competition binding with [^{3}H]*N*-methylscopolamine (K_d/applied conc: M$_5$, 0.20/0.3 nM) using the whole CHO-hM$_5$R cells.[78] [i]Determined by competition binding with [^{3}H]prazosin (K_d/applied conc: α_{1A}, 0.25/0.4 nM) using membranes from HEK293T cells transiently transfected with cDNA of human adrenoceptors α_{1A}.[79,80] [j]Determined by competition binding with [^{3}H]RX821002 (α_{2A}, 0.6/0.5 nM) using membranes from HEK293T cells transiently transfected with cDNA of human adrenoceptors α_{2A}.[79,80] [k]Determined by competition binding with [^{3}H]CGP12177 (β_1, 0.075/0.2 nM) using membranes from HEK293T cells transiently transfected with cDNA of human adrenoceptors β_1.[79,80] [l]Determined by competition binding with [^{3}H]CGP12177 (β_2, 0.070/0.2 nM) using membranes from HEK293T cells transiently transfected with cDNA of human adrenoceptors β_2.[79,80] [m]Determined by competition binding with [^{3}H]diprenorphine (μOR, 0.090/0.3 nM) using membranes from HEK293T cells transiently transfected with cDNA of human μ opioid receptor (μOR).[79,80] [n]Determined by competition binding with [^{3}H]WAY600135 (5-HT$_{1A}$, 0.080/0.2 nM) using membranes from HEK293T cells transiently transfected with cDNA of human serotonin 1A receptor (5-HT$_{1A}$).[79,80]

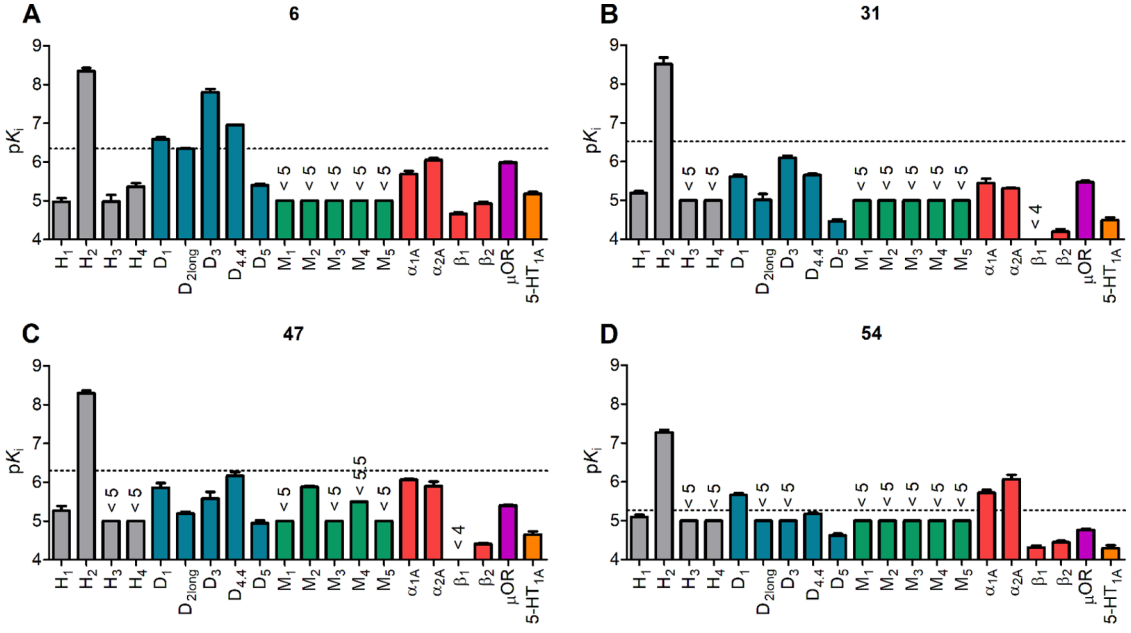

Figure 4. Selectivity over representative aminergic GPCRs, including histaminergic (gray), dopaminergic (blue), muscarinic (green), adrenergic (red), opioid (magenta), and serotonergic (orange) receptors, were determined by radioligand competition binding experiments and compared to the affinity at the H$_2$R of (A) **6**, (B) **31**, (C) **47**, and (D) **54**. The dashed line indicates an at least 100-fold selectivity for the H$_2$R of the respective compound. Bars represent the mean ± SEM of three to four individual experiments each performed in triplicate.

https://doi.org/10.1021/acs.jmedchem.1c00692
J. Med. Chem. 2021, 64, 8684−8709

and the receptor (Figure 3D, right). For **32**, this contact and, therefore, the van der Waals interaction are reduced due to the replacement of the methyl group with a proton at the heterocycle (Figure 3D, center). For **31**, this interaction is completely missing due to the presence of an additional nitrogen atom in the ring (Figure 3D, left). In summary, the docking studies at the active-state models of the hH$_2$R and the hD$_2$R suggest that the amino acids at the positions 3.28, 3.32, E2.49, E2.51, 5.42, and 7.35 are responsible for different affinities of **6**, **31**, and **32** at the hH$_2$R, hD$_2$R, and hD$_3$R. However, this participation has to be verified in detail by the corresponding mutagenesis experiments in future studies.

Off-Target Studies. To be able to differentiate between the on-target and off-target effects, the ligands should selectively bind to the H$_2$R. Therefore, the selected compounds **6**, **31**, **47**, and **54** were additionally investigated in radioligand competition binding studies for their ability to bind to other peripheral and central aminergic GPCRs (off-target studies). Some of these receptors are frequently found antitarget receptors (e.g., α_{1A} adrenergic, M$_{1-5}$ muscarinic). The results are summarized in Table 7 and indicate that the most promising thiadiazoles **31** and **47** have a more than 100-fold higher affinity at the H$_2$R compared to the other tested GPCRs (cf. selectivity profiles B and C in Figure 4). The thiazole **6**, tested as a control, also showed a moderate affinity to D$_1$ and D$_{4.4}$ receptors (D$_1$R: pK_i = 6.59; D$_{4.4}$R: pK_i = 6.96, cf. Table 7) in addition to the already published high affinity for the D$_3$R (pK_i = 7.80, cf. Table 2). Although triazole **54** showed low affinities (p$K_i \leq$ 6.07) at the 14 additionally tested aminergic GPCRs, it did not achieve a sufficient selectivity (factor >100, cf. selectivity profile D in Figure 4) due to the double-digit nanomolar affinity for the H$_2$R (pK_i = 7.27, cf. Table 1). Since the selectivity of a ligand in tissue/in in vivo experiments is not only dependent on its affinity but also on the relative abundance of the respective receptor, we also estimated the "total selectivity" of **6**, **31**, **47**, and **54** in seven different brain regions (for details, see the SI).

SUMMARY AND CONCLUSIONS

In summary, we aimed for the development of novel, subtype-selective H$_2$R ligands, which also have a selectivity over dopamine D$_{2long/3}$ receptors. To achieve this goal, we synthesized and characterized a series of 40 compounds containing a carbamoylguanidine as a key motif, as well as varying heterocycles, spacers, and side residues. We observed that the replacement of the thiazole by a thiadiazole ring in N^G-carbamoylated thiazolylpropylguanidines resulted in potent H$_2$R agonists with affinities in the low one-digit nanomolar range. Furthermore, ligands containing this modification possess a significantly increased selectivity for the hH$_2$R over dopamine hD$_{2long/3}$ receptors. To identify the molecular interactions leading to this selectivity toward the hD$_{2long/3}$ receptors, molecular docking studies with **6**,[23] **31** (UR-KAT505), and **32** (UR-KAT583) on the active-state models of the hH$_2$R and the hD$_2$R were performed. We found that 3.28, 3.32, E2.49, E2.51, 5.42, and 7.35 are most likely the responsible amino acids, which will be confirmed in future receptor mutagenesis experiments. Within the synthesized thiadiazole-containing ligand series, compounds **31** and **47** (UR-KAT533) turned out to be the most promising candidates reaching up to 1000-fold selectivity over the other three receptor subtypes (hH$_{1,3,4}$R). **31** showed the highest selectivity for the hH$_2$R over the hD$_{2long}$R (>2000-fold) and 260-fold selectivity for the hH$_2$R over the hD$_3$R. **47**, on the other hand, showed very good selectivity for the hH$_2$R over the hD$_{2long}$R (>1000-fold) and the highest selectivity for the hH$_2$R over the hD$_3$R (>520-fold). Moreover, **31** and **47** were shown to be selective H$_2$R agonists (>100-fold) relative to 14 additional peripheral and central GPCRs (including dopaminergic, muscarinic, adrenergic, serotonergic, and opioid receptors). These key characteristics render **31** and **47** the most affine and selective monomeric carbamoylguanidine-type agonists known so far. Therefore, we plan to employ them as pharmacological tools for further investigations on the physiological and pathophysiological role of the H$_2$R and hope that these studies can contribute to clarify the largely unknown function of H$_2$ receptors in the CNS.

EXPERIMENTAL SECTION

Chemistry: General Conditions. Unless otherwise stated, chemicals and solvents were from commercial suppliers and were used as received. All of the solvents were of analytical grade or were distilled prior to use. For column chromatography, silica gel 60 (0.04−0.063 mm, Merck, Darmstadt, Germany) was used. Flash chromatography was performed on an Intelli Flash-310 workstation from Varian Deutschland GmbH (Darmstadt, Germany) with SuperFlash (SF) columns (Si50, 4−40 g) from Agilent Technologies (Santa Clara, CA). Reactions were monitored by thin-layer chromatography (TLC) on Merck silica gel 60 F254 aluminum sheets, and spots were visualized with UV light at 254 nm or ninhydrin staining. NMR spectra were recorded on a Bruker Avance 300 (^{1}H: 300 MHz, ^{13}C: 76 MHz), a Bruker Avance 400 (^{1}H: 400 MHz, ^{13}C: 101 MHz), and a Bruker Avance 600 (^{1}H: 600 MHz, ^{13}C: 151 MHz) (Bruker, Karlsruhe, Germany) NMR spectrometer with deuterated solvents from Deutero (Kastellaun, Germany). All chemical shifts are reported in the δ-scale as parts per million (ppm, multiplicity, coupling constant (J), number of protons) relative to the solvent residual peaks as the internal standard.[81,82] The spectra were analyzed by the first order, and coupling constants are given in hertz (Hz). Abbreviations for the multiplicities of the signals are singlet (s), doublet (d), triplet (t), quartet (q), quintet (quint), multiplet (m), doublet of doublets (dd), and broad singlet (br s). High-resolution mass spectrometry (HRMS) was performed on a Q-TOF 6540 ultrahigh definition (UHD) LC/MS system (Agilent Technologies) using an electrospray ionization (ESI) source or on an AccuTOF GCX GC/MS system (Jeol, Peabody, MA) using an electron ionization (EI) source. Preparative HPLC was performed with a system from Knauer (Berlin, Germany) consisting of two K-1800 pumps, a K-2001 detector, and the column was a Phenomenex Kinetex (250 × 21 mm^2, 5 μm) (Phenomenex, Aschaffenburg, Germany). As a mobile phase, mixtures of MeCN and 0.1% aqueous (aq) TFA were used. The UV detection was carried out at 220 nm. Prior to lyophilization (a ScanVac CoolSafe 4-15L freeze dryer from Labogene (LMS, Brigachtal, Germany), equipped with a RZ 6 rotary vane vacuum pump (Vacuubrand, Wertheim, Germany)), MeCN was removed under reduced pressure. Analytical HPLC experiments were performed on a 1100 HPLC system from Agilent Technologies equipped with an Instant Pilot controller, a G1312A binary pump, a G1329A ALS autosampler, a G1379A vacuum degasser, a G1316A column compartment, and a G1315B diode array detector (DAD). The column was a Phenomenex Kinetex XB-C18 column (250 × 4.6 mm^2, 5 μm) (Phenomenex, Aschaffenburg, Germany), tempered at 30 °C. As a mobile phase, mixtures of MeCN/aqueous TFA were used. The following linear gradients were applied. Compounds **30**−**51** and **57**−**70**: MeCN/TFA (0.05%) (v/v) 0 min: 10:90, 30 min: 90:10, 33 min: 95:5, 40 min: 95:5; flow rate: 0.8 mL/min, t_0 = 3.21 min. Compounds **52**−**56**: MeCN/TFA (0.05%) (v/v) 0 min: 10:90, 25 min: 95:5, 35 min: 95:5; flow rate: 1.0 mL/min, t_0 = 2.67 min. The injection volume was 5−50 μL. Absorbance was detected at 220 nm. Compound concentration was between 100 and 1000 μM.

Compound Characterization. Target compounds (**30**−**70**) were characterized by ^{1}H NMR (for spectra, see the SI), ^{13}C NMR (for spectra, see the SI), and two-dimensional (2D) NMR (correlation spectroscopy (COSY), heteronuclear single quantum correlation

https://doi.org/10.1021/acs.jmedchem.1c00692
J. Med. Chem. 2021, 64, 8684−8709

(HSQC), heteronuclear multiple bond correlation (HMBC)) spectroscopy, HRMS, and reversed-phase HPLC (RP-HPLC) analysis. The purities (for chromatograms, see the SI) of the H_2R ligands used for pharmacological investigation were ≥95%. For biological testing, the target compounds **30**−**70** (TFA or HCl salts) were dissolved in dimethyl sulfoxide (DMSO), DMSO/H_2O 1:1 (v/v), or DMSO/20 mM aq HCl 1:1 (v/v) to obtain a final concentration of 10 mM.

Screening for Pan Assay Interference Compounds (PAINS). Screening of all target compounds (**30**−**70**) for PAINS via the public tool http://zinc15.docking.org/patterns/home[83] gave no hits.

General Procedure for the Synthesis of the Carbamoylguanidine-Type Ligands (30−36, 38−57, and 59−70). The reaction was performed in analogy to the published procedure for bivalent carbamoylguanidine-type ligands.[22] In this general procedure, mercuric chloride ($HgCl_2$) is used as a reagent, which is very toxic and potentially carcinogenic. It should be used only in a well-ventilated fume hood after reading the safety precautions and wearing proper lab safety equipment (gloves, safety goggles, and lab coats). Future synthetic work should consider replacements for $HgCl_2$. The guanidinylating reagents **18**−**29** (1−1.1 equiv) and 1−2 equiv of the respective amines **8**−**17** were dissolved in CH_2Cl_2 (3−20 mL). NEt_3 (2.5−3 equiv) and $HgCl_2$ (1.1−2 equiv) were added to the mixture and stirring was continued for 4−48 h. The precipitate was removed by filtration through Celite 545 or centrifugation (4000*g*, 5 min). In the case of **52**−**56**, the reaction was quenched with 7 N NH_3 (5 mL) in MeOH prior to filtration. The solvent was removed in a vacuum. The crude product was purified by flash or column chromatography on silica gel (gradient: 0−20 min: petroleum ether/ethyl acetate (PE/EtOAc) 100:0−50:50, SF 8−12 g, gradient: CH_2Cl_2/MeOH 90:10 to CH_2Cl_2/MeOH/25% NH_3 in H_2O 50:50:1, or isocratic: CH_2Cl_2/7 N NH_3 in MeOH 99:1) and dried in a vacuum. The isolated Boc-/trityl (Trt)-protected intermediates were characterized by LC-MS (data are shown in Table S7 in the SI). Subsequently, the deprotection was performed by stirring the respective compound with 30−70% TFA in CH_2Cl_2 (5−14 mL) for 7−18 h. The obtained carbamoylguanidines (cf. **30**−**36**, **38**−**52**, **55**, **57**, and **59**−**70**) were purified by preparative HPLC. In the case of **53**, **54**, and **56**, the HCl salts were synthesized according to the following procedure. After deprotection with TFA, the ligands were purified by column chromatography (isocratic: CH_2Cl_2/7 N NH_3 in MeOH 90:10), yielding the free base. The free base was dissolved in 1,4-dioxane (10 mL), and 1−2 N HCl (5 mL) in diethyl ether (Et_2O) was added dropwise so that the HCl salt precipitated. The suspension was concentrated in a vacuum, and the solid was washed with Et_2O (3 × 15 mL). After removing the solvent in a vacuum, compounds **53**, **54**, and **56** were obtained as HCl salts.

*1-(Amino{[3-(5-methyl-1,3,4-thiadiazol-2-yl)propyl]amino}-methylene)-3-(pentyl)urea Hydrotrifluoroacetate (**30**).* **30** was prepared from amine **10** (29 mg, 0.19 mmol, 1.1 equiv), **18** (51 mg, 0.17 mmol, 1 equiv), NEt_3 (58 μL, 0.42 mmol, 2.5 equiv), and $HgCl_2$ (91 mg, 0.34 mmol, 2 equiv) according to the general procedure, yielding the product as a white, foamlike, and hygroscopic solid (25 mg, 34%). R_f = 0.01 (PE/EtOAc 3:7). RP-HPLC: 98% (t_R = 13.5 min, k = 3.21). ^{1}H NMR (600 MHz, DMSO-d_6): δ 10.46 (br s, 1H), 9.06 (br s, 1H), 8.54 (br s, 2H), 7.51 (br s, 1H), 3.37−3.29 (m, 2H), 3.12−3.04 (m, 4H), 2.68 (s, 3H), 1.96 (quint, J = 7.4 Hz, 2H), 1.44 (quint, J = 7.2 Hz, 2H), 1.32−1.20 (m, 4H), 0.86 (t, J = 7.1 Hz, 3H). ^{13}C NMR (151 MHz, DMSO-d_6): δ 169.15, 165.01, 159.81 (q, J = 31.9 Hz, TFA), 153.89, 153.69, 117.36 (q, J = 299.5 Hz, TFA), 40.02, 19.11, 28.61, 28.39, 27.94, 26.31, 21.75, 15.10, 13.85. HRMS (ESI-MS): m/z [M + H$^+$] calcd for $C_{13}H_{25}NOS^+$: 313.1805; found: 313.1827. Molecular formula (MF): $C_{13}H_{24}N_6OS{\cdot}C_2HF_3O_2$. Molecular weight (MW): (312.44 + 114.02).

*1-(Amino{[3-(5-amino-1,3,4-thiadiazol-2-yl)propyl]amino}-methylene)-3-(pentyl)urea Dihydrotrifluoroacetate (**31**).* **31** was prepared from amine **11** (53 mg, 0.18 mmol, 1 equiv), **18** (50 mg, 0.19 mmol, 1.1 equiv), NEt_3 (61 μL, 0.44 mmol, 2.5 equiv), and $HgCl_2$ (96 mg, 0.35 mmol, 2 equiv) according to the general procedure, yielding the product as a white, foamlike, and hygroscopic solid (19 mg, 19%). R_f = 0.49 (CH_2Cl_2/MeOH 9:1). RP-HPLC: 99% (t_R = 11.4 min, k = 2.55). ^{1}H NMR (600 MHz, DMSO-d_6): δ 10.37 (br s, 1H), 9.04 (br s, 1H), 8.52 (br s, 2H), 8.10−7.34 (m, 4H), 3.30 (q, J = 6.7 Hz, 2H), 3.09 (q, J = 6.6 Hz, 2H), 2.86 (t, J = 7.5 Hz, 2H), 1.89 (quint, J = 7.4 Hz, 2H), 1.44 (quint, J = 7.1 Hz, 2H), 1.31−1.22 (m, 4H), 0.86 (t, J = 7.0 Hz, 3H). ^{13}C NMR (151 MHz, DMSO-d_6): δ 168.77, 158.93 (q, J = 34.3 Hz, TFA), 157.42, 153.86, 153.68, 116.45 (q, J = 297.7 Hz, TFA), 40.05, 39.21, 28.60, 28.39, 27.34, 26.52, 21.75, 13.86. HRMS (ESI-MS): m/z [M + H$^+$] calcd for $C_{12}H_{24}N_7OS^+$: 314.1758; found: 314.1761. MF: $C_{12}H_{23}N_7OS{\cdot}C_4H_2F_6O_4$. MW: (313.42 + 228.05).

*1-(Amino{[3-(2-aminothiazol-5-yl)propyl]amino}methylene)-3-(pentyl)urea Dihydrotrifluoroacetate (**32**).* **32** was prepared from amine **12** (30 mg, 0.12 mmol, 1 equiv), **18** (39 mg, 0.13 mmol, 1.1 equiv), NEt_3 (41 μL, 0.29 mmol, 2.5 equiv), and $HgCl_2$ (64 mg, 0.23 mmol, 2 equiv) according to the general procedure, yielding the product as a white, foamlike, and hygroscopic solid (16.9 mg, 26%). R_f = 0.56 (CH_2Cl_2/MeOH 9:1). RP-HPLC: 99% (t_R = 11.0 min, k = 2.43). ^{1}H NMR (600 MHz, DMSO-d_6) δ 10.45 (br s, 1H), 9.41−8.85 (m, 3H), 8.50 (br s, 2H), 7.48 (br s, 1H), 7.07 (s, 1H), 3.26 (q, J = 6.6 Hz, 2H), 3.08 (q, J = 6.6 Hz, 2H), 2.63 (t, J = 7.5 Hz, 2H), 1.77 (quint, J = 7.3 Hz, 2H), 1.42 (quint, J = 7.2 Hz, 2H), 1.32−1.18 (m, 4H), 0.85 (t, J = 7.0 Hz, 3H). ^{13}C NMR (151 MHz, DMSO-d_6) δ 169.37, 159.06 (q, J = 33.2 Hz, TFA), 153.82, 153.68, 123.95, 123.48, 116.62 (q, J = 296.7 Hz, TFA), 39.87, 39.10, 28.60, 28.46, 28.38, 23.29, 21.75, 13.86. HRMS (ESI-MS): m/z [M + H$^+$] calcd for $C_{13}H_{25}N_6OS^+$: 313.1805; found: 313.1807. MF: $C_{13}H_{24}N_6OS{\cdot}C_4H_2F_6O_4$. MW: (312.44 + 228.05).

*1-(Amino{[4-(2-amino-4-methylthiazol-5-yl)phenyl]amino}-methylene)-3-(pentyl)urea Dihydrotrifluoroacetate (**33**).* **33** was prepared from amine **15** (60 mg, 0.20 mmol, 1 equiv), **18** (66 mg, 0.22 mmol, 1.1 equiv), NEt_3 (68 μL, 0.49 mmol, 2.5 equiv), and $HgCl_2$ (107 mg, 0.39 mmol, 2 equiv) according to the general procedure, yielding the product as a white, foamlike, and hygroscopic solid (55 mg, 45%). R_f = 0.45 (CH_2Cl_2/MeOH 9:1). RP-HPLC: 100% (t_R = 11.8 min, k = 2.68). ^{1}H NMR (600 MHz, DMSO-d_6) δ 10.72 (br s, 1H), 10.13 (br s, 1H), 9.33−7.91 (m, 4H), 7.59 (t, J = 5.6 Hz, 1H), 7.51−7.45 (m, 2H), 7.41−7.35 (m, 2H), 3.11 (t, J = 7.0 Hz, 2H), 2.25 (s, 3H), 1.44 (quint, J = 7.1 Hz, 2H), 1.33−1.19 (m, 4H), 0.86 (t, J = 7.1 Hz, 3H). ^{13}C NMR (151 MHz, DMSO-d_6): δ 166.94, 159.14 (q, J = 33.1 Hz, TFA), 153.48, 153.36, 138.18, 137.69, 132.72, 130.37, 129.35, 126.20, 116.55 (q, J = 298.0 Hz, TFA), 115.92, 39.20, 28.53, 28.39, 21.75, 14.43, 13.87. HRMS (ESI-MS): m/z [M + H$^+$] calcd for $C_{17}H_{25}N_6OS^+$: 361.1805; found: 361.1806. MF: $C_{17}H_{24}N_6OS{\cdot}C_4H_2F_6O_4$. MW: (380.48 + 228.05).

*1-(Amino{[3-(2-amino-4-methylthiazol-5-yl)phenyl]amino}-methylene)-3-(pentyl)urea Dihydrotrifluoroacetate (**34**).* **34** was prepared from amine **16** (30 mg, 0.10 mmol, 1 equiv), **18** (33 mg, 0.11 mmol, 1.1 equiv), NEt_3 (33 μL, 0.25 mmol, 2.5 equiv), and $HgCl_2$ (53 mg, 0.20 mmol, 2 equiv) according to the general procedure, yielding the product as a white, foamlike, and hygroscopic solid (28 mg, 48%). R_f = 0.55 (CH_2Cl_2/MeOH 9:1). RP-HPLC: 100% (t_R = 12.0 min, k = 2.74). ^{1}H NMR (600 MHz, DMSO-d_6) δ 10.64 (br s, 1H), 10.00 (br s, 1H), 9.30−7.78 (m, 4H), 7.57 (t, J = 5.6 Hz, 1H), 7.52 (t, J = 7.9 Hz, 1H), 7.39−7.35 (m, 1H), 7.34 (t, J = 2.0 Hz, 1H), 7.29−7.24 (m, 1H), 3.11 (t, J = 7.0 Hz, 2H), 2.25 (s, 3H), 1.44 (quint, J = 7.1 Hz, 2H), 1.34−1.19 (m, 4H), 0.86 (t, J = 7.1 Hz, 3H). ^{13}C NMR (151 MHz, DMSO-d_6) δ 166.86, 159.00 (q, J = 32.8 Hz, TFA), 153.52, 153.34, 134.31, 133.13, 130.40, 127.21, 125.21, 124.28, 116.66 (q, J = 296.3 Hz, TFA), 115.89, 39.17, 28.54, 28.38, 21.74, 14.82, 13.88. HRMS (ESI-MS): m/z [M + H$^+$] calcd for $C_{17}H_{25}N_6OS^+$: 361.1805; found: 361.1811. MF: $C_{17}H_{24}N_6OS{\cdot}C_4H_2F_6O_4$. MW: (360.48 + 228.05).

*1-(Amino{[(2-amino-4,5,6,7-tetrahydrobenzo[d]thiazol-6-yl)-methyl]amino}methylene)-3-(pentyl)urea Dihydrotrifluoroacetate (**35**).* **35** was prepared from amine **17** (77 mg, 0.18 mmol, 1.1 equiv), **18** (50 mg, 0.17 mmol, 1 equiv), NEt_3 (57 μL, 0.41 mmol, 2.5 equiv), and $HgCl_2$ (90 mg, 0.33 mmol, 2 equiv) according to the general procedure, yielding the product as a white, foamlike, and hygroscopic solid (21 mg, 22%). R_f = 0.59 (CH_2Cl_2/MeOH 9:1). RP-HPLC: 100% (t_R = 10.6 min, k = 2.30). ^{1}H NMR (600 MHz, DMSO-d_6): δ 10.56 (br s, 1H), 9.28−8.81 (m, 3H), 8.56 (br s, 2H), 7.51 (br s, 1H), 3.36−3.22 (m, 2H), 3.08 (q, J = 6.6 Hz, 2H), 2.67−2.58 (m, 1H), 2.56−2.50 (m, 1H), 2.47−2.36 (m, 1H), 2.23−2.16 (m, 1H), 2.10−2.00 (m, 1H), 1.92−1.83 (m, 1H), 1.50−1.38 (m, 3H), 1.31−1.17 (m, 4H), 0.85 (t, J

https://doi.org/10.1021/acs.jmedchem.1c00692
J. Med. Chem. 2021, 64, 8684−8709

= 7.1 Hz, 3H). ^{13}C NMR (151 MHz, DMSO-d_6): δ 168.63, 159.46 (q, J = 32.8 Hz, TFA), 154.08, 153.83, 134.60, 116.85 (q, J = 296.5 Hz, TFA), 113.20, 44.62, 40.05, 39.16, 33.22, 28.63, 28.42, 25.52, 24.53, 22.00, 21.78, 13.88. HRMS (ESI-MS): m/z [M + H$^+$] calcd for $C_{15}H_{27}N_6OS^+$: 339.1962; found: 339.1964. MF: $C_{15}H_{26}N_6OS\cdot C_4H_2F_6O_4$. MW: (338.47 + 228.05).

*1-(Amino{[3-(5-amino-1,3,4-thiadiazol-2-yl)propyl]amino}-methylene)-3-(hexyl)urea Dihydrotrifluoroacetate (**36**).* **36** was prepared from amine **11** (22 mg, 0.086 mmol, 1 equiv), **19** (30 mg, 0.095 mmol, 1.1 equiv), NEt_3 (30 μL, 0.215 mmol, 2.5 equiv), and $HgCl_2$ (47 mg, 0.172 mmol, 2 equiv) according to the general procedure, yielding the product as a white, foamlike, and hygroscopic solid (8.44 mg, 18%). RP-HPLC: 96% (t_R = 12.9 min, k = 3.02). ^{1}H NMR (600 MHz, DMSO-d_6) δ 10.15 (br s, 1H), 9.01 (br s, 1H), 8.50 (br s, 2H), 8.03−7.24 (m, 3H), 3.30 (q, J = 6.7 Hz, 2H), 3.09 (q, J = 6.6 Hz, 2H), 2.86 (t, J = 7.5 Hz, 2H), 1.89 (quint, J = 7.4 Hz, 2H), 1.43 (quint, J = 6.9 Hz, 2H), 1.31−1.21 (m, 6H), 0.89−0.83 (m, 2H). ^{13}C NMR (151 MHz, DMSO-d_6) δ 168.77, 157.42, 158.59 (q, J = 34.2 Hz, TFA), 153.79, 153.60, 116.18 (q, J = 293.6 Hz, TFA), 39.97, 39.14, 30.87, 28.87, 27.29, 26.52, 25.86, 22.01, 13.87. HRMS (ESI-MS): m/z [M + H$^+$] calcd for $C_{13}H_{26}N_7OS^+$: 328.1914; found: 328.1917. MF: $C_{13}H_{25}N_7OS\cdot C_4H_2F_6O_4$. MW: (327.45 + 228.05).

*1-(Amino{[3-(5-methyl-1,3,4-thiadiazol-2-yl)propyl]amino}-methylene)-3-(8-aminooctyl)urea Dihydrotrifluoroacetate (**38**).* **38** was prepared from amine **10** (17 mg, 0.11 mmol, 1.1 equiv), **20** (46 mg, 0.1 mmol, 1 equiv), NEt_3 (35 μL, 0.25 mmol, 2.5 equiv), and $HgCl_2$ (54 mg, 0.2 mmol, 2 equiv) according to the general procedure, yielding the product as a white, foamlike, and hygroscopic solid (22 mg, 37%). R_f = 0.48 (CH_2Cl_2/MeOH 9:1). RP-HPLC: 97% (t_R = 9.1 min, k = 1.83). ^{1}H NMR (600 MHz, DMSO-d_6): δ 10.54 (br s, 1H), 9.05 (br s, 1H), 8.53 (br s, 2H), 7.77 (br s, 3H), 7.52 (br s, 1H), 3.40−3.29 (m, 4H), 3.11−3.05 (m, 4H), 2.76 (t, J = 6.7 Hz, 2H), 2.67 (s, 3H), 1.96 (quint, J = 7.3 Hz, 2H), 1.51 (quint, J = 7.3 Hz, 2H), 1.46−1.39 (m, 2H), 1.32−1.21 (m, 8H). ^{13}C NMR (151 MHz, DMSO-d_6): δ 169.62, 165.49, 159.38 (q, J = 31.3 Hz, TFA), 154.36, 154.18, 117.44 (q, J = 297.3 Hz, TFA), 40.48, 40.52, 39.26, 29.37, 28.91, 28.89, 28.40, 27.42, 26.77, 26.55, 26.19, 15.57. HRMS (ESI-MS): m/z [M + H$^+$] calcd for $C_{16}H_{32}N_7OS^+$: 370.2384; found: 370.2388 MF: $C_{16}H_{31}N_7OS\cdot C_4H_2F_6O_4$. MW: (369.53 + 228.05).

*1-(Amino{[3-(5-amino-1,3,4-thiadiazol-2-yl)propyl]amino}-methylene)-3-(8-aminooctyl)urea Trihydrotrifluoroacetate (**39**).* **39** was prepared from amine **11** (15 mg, 0.054 mmol, 1 equiv), **20** (25 mg, 0.05 mmol, 1.1 equiv), NEt_3 (19 μL, 0.14 mmol, 2.5 equiv), and $HgCl_2$ (29 mg, 0.11 mmol, 2 equiv) according to the general procedure, yielding the product as a white, foamlike, and hygroscopic solid (10 mg, 26%). RP-HPLC: 96% (t_R = 7.9 min, k = 1.46). ^{1}H NMR (600 MHz, DMSO-d_6): δ 10.39 (br s, 1H), 9.05 (br s, 1H), 8.54 (br s, 2H), 7.88−7.29 (m, 6H), 3.32 (q, J = 6.7 Hz, 2H), 3.11 (q, J = 6.6 Hz, 2H), 2.87 (t, J = 7.5 Hz, 2H), 2.82−2.74 (m, 2H), 1.91 (quint, J = 7.4 Hz, 2H), 1.53 (quint, J = 7.4 Hz, 2H), 1.45 (q, J = 6.7 Hz, 2H), 1.28 (s, 8H). ^{13}C NMR (151 MHz, DMSO-d_6): δ 168.65, 158.58 (q, J = 33.5 Hz, TFA), 157.35, 153.84, 153.67, 116.53 (q, J = 296.1 Hz, TFA), 39.94, 39.16, 38.80, 28.90, 28.44, 27.38, 26.96, 26.49, 26.10, 25.72. HRMS (ESI-MS): m/z [M + H$^+$] calcd for $C_{15}H_{31}N_8OS^+$: 370.2384; found: 370.2388. MF: $C_{15}H_{30}N_8OS\cdot C_6H_3F_9O_6$. MW: (369.53 + 342.07).

*1-(Amino{[4-(2-amino-4-methylthiazol-5-yl)phenyl]amino}-methylene)-3-(cyclohexyl)urea Dihydrotrifluoroacetate (**40**).* **40** was prepared from amine **15** (50 mg, 0.16 mmol, 1 equiv), **21** (57 mg, 0.18 mmol, 1.1 equiv), NEt_3 (57 μL, 0.41 mmol, 2.5 equiv), and $HgCl_2$ (89 mg, 0.33 mmol, 2 equiv) according to the general procedure, yielding the product as a white, foamlike, and hygroscopic solid (51 mg, 53%). R_f = 0.54 (CH_2Cl_2/MeOH 9:1). RP-HPLC: 100% (t_R = 11.6 min, k = 2.61). ^{1}H NMR (600 MHz, DMSO-d_6): δ 10.87 (br s, 1H), 10.18 (br s, 1H), 9.39−8.20 (m, 4H), 7.64 (d, J = 7.6 Hz, 1H), 7.54−7.48 (m, 2H), 7.43−7.37 (m, 2H), 3.55−3.44 (m, 1H), 2.27 (s, 3H), 1.86−1.73 (m, 2H), 1.71−1.60 (m, 2H), 1.58−1.48 (m, 1H), 1.36−1.12 (m, 5H). ^{13}C NMR (151 MHz, DMSO-d_6): δ 167.25, 159.13 (q, J = 33.7 Hz, TFA), 153.55, 152.60, 136.24, 133.04, 129.92, 129.45, 126.26, 116.57 (q, J = 297.3 Hz, TFA), 115.79, 48.40, 32.05, 24.96, 24.12, 13.95. HRMS (ESI-MS): m/z [M + H$^+$] calcd for $C_{18}H_{25}N_6OS^+$: 373.1805; found: 373.1804. MF: $C_{18}H_{24}N_6OS\cdot C_4H_2F_6O_4$. MW: (372.49 + 228.05).

*1-(Amino{[3-(2-amino-4-methyloxazol-5-yl)propyl]amino}-methylene)-3-(2-cyclohexylpropyl)urea Dihydrotrifluoroacetate (**41**).* **41** was prepared from amine **9** (35 mg, 0.1 mmol, 1 equiv), **22** (36 mg, 0.1. mmol, 1 equiv), NEt_3 (35 μL, 0.25 mmol, 2.5 equiv), and $HgCl_2$ (54 mg, 0.2 mmol, 2 equiv) according to the general procedure, yielding the product as a white, foamlike, and hygroscopic solid (14.1 mg, 24%). R_f = 0.52 (CH_2Cl_2/MeOH 9:1). RP-HPLC: 97% (t_R = 15.0 min, k = 3.67). ^{1}H NMR (600 MHz, DMSO-d_6) δ 10.38 (br s, 1H), 9.00 (br s, 3H), 8.51 (br s, 2H), 7.48 (br s, 1H), 3.28 (q, J = 6.7 Hz, 2H), 3.19−3.12 (m, 1H), 2.99−2.92 (m, 1H), 2.59 (t, J = 7.3 Hz, 2H), 2.01 (s, 3H), 1.80−1.69 (m, 4H), 1.66−1.56 (m, 4H), 1.51−1.44 (m, 1H), 1.26−0.91 (m, 7H), 0.81 (d, J = 6.9 Hz, 3H). ^{13}C NMR (151 MHz, DMSO-d_6) δ 158.83 (q, J = 32.5 Hz, TFA), 157.40, 153.84, 153.74, 139.03, 120.74, 116.81 (q, J = 295.7 Hz, TFA), 42.87, 40.06, 39.24, 37.79, 30.29, 27.92, 26.24, 26.17, 26.07, 25.93, 20.21, 14.04, 7.95. HRMS (ESI-MS): m/z [M + H$^+$] calcd for $C_{18}H_{33}N_6O_2^+$: 365.2660; found: 365.2660. MF: $C_{18}H_{32}N_6O_2\cdot C_4H_2F_6O_4$. MW: (364.26 + 228.05).

*1-(Amino{[3-(5-methyl-1,3,4-thiadiazol-2-yl)propyl]amino}-methylene)-3-(2-cyclohexylpropyl)urea Hydrotrifluoroacetate (**42**).* **42** was prepared from amine **10** (22 mg, 0.14 mmol, 1.1 equiv), **22** (46 mg, 0.13 mmol, 1 equiv), NEt_3 (43 μL, 0.32 mmol, 2.5 equiv), and $HgCl_2$ (70 mg, 0.26 mmol, 2 equiv) according to the general procedure, yielding the product as a white, foamlike, and hygroscopic solid (12 mg, 19%). R_f = 0.54 (CH_2Cl_2/MeOH 9:1). RP-HPLC: 97% (t_R = 17.9 min, k = 4.58). ^{1}H NMR (600 MHz, DMSO-d_6): δ 10.19 (br s, 1H), 9.02 (br s, 1H), 8.51 (br s, 2H), 7.47 (br s, 1H), 3.35−3.31 (m, 2H), 3.17−3.04 (m, 3H), 2.97−2.89 (m, 1H), 2.68 (s, 3H), 1.97 (quint, J = 7.4 Hz, 2H), 1.75−1.66 (m, 2H), 1.64−1.53 (m, 3H), 1.51−1.42 (m, 1H), 1.25−0.90 (m, 6H), 0.80 (d, J = 6.9 Hz, 3H). ^{13}C NMR (151 MHz, DMSO-d_6): δ 169.62, 165.49, 159.43 (q, J = 32.2 Hz, TFA), 154.23, 154.15, 117.50 (q, J = 296.6 Hz, TFA), 43.35, 40.51, 38.25, 30.76, 28.38, 26.78, 26.71, 26.64, 26.54, 15.58, 14.52. HRMS (ESI-MS): m/z [M + H$^+$] calcd for $C_{17}H_{31}N_6OS^+$: 367.2275; found: 367.2301. MF: $C_{17}H_{30}N_6OS\cdot C_2HF_3O_2$. MW: (366.53 + 114.02).

*1-(Amino{[3-(5-amino-1,3,4-thiadiazol-2-yl)propyl]amino}-methylene)-3-(2-cyclohexylpropyl)urea Dihydrotrifluoroacetate (**43**).* **43** was prepared from amine **11** (20 mg, 0.08 mmol, 1 equiv), **22** (31 mg, 0.09 mmol, 1.1 equiv), NEt_3 (27 μL, 0.20 mmol, 2.5 equiv), and $HgCl_2$ (43 mg, 0.16 mmol, 2 equiv) according to the general procedure, yielding the product as a white, foamlike, and hygroscopic solid (8 mg, 17%). RP-HPLC: 99% (t_R = 15.5 min, k = 3.83). ^{1}H NMR (600 MHz, DMSO-d_6): δ 10.01 (br s, 1H), 8.98 (br s, 1H), 8.48 (br s, 2H), 7.46 (br s, 3H), 3.29 (q, J = 6.7 Hz, 2H), 3.16−3.09 (m, 1H), 2.96−2.89 (m, 1H), 2.84 (t, J = 7.5 Hz, 2H), 1.88 (quint, J = 7.3 Hz, 2H), 1.72−1.66 (m, 2H), 1.63−1.53 (m, 3H), 1.50−1.41 (m, 1H), 1.25−0.88 (m, 6H), 0.79 (d, J = 6.9 Hz, 3H). ^{13}C NMR (151 MHz, DMSO-d_6): δ 168.60, 158.58 (q, J = 33.5 Hz, TFA), 157.33, 153.90, 153.68, 116.46 (q, J = 296.2 Hz, TFA), 42.88, 40.01, 39.45, 37.77, 30.28, 27.91, 27.37, 26.49, 26.24, 26.17, 26.07, 14.06. HRMS (ESI-MS): m/z [M + H$^+$] calcd for $C_{16}H_{30}N_7OS^+$: 368.2227; found: 368.2230. MF: $C_{16}H_{29}N_7OS\cdot C_4H_2F_6O_4$. MW: (367.52 + 228.05).

*1-(Amino{[4-(2-amino-4-methylthiazol-5-yl)phenyl]amino}-methylene)-3-(2-cyclohexylpropyl)urea Dihydrotrifluoroacetate (**44**).* **44** was prepared from amine **15** (32 mg, 0.11 mmol, 1.1 equiv), **22** (34 mg, 0.10 mmol, 1 equiv), NEt_3 (33 μL, 0.24 mmol, 2.5 equiv), and $HgCl_2$ (52 mg, 0.19 mmol, 2 equiv) according to the general procedure, yielding the product as a white, foamlike, and hygroscopic solid (41 mg, 64%). R_f = 0.50 (CH_2Cl_2/MeOH 9:1). RP-HPLC: 100% (t_R = 15.6 min, k = 3.86). ^{1}H NMR (600 MHz, DMSO-d_6): δ 10.86 (br s, 1H), 10.42 (br s, 1H), 9.48−8.14 (m, 4H), 7.61 (t, J = 5.8 Hz, 1H), 7.54−7.47 (m, 2H), 7.43−7.37 (m, 2H), 3.21−3.12 (m, 1H), 3.01−2.92 (m, 1H), 2.27 (s, 3H), 1.75−1.66 (m, 2H), 1.65−1.55 (m, 3H), 1.52−1.44 (m, 1H), 1.28−0.90 (m, 6H), 0.81 (d, J = 6.9 Hz, 3H). ^{13}C NMR (151 MHz, DMSO-d_6): δ 167.22, 159.16 (q, J = 33.8 Hz, TFA), 153.50, 136.35, 133.09, 129.90, 129.43, 126.13, 116.56 (q, J = 297.3 Hz, TFA), 115.82, 42.99, 39.71, 37.75, 30.29, 27.92, 26.23, 26.17, 26.06, 14.07, 13.99. HRMS (ESI-MS): m/z [M + H$^+$] calcd for $C_{21}H_{31}N_6OS^+$:

https://doi.org/10.1021/acs.jmedchem.1c00692
J. Med. Chem. 2021, 64, 8684−8709

415.2275; found: 415.2275. MF: $C_{21}H_{30}N_6OS{\cdot}C_4H_2F_6O_4$. MW: (414.57 + 228.05).

*1-(Amino{[3-(2-amino-4-methyloxazol-5-yl)propyl]amino}-methylene)-3-(benzyl)urea Dihydrotrifluoroacetate (**45**).* **45** was prepared from amine **9** (35 mg, 0.1 mmol, 1 equiv), **23** (32 mg, 0.1 mmol, 1 equiv), NEt_3 (35 μL, 0.25 mmol, 2.5 equiv), and $HgCl_2$ (54 mg, 0.2 mmol, 2 equiv) according to the general procedure, yielding the product as a white, foamlike, and hygroscopic solid (14.9 mg, 27%). R_f = 0.52 (CH_2Cl_2/MeOH 9:1). RP-HPLC: 96% (t_R = 10.4 min, k = 2.24). ^{1}H NMR (600 MHz, DMSO-d_6) δ 10.51 (br s, 1H), 9.14−8.85 (m, 3H), 8.55 (br s, 2H), 8.00 (br s, 1H), 7.39−7.19 (m, 5H), 4.31 (d, J = 5.8 Hz, 2H), 3.27 (q, J = 6.7 Hz, 2H), 2.57 (t, J = 7.3 Hz, 2H), 1.99 (s, 3H), 1.75 (quint, J = 7.2 Hz, 2H). ^{13}C NMR (151 MHz, DMSO-d_6) δ 158.79 (q, J = 32.4 Hz, TFA), 157.42, 153.82, 153.77, 139.01, 138.68, 128.40, 127.22, 127.11, 120.81, 116.87 (q, J = 298.7 Hz, TFA), 42.77, 40.06, 25.92, 20.22, 7.98. HRMS (ESI-MS): m/z [M + H$^+$] calcd for $C_{16}H_{23}N_6O_2^+$: 331.1877; found: 331.1882. MF: $C_{16}H_{22}N_6O_2{\cdot}C_4H_2F_6O_4$. MW: (330.39 + 228.05).

*1-(Amino{[3-(5-methyl-1,3,4-thiadiazol-2-yl)propyl]amino}-methylene)-3-(benzyl)urea Hydrotrifluoroacetate (**46**).* **46** was prepared from amine **10** (25 mg, 0.16 mmol, 1.1 equiv), **23** (47 mg, 0.15 mmol, 1 equiv), NEt_3 (50 μL, 0.36 mmol, 2.5 equiv), and $HgCl_2$ (79 mg, 0.29 mmol, 2 equiv) according to the general procedure, yielding the product as a white, foamlike, and hygroscopic solid (13.5 mg, 20%). R_f = 0.54 (CH_2Cl_2/MeOH 9:1). RP-HPLC: 98% (t_R = 12.6 min, k = 2.93). ^{1}H NMR (600 MHz, DMSO-d_6): δ 10.40−10.08 (m, 1H), 9.03 (br s, 1H), 8.54 (br s, 2H), 8.05−7.95 (m, 1H), 7.38−7.22 (m, 5H), 4.31 (d, J = 5.8 Hz, 2H), 3.39−3.28 (m, 2H), 3.07 (t, J = 7.6 Hz, 2H), 2.67 (s, 3H), 1.96 (quint, J = 7.2 Hz, 2H). ^{13}C NMR (151 MHz, DMSO-d_6): δ 169.62, 165.50, 159.42 (q, J = 30.9 Hz, TFA), 154.24, 139.13, 128.88, 127.70, 127.58, 117.47 (q, J = 296.9 Hz, TFA), 43.24, 40.55, 28.35, 26.79, 15.58. HRMS (ESI-MS): m/z [M + H$^+$] calcd for $C_{15}H_{21}N_6OS^+$: 333.1492; found: 333.1501. MF: $C_{15}H_{20}N_6OS{\cdot}C_2HF_3O_2$. MW: (332.43 + 114.02).

*1-(Amino{[3-(5-amino-1,3,4-thiadiazol-2-yl)propyl]amino}-methylene)-3-(benzyl)urea Dihydrotrifluoroacetate (**47**).* **47** was prepared from amine **11** (48 mg, 0.19 mmol, 1.2 equiv), **23** (50 mg, 0.16 mmol, 1 equiv), NEt_3 (54 μL, 0.39 mmol, 2.5 equiv), and $HgCl_2$ (84 mg, 0.31 mmol, 2 equiv) according to the general procedure, yielding the product as a white, foamlike, and hygroscopic solid (20.8 mg, 23%). RP-HPLC: 98% (t_R = 10.4 min, k = 2.24). ^{1}H NMR (600 MHz, DMSO-d_6) δ 10.46 (br s, 1H), 9.06 (br s, 1H), 8.56 (br s, 2H), 8.35−7.51 (m, 2H), 7.36−7.22 (m, 5H), 4.31 (d, J = 5.8 Hz, 2H), 3.30 (q, J = 6.7 Hz, 2H), 2.86 (t, J = 7.6 Hz, 2H), 1.89 (quint, J = 7.3 Hz, 2H). ^{13}C NMR (151 MHz, DMSO-d_6) δ 169.07, 158.95 (q, J = 34.7 Hz, TFA), 157.58, 153.84 (2C), 138.70, 128.41 (2C), 127.24 (2C), 127.10, 116.14 (q, J = 295.1 Hz, TFA) 42.78, 40.00, 27.16, 26.59. HRMS (ESI-MS): m/z [M + H$^+$] calcd for $C_{14}H_{20}N_7OS^+$: 334.1445; found: 334.1447. MF: $C_{14}H_{19}N_7OS{\cdot}C_4H_2F_6O_4$. MW: (333.41 + 228.05).

*1-(Amino{[3-(2-aminothiazol-5-yl)propyl]amino}methylene)-3-(benzyl)urea Dihydrotrifluoroacetate (**48**).* **48** was prepared from amine **12** (30 mg, 0.12 mmol, 1 equiv), **23** (41 mg, 0.13 mmol, 1.1 equiv), NEt_3 (41 μL, 0.29 mmol, 2.5 equiv), and $HgCl_2$ (64 mg, 0.23 mmol, 2 equiv) according to the general procedure, yielding the product as a white, foamlike, and hygroscopic solid (20.4 mg, 30%). R_f = 0.56 (CH_2Cl_2/MeOH 9:1). RP-HPLC: 100% (t_R = 10.2 min, k = 2.18). ^{1}H NMR (600 MHz, DMSO-d_6) δ 10.68 (br s, 1H), 9.10 (br s, 3H), 8.57 (br s, 2H), 8.01 (br s, 1H), 7.43−7.20 (m, 5H), 7.06 (s, 1H), 4.32 (d, J = 5.9 Hz, 2H), 3.27 (q, J = 6.6 Hz, 2H), 2.64 (t, J = 7.5 Hz, 2H), 1.79 (quint, J = 7.3 Hz, 2H). ^{13}C NMR (151 MHz, DMSO-d_6) δ 169.35, 159.24 (q, J = 32.7 Hz, TFA), 153.88, 153.83, 138.72, 128.40 (2C), 127.22 (2C), 127.09, 123.96, 123.88, 116.7 (q, J = 298.4 Hz, TFA), 42.76, 39.94, 28.49, 23.30. HRMS (ESI-MS): m/z [M + H$^+$] calcd for $C_{15}H_{21}N_6OS^+$: 333.1492; found: 333.1495. MF: $C_{15}H_{20}N_6OS{\cdot}C_4H_2F_6O_4$. MW: (332.43 + 228.05).

*1-(Amino{[4-(2-amino-4-methylthiazol-5-yl)phenyl]amino}-methylene)-3-(benzyl)urea Dihydrotrifluoroacetate (**49**).* **49** was prepared from amine **15** (60 mg, 0.20 mmol, 1 equiv), **23** (70 mg, 0.22 mmol, 1.1 equiv), NEt_3 (68 μL, 0.49 mmol, 2.5 equiv), and $HgCl_2$ (107 mg, 0.39 mmol, 2 equiv) according to the general procedure, yielding the product as a white, foamlike, and hygroscopic solid (58 mg, 48%). R_f = 0.46 (CH_2Cl_2/MeOH 9:1). RP-HPLC: 99% (t_R = 10.9 min, k = 2.40). ^{1}H NMR (600 MHz, DMSO-d_6) δ 11.69−10.16 (m, 2H), 9.42−8.58 (m, 4H), 8.15 (t, J = 5.9 Hz, 1H), 7.54−7.49 (m, 2H), 7.45−7.39 (m, 2H), 7.38−7.25 (m, 5H), 4.35 (d, J = 5.8 Hz, 2H), 2.27 (s, 3H). ^{13}C NMR (151 MHz, DMSO-d_6): δ 167.46, 159.52 (q, J = 33.6 Hz, TFA), 153.62, 138.52, 135.20, 133.36, 129.52, 128.43, 127.33, 127.17, 126.19, 116.55 (q, J = 295.9 Hz, TFA), 115.73, 42.88, 13.63. HRMS (ESI-MS): m/z [M + H$^+$] calcd for $C_{19}H_{21}N_6OS^+$: 381.1492; found: 381.1491. MF: $C_{19}H_{20}N_6OS{\cdot}C_4H_2F_6O_4$. MW: (380.47 + 228.05).

*1-(Amino{[3-(2-amino-4-methylthiazol-5-yl)phenyl]amino}-methylene)-3-(benzyl)urea Dihydrotrifluoroacetate (**50**).* **50** was prepared from amine **16** (30 mg, 0.10 mmol, 1 equiv), **23** (35 mg, 0.22 mmol, 1.1 equiv), NEt_3 (33 μL, 0.25 mmol, 2.5 equiv), and $HgCl_2$ (53 mg, 0.20 mmol, 2 equiv) according to the general procedure, yielding the product as a white, foamlike, and hygroscopic solid (27 mg, 44%). R_f = 0.52 (CH_2Cl_2/MeOH 9:1). RP-HPLC: 100% (t_R = 11.1 min, k = 2.46). ^{1}H NMR (600 MHz, DMSO-d_6): δ 10.90 (br s, 1H), 10.54 (br s, 1H), 8.42−9.20 (m, 4H), 8.11 (t, J = 5.9 Hz, 1H), 7.53 (t, J = 8.0 Hz, 1H), 7.42−7.23 (m, 8H), 4.34 (d, J = 5.8 Hz, 2H), 2.26 (s, 3H). ^{13}C NMR (151 MHz, DMSO-d_6): δ 167.32, 159.14 (q, J = 33.5 Hz, TFA), 153.64, 153.60, 138.50, 136.81, 134.48, 132.36, 130.47, 128.42, 127.30, 127.16, 125.36, 124.75, 116.52 (q, J = 295.6 Hz, TFA), 115.65, 42.85, 14.04. HRMS (ESI-MS): m/z [M + H$^+$] calcd for $C_{19}H_{21}N_6OS^+$: 381.1492; found: 381.1498. MF: $C_{19}H_{20}N_6OS{\cdot}C_4H_2F_6O_4$. MW: (380.47 + 228.05).

*1-(Amino{[(2-amino-4,5,6,7-tetrahydrobenzo[d]thiazol-6-yl)-methyl]amino}methylene)-3-(benzyl)urea Dihydrotrifluoroacetate (**51**).* **51** was prepared from amine **17** (85 mg, 0.20 mmol, 1 equiv), **23** (71 mg, 0.22 mmol, 1.1 equiv), NEt_3 (76 μL, 0.55 mmol, 2.5 equiv), and $HgCl_2$ (119 mg, 0.44 mmol, 2 equiv) according to the general procedure, yielding the product as a white, foamlike, and hygroscopic solid (45 mg, 38%). R_f = 0.48 (CH_2Cl_2/MeOH 9:1). RP-HPLC: 100% (t_R = 9.8 min, k = 2.05). ^{1}H NMR (600 MHz, DMSO-d_6): δ 10.65 (br s, 1H), 9.27−8.84 (m, 3H), 8.61 (br s, 2H), 8.03 (br s, 1H), 7.35−7.30 (m, 2H), 7.30−7.23 (m, 3H), 4.31 (d, J = 5.8 Hz, 2H), 3.28 (q, J = 6.8 Hz, 2H), 2.63 (dd, J = 16.2, 5.0 Hz, 1H), 2.55−2.50 (m, 1H), 2.47−2.36 (m, 1H), 2.23−2.15 (m, 1H), 2.10−2.01 (m, 1H), 1.91−1.83 (m, 1H), 1.50−1.40 (m, 1H). ^{13}C NMR (151 MHz, DMSO-d_6): δ 168.60, 159.33 (q, J = 32.7 Hz, TFA), 154.04, 153.98, 138.73, 134.64, 128.44, 127.26, 127.14, 116.82 (q, J = 299.9 Hz, TFA), 113.21, 44.67, 42.80, 33.20, 25.53, 24.54, 22.01. HRMS (ESI-MS): m/z [M + H$^+$] calcd for $C_{17}H_{23}N_6OS^+$: 359.1649; found: 359.1645. MF: $C_{17}H_{22}N_6OS{\cdot}C_4H_2F_6O_4$. MW: (358.46 + 228.05).

*1-(Amino{[3-(1H-imidazol-4-yl)propyl]amino}methylene)-3-((R)-(1-phenylethyl))urea Dihydrotrifluoroacetate (**52**).* **52** was prepared from **8** (327 mg, 0.89 mmol, 1 equiv), **24** (300 mg, 0.89 mmol, 1 equiv), $HgCl_2$ (265 mg, 0.98 mmol, 1.1 equiv), and NEt_3 (372 μL, 2.67 mmol, 3 equiv) according to the general procedure, yielding a 429.1 mg (73%) of Trt-/Boc-protected intermediate. Thereof, 306 mg was deprotected in the next step, yielding **52** as a white, foamlike, and hygroscopic solid after purification by preparative HPLC (129.7 mg, 51%). RP-HPLC: 100% (t_R = 8.3 min, k = 2.11). ^{1}H NMR (300 MHz, MeOD) δ 8.75 (d, J = 1.4 Hz, 1H), 7.35−7.18 (m, 6H), 4.94−4.85 (m, 1H), 3.38−3.29 (m, 2H), 2.81 (t, J = 7.3 Hz, 2H), 2.00 (quint, J = 7.4 Hz, 2H), 1.47 (d, J = 7.0 Hz, 3H). ^{13}C NMR (75 MHz, MeOD) δ 161.87 (q, J = 34.4 Hz, TFA), 154.56, 153.29, 143.49, 133.46, 132.86, 128.72 (2C), 126.89, 125.56 (2C), 116.7 (q, J = 288.2 Hz, TFA), 114.97, 49.71, 39.99, 26.73, 21.29, 21.10. HRMS (ESI-MS): m/z [M + H$^+$] calcd for $C_{16}H_{23}N_6O^+$: 315.1928, found: 315.1932. MF: $C_{16}H_{22}N_6O{\cdot}C_4H_2F_6O_4$. MW: (314.39 + 228.05).

*1-(Amino{[3-(5-amino-1,3,4-thiadiazol-2-yl)propyl]amino}-methylene)-3-((R)-(1-phenylethyl))urea Dihydrochloride (**53**).* **53** was prepared from **11** (407 mg, 1.47 mmol, 1 equiv), **24** (494 mg, 1.47 mmol, 1 equiv), $HgCl_2$ (438 mg, 1.61 mmol, 1.1 equiv), and NEt_3 (613 μL, 4.40 mmol, 3 equiv) according to the general procedure, yielding the product as a white, foamlike, and hygroscopic solid (50 mg, 8%). RP-HPLC: 100% (t_R = 9.3 min, k = 2.48). ^{1}H NMR (300 MHz, MeOD) δ 7.37−7.20 (m, 5H), 4.89−4.85 (m, 1H), 3.49−3.35 (m,

https://doi.org/10.1021/acs.jmedchem.1c00692
J. Med. Chem. 2021, 64, 8684−8709

2H), 3.02 (t, J = 7.2 Hz, 2H), 2.09 (quint, J = 6.8 Hz, 2H), 1.47 (d, J = 6.9 Hz, 3H). ^{13}C NMR (75 MHz, MeOD) δ 143.33, 128.26 (2C), 126.97, 125.65 (2C), 49.80, 40.08, 26.80, 26.63, 21.44, 4 C-signals are missing due to the low concentration of the sample. HRMS (ESI-MS): m/z [M + H$^+$] calcd for $C_{15}H_{22}N_7OS^+$: 348.1601, found: 348.1605. MF: $C_{15}H_{21}N_7OS{\cdot}H_2Cl_2$. MW: (347.44 + 72.92).

*1-(Amino{[3-(1H-1,2,4-triazol-5-yl)propyl]amino}methylene)-3-((R)-(1-phenylethyl))urea Dihydrochloride (**54**).* **54** was prepared from **13** (420 mg, 1.14 mmol, 1 equiv), **24** (423 mg, 1.25 mmol, 1.1 equiv), $HgCl_2$ (340 mg, 1.25 mmol, 1.1 equiv), and NEt_3 (474 μL, 3.42 mmol, 3 equiv) according to the general procedure, yielding 560 mg (75%) of Trt-/Boc-protected intermediate. Thereof, 540 mg was deprotected in the next step, yielding **54** as a white, foamlike, and hygroscopic solid after purification by preparative HPLC (200 mg, 63%). RP-HPLC: 100% (t_R = 9.1 min, k = 2.41). ^{1}H NMR (300 MHz, MeOD) δ 9.27 (s, 1H), 7.41−7.19 (m, 5H), 4.88 (q, J = 6.8 Hz, 1H), 3.56−3.37 (m, 2H), 3.21−3.01 (m, 2H), 2.15 (quint, J = 7.3 Hz, 2H), 1.46 (d, J = 7.0 Hz, 3H). ^{13}C NMR (75 MHz, MeOD) δ 155.98, 155.71, 154.19, 144.64, 143.46, 129.56 (2C), 128.27, 126.95 (2C), 51.11, 41.42, 26.36, 22.97, 22.84. HRMS (ESI-MS): m/z [M + H$^+$] calcd for $C_{15}H_{22}N_7O^+$: 316,1880, found: 316.1883. MF: $C_{15}H_{21}N_7O{\cdot}H_2Cl_2$. MW: (315.38 + 72.92).

*1-(Amino{[3-(4-((dimethylamino)methyl)-1H-1,2,3-triazol-1-yl)-propyl]amino}methylene)-3-((R)-(1-phenylethyl))urea Trihydrotrifluoroacetate (**55**).* **55** was prepared from **14** (298 mg, 1.63 mmol, 1 equiv), **24** (549 mg, 1.63 mmol, 1 equiv), $HgCl_2$ (486 mg, 1.79 mmol, 1.1 equiv), and NEt_3 (680 μL, 4.88 mmol, 3 equiv) according to the general procedure, yielding the product as a white, foamlike, and hygroscopic solid (50 mg, 5%). RP-HPLC: 98% (t_R = 8.3 min, k = 2.11). ^{1}H NMR (300 MHz, MeOD) δ 8.22 (s, 1H), 7.36−7.20 (m, 5H), 4.90−4.85 (m, 1H), 4.55 (t, J = 6.7 Hz, 2H), 4.42 (s, 2H), 3.34 (t, J = 6.7 Hz, 2H), 2.88 (s, 6H), 2.25 (p, J = 6.9 Hz, 2H), 1.47 (d, J = 7.0 Hz, 3H). ^{13}C NMR (75 MHz, MeOD) δ 156.03, 144.86, 138.09, 129.63 (2C), 128.33, 128.05, 126.97 (2C), 52.42, 51.09, 48.65, 42.92 (2C), 39.51, 29.69, 22.70, the 1C signal is missing due to the low concentration of the sample. HRMS (ESI-MS): m/z [M + H$^+$] calcd for $C_{18}H_{29}N_8O^+$: 373.2459, found: 373.2463. MF: $C_{18}H_{28}N_8O{\cdot}C_6H_3F_9O_6$. MW: (372.48 + 342.07).

*1-(Amino{[3-(5-amino-1,3,4-thiadiazol-2-yl)propyl]amino}-methylene)-3-(1-(3-fluorophenyl)ethyl)urea Dihydrochloride (**56**).* **56** was prepared from **11** (130 mg, 0.50 mmol, 1 equiv), **25** (179 mg, 0.50 mmol, 1 equiv), $HgCl_2$ (150 mg, 0.55 mmol, 1.1 equiv), and NEt_3 (211 μL, 1.51 mmol, 3 equiv) according to the general procedure, yielding the product as a white, foamlike, and hygroscopic solid (70 mg, 32%). RP-HPLC: 100% (t_R = 9.8 min, k = 2.67). ^{1}H NMR (300 MHz, MeOD) δ 7.40−7.29 (m, 1H), 7.20−7.06 (m, 2H), 7.02−6.92 (m, 1H), 4.91−4.86 (m, 1H), 3.46−3.38 (m, 2H), 3.03 (t, J = 7.4 Hz, 2H), 2.08 (p, J = 7.1 Hz, 2H), 1.47 (d, J = 7.0 Hz, 3H). ^{13}C NMR (75 MHz, MeOD) δ 172.03, 164.29 (d, J = 244.2 Hz), 159.72, 155.61, 154.34, 147.72 (d, J = 7.0 Hz), 131.41 (d, J = 8.2 Hz), 122.88 (d, J = 2.7 Hz), 114.92 (d, J = 21.3 Hz), 113.81 (d, J = 22.2 Hz), 50.76, 41.44, 28.22, 27.50, 22.63. HRMS (ESI-MS): m/z [M + H$^+$] calcd for $C_{15}H_{21}FN_7OS^+$: 366.1507, found: 366.1509. MF: $C_{15}H_{20}FN_7OS{\cdot}H_2Cl_2$. MW: (365.43 + 72.92).

*1-(Amino{[3-(5-amino-1,3,4-thiadiazol-2-yl)propyl]amino}-methylene)-3-(2-methyl-3-(p-tolyl)propyl)urea Dihydrotrifluoroacetate (**57**).* **57** was prepared from amine **11** (66 mg, 0.26 mmol, 1.1 equiv), **26** (85 mg, 0.22 mmol, 1 equiv), NEt_3 (78 μL, 0.56 mmol, 2.5 equiv), and $HgCl_2$ (121 mg, 0.45 mmol, 2 equiv) according to the general procedure, yielding the product as a white, foamlike, and hygroscopic solid (24 mg, 18%). RP-HPLC: 98% (t_R = 15.0 min, k = 3.67). ^{1}H NMR (600 MHz, DMSO-d_6): δ 10.28 (br s, 1H), 9.01 (br s, 1H), 8.50 (br s, 2H), 7.40−8.03 (s, 3H), 7.11−6.99 (m, 4H), 3.29 (q, J = 6.7 Hz, 2H), 3.12−3.02 (m, 1H), 2.96−2.89 (m, 1H), 2.85 (t, J = 7.5 Hz, 2H), 2.62−2.54 (m, 1H), 2.36−2.27 (m, 1H), 2.25 (s, 3H), 1.93−1.82 (m, 3H), 0.78 (d, J = 6.7 Hz, 3H). ^{13}C NMR (151 MHz, DMSO-d_6) δ 168.81, 158.87 (q, J = 34.7 Hz, TFA), 157.45, 153.77, 136.97, 134.72, 128.81, 128.78, 116.33 (q, J = 294.0 Hz, TFA), 44.05, 40.06, 39.98, 34.86, 27.30, 26.53, 20.61, 17.08. HRMS (ESI-MS): m/z [M + H$^+$] calcd for $C_{18}H_{28}N_7OS^+$: 390.2071; found: 390.2077. MF: $C_{18}H_{27}N_7OS{\cdot}C_4H_2F_6O_4$. MW: (389.52 + 228.05).

*1-(Amino{[3-(2-aminothiazol-5-yl)propyl]amino}methylene)-3-(2-methyl-3-(p-tolyl)propyl)urea Dihydrotrifluoroacetate (**59**).* **59** was prepared from amine **12** (37 mg, 0.15 mmol, 1.1 equiv), **26** (50 mg, 0.13 mmol, 1 equiv), NEt_3 (46 μL, 0.33 mmol, 2.5 equiv), and $HgCl_2$ (72 mg, 0.26 mmol, 2 equiv) according to the general procedure, yielding the product as a white, foamlike, and hygroscopic solid (18.2 mg, 23%). R_f = 0.55 (CH_2Cl_2/MeOH 9:1). RP-HPLC: 99% (t_R = 14.5 min, k = 3.52). ^{1}H NMR (600 MHz, DMSO-d_6) δ 10.51 (br s, 1H), 9.46−8.69 (m, 3H), 8.51 (br s, 2H), 7.56 (br s, 1H), 7.13−6.97 (m, 5H), 3.27 (q, J = 6.6 Hz, 2H), 3.13−3.03 (m, 1H), 2.98−2.87 (m, 1H), 2.64 (t, J = 7.5 Hz, 2H), 2.60−2.55 (m, 1H), 2.35−2.28 (m, 1H), 2.25 (s, 3H), 1.92−1.82 (m, 1H), 1.78 (quint, J = 7.3 Hz, 2H), 0.79 (d, J = 6.7 Hz, 3H). ^{13}C NMR (151 MHz, DMSO-d_6) δ 169.30, 159.18 (q, J = 32.9 Hz, TFA) 153.81, 153.77, 136.97, 134.72, 128.81 (2C), 128.77 (2C), 123.96 (2C), 116.69 (q, J = 297.1 Hz, TFA), 44.64, 40.06, 39.90, 34.87, 28.52, 23.30, 20.61, 17.07. HRMS (ESI-MS): m/z [M + H$^+$] calcd for $C_{19}H_{29}N_6OS^+$: 389.2118; found: 389.2122. MF: $C_{19}H_{28}N_6OS{\cdot}C_4H_2F_6O_4$. MW: (388.53 + 228.05).

*1-(Amino{[4-(2-amino-4-methylthiazol-5-yl)phenyl]amino}-methylene)-3-(2-methyl-3-(p-tolyl)propyl)urea Dihydrotrifluoroacetate (**60**).* **60** was prepared from amine **15** (50 mg, 0.16 mmol, 1 equiv), **26** (68 mg, 0.18 mmol, 1.1 equiv), NEt_3 (57 μL, 0.41 mmol, 2.5 equiv), and $HgCl_2$ (89 mg, 0.33 mmol, 2 equiv) according to the general procedure, yielding the product as a white, foamlike, and hygroscopic solid (58 mg, 55%). R_f = 0.64 (CH_2Cl_2/MeOH 9:1). RP-HPLC: 100% (t_R = 15.2 min, k = 3.74). ^{1}H NMR (600 MHz, DMSO-d_6): δ 10.88 (br s, 1H), 10.47 (br s, 1H), 9.29−8.29 (m, 4H), 7.70 (t, J = 5.8 Hz, 1H), 7.55−7.48 (m, 2H), 7.44−7.38 (m, 2H), 7.12−7.02 (m, 4H), 3.15−3.08 (m, 1H), 3.00−2.93 (m, 1H), 2.60 (dd, J = 13.5, 6.1 Hz, 1H), 2.32 (dd, J = 13.5, 8.2 Hz, 1H), 2.29−2.24 (m, 6H), 1.93−1.83 (m, 1H), 0.81 (d, J = 6.7 Hz, 3H). ^{13}C NMR (151 MHz, DMSO-d_6) δ 167.31, 159.20 (q, J = 33.5 Hz, TFA), 153.55, 153.50, 136.94, 134.75, 133.23, 129.70, 129.47, 128.81, 128.79, 126.11, 116.59 (q, J = 295.9 Hz, TFA), 115.77, 44.74, 39.60, 34.83, 20.62, 17.09, 13.82. HRMS (ESI-MS): m/z [M + H$^+$] calcd for $C_{23}H_{29}N_6OS^+$: 437.2118; found: 437.2118. MF: $C_{23}H_{28}N_6OS{\cdot}C_4H_2F_6O_4$. MW: (436.58 + 228.05).

*1-(Amino{[3-(2-amino-4-methylthiazol-5-yl)phenyl]amino}-methylene)-3-(2-methyl-3-(p-tolyl)propyl)urea Dihydrotrifluoroacetate (**61**).* **61** was prepared from amine **16** (20 mg, 0.07 mmol, 1 equiv), **26** (28 mg, 0.073 mmol, 1.1 equiv), NEt_3 (23 μL, 0.17 mmol, 2.5 equiv), and $HgCl_2$ (36 mg, 0.13 mmol, 2 equiv) according to the general procedure, yielding the product as a white, foamlike, and hygroscopic solid (16 mg, 34%). R_f = 0.58 (CH_2Cl_2/MeOH 9:1). RP-HPLC: 100% (t_R = 15.4 min, k = 3.80). ^{1}H NMR (600 MHz, DMSO-d_6): δ 10.81 (br s, 1H), 10.37 (br s, 1H), 9.30−8.53 (m, 4H), 7.68 (t, J = 5.8 Hz, 1H), 7.59−7.53 (m, 1H), 7.43−7.38 (m, 2H), 7.35−7.30 (m, 1H), 3.15−3.06 (m, 1H), 3.00−2.91 (m, 1H), 2.63−2.55 (m, 1H), 2.35−2.20 (m, 7H), 1.93−1.82 (m, 1H), 0.80 (d, J = 6.7 Hz, 3H). ^{13}C NMR (151 MHz, DMSO-d_6): δ 167.56, 158.84 (q, J = 34.5 Hz, TFA), 153.56, 136.92, 134.76, 134.56, 131.80, 130.57, 128.81, 128.79, 127.35, 125.47, 125.10, 116.83 (q, J = 295.7 Hz, TFA), 115.54, 44.71, 40.06, 34.85, 20.61, 17.07, 13.50. HRMS (ESI-MS): m/z [M + H$^+$] calcd for $C_{23}H_{29}N_6OS^+$: 437.2118; found: 437.2116. MF: $C_{23}H_{28}N_6OS{\cdot}C_4H_2F_6O_4$. MW: (436.58 + 228.05).

*1-(Amino{[(2-amino-4,5,6,7-tetrahydrobenzo[d]thiazol-6-yl)-methyl]amino}methylene)-3-(2-methyl-3-(p-tolyl)propyl)urea Dihydrotrifluoroacetate (**62**).* **62** was prepared from amine **17** (82 mg, 0.19 mmol, 1.1 equiv), **26** (80 mg, 0.21 mmol, 1 equiv), NEt_3 (67 μL, 0.48 mmol, 2.5 equiv), and $HgCl_2$ (104 mg, 0.38 mmol, 2 equiv) according to the general procedure, yielding the product as a white, foamlike, and hygroscopic solid (22 mg, 16%). R_f = 0.49 (CH_2Cl_2/MeOH 9:1). RP-HPLC: 99% (t_R = 14.1 min, k = 3.39). ^{1}H NMR (600 MHz, DMSO-d_6): δ 10.36 (br s, 1H), 9.10 (br s, 1H), 8.90−8.32 (m, 4H), 7.58 (br s, 1H), 7.12−7.02 (m, 4H), 3.33−3.26 (m, 2H), 3.14−3.03 (m, 1H), 2.97−2.86 (m, 1H), 2.67−2.56 (m, 2H), 2.48−2.36 (m, 2H), 2.34−2.28 (m, 1H), 2.26 (s, 3H), 2.24−2.15 (m, 1H), 2.10−2.01 (m, 1H), 1.93−1.82 (m, 2H), 1.51−1.41 (m, 1H), 0.79 (d, J = 6.6 Hz, 3H). ^{13}C NMR (151 MHz, DMSO-d_6) δ 168.13, 158.75 (q, J = 31.4 Hz, TFA), 153.94,

https://doi.org/10.1021/acs.jmedchem.1c00692
J. Med. Chem. 2021, 64, 8684−8709

153.71, 136.95, 134.73, 128.81, 128.77, 117.06 (q, J = 297.8 Hz, TFA), 113.15, 44.66, 40.06, 34.86, 33.27, 25.59, 24.70, 22.44, 20.61, 17.08. HRMS (ESI-MS): m/z [M + H$^+$] calcd for $C_{21}H_{31}N_6OS^+$: 415.2275; found: 415.2278. MF: $C_{21}H_{30}N_6OS{\cdot}C_4H_2F_6O_4$. MW: (414.57 + 228.05).

*1-(Amino{[3-(5-amino-1,3,4-thiadiazol-2-yl)propyl]amino}-methylene)-3-(2-methyl-5-phenylpentyl)urea Dihydrotrifluoroacetate (**63**).* **63** was prepared from amine **11** (20 mg, 0.077 mmol, 1 equiv), **27** (33.5 mg, 0.085 mmol, 1.1 equiv), NEt_3 (27 μL, 0.19 mmol, 2.5 equiv), and $HgCl_2$ (42 mg, 0.15 mmol, 2 equiv) according to the general procedure, yielding the product as a white, foamlike, and hygroscopic solid (5.94 mg, 12%). RP-HPLC: 97% (t_R = 16.4 min, k = 4.11). ^{1}H NMR (600 MHz, DMSO-d_6) δ 9.92 (br s, 1H), 8.98 (br s, 1H), 8.49 (br s, 2H), 7.62−7.29 (m, 3H), 7.27−7.22 (m, 2H), 7.16 (d, J = 25.0 Hz, 3H), 3.29 (q, J = 6.7 Hz, 2H), 3.07−3.00 (m, 1H), 2.95−2.87 (m, 1H), 2.84 (t, J = 7.5 Hz, 2H), 2.58−2.52 (m, 2H), 1.88 (quint, J = 7.4 Hz, 2H), 1.66−1.48 (m, 3H), 1.36−1.27 (m, 1H), 1.13−1.05 (m, 1H), 0.83 (d, J = 6.7 Hz, 3H). ^{13}C NMR (151 MHz, DMSO-d_6) δ 168.58, 158.46 (q, J = 33.9 Hz, TFA), 157.32, 153.69 (2C), 142.12, 128.23 (2C), 128.20 (2C), 125.62, 44.92, 40.00, 35.31, 33.21, 32.61, 28.31, 27.38, 26.48, 17.41, second TFA quartet at approx. 116 ppm was not visible. HRMS (ESI-MS): m/z [M + H$^+$] calcd for $C_{19}H_{30}N_7OS^+$: 404.2227; found: 404.2232. MF: $C_{19}H_{29}N_7OS{\cdot}C_4H_2F_6O_4$. MW: (403.55 + 228.05).

*1-(Amino{[4-(2-amino-4-methylthiazol-5-yl)phenyl]amino}-methylene)-3-(2-methyl-5-phenylpentyl)urea Dihydrotrifluoroacetate (**64**).* **64** was prepared from amine **15** (50 mg, 0.16 mmol, 1 equiv), **27** (71 mg, 0.18 mmol, 1.1 equiv), NEt_3 (57 μL, 0.41 mmol, 2.5 equiv), and $HgCl_2$ (89 mg, 0.33 mmol, 2 equiv) according to the general procedure, yielding the product as a white, foamlike, and hygroscopic solid (45 mg, 41%). R_f = 0.64 (CH_2Cl_2/MeOH 9:1). RP-HPLC: 100% (t_R = 16.2 min, k = 4.05). ^{1}H NMR (600 MHz, DMSO-d_6): δ 10.84 (br s, 1H), 10.33 (br s, 1H), 9.15−8.40 (m, 2H), 7.64 (t, J = 5.8 Hz, 1H), 7.55−7.47 (m, 2H), 7.42−7.38 (m, 2H), 7.30−7.23 (m, 2H), 7.21−7.14 (m, 3H), 3.11−3.04 (m, 1H), 2.99−2.91 (m, 1H), 2.60−2.52 (m, 2H), 2.27 (s, 3H), 1.69−1.50 (m, 3H), 1.38−1.29 (m, 1H), 1.17−1.06 (m, 1H), 0.85 (d, J = 6.7 Hz, 3H). ^{13}C NMR (151 MHz, DMSO-d_6): δ 167.14, 158.99 (q, J = 34.7 Hz, TFA), 153.54, 153.49, 142.13, 132.98, 130.03, 129.41, 128.23, 126.16, 125.63, 116.47 (q, J = 295.5 Hz, TFA), 115.83, 45.00, 35.32, 33.22, 32.58, 28.33, 17.41, 14.10. HRMS (ESI-MS): m/z [M + H$^+$] calcd for $C_{24}H_{31}N_6OS^+$: 451.2275; found: 451.2274. MF: $C_{24}H_{30}N_6OS{\cdot}C_4H_2F_6O_4$. MW: (450.61 + 228.05).

*1-(Amino{[3-(2-amino-4-methylthiazol-5-yl)phenyl]amino}-methylene)-3-(2-methyl-5-phenylpentyl)urea Dihydrotrifluoroacetate (**65**).* **65** was prepared from amine **16** (20 mg, 0.07 mmol, 1 equiv), **27** (29 mg, 0.073 mmol, 1.1 equiv), NEt_3 (23 μL, 0.17 mmol, 2.5 equiv), and $HgCl_2$ (36 mg, 0.13 mmol, 2 equiv) according to the general procedure, yielding the product as a white, foamlike, and hygroscopic solid (18 mg, 38%). R_f = 0.58 (CH_2Cl_2/MeOH 9:1). RP-HPLC: 99% (t_R = 16.3 min, k = 4.08). ^{1}H NMR (600 MHz, DMSO-d_6): δ 10.80 (br s, 1H), 10.29 (br s, 1H), 9.17−8.26 (m, 2H), 7.63 (t, J = 5.8 Hz, 1H), 7.55 (t, J = 7.9 Hz, 1H), 7.42−7.36 (m, 2H), 7.32−7.24 (m, 3H), 7.21−7.14 (m, 3H), 3.12−3.04 (m, 1H), 2.99−2.92 (m, 1H), 2.62−2.51 (m, 2H), 2.27 (s, 3H), 1.68−1.50 (m, 3H), 1.37−1.29 (m, 1H), 1.16−1.08 (m, 1H), 0.85 (d, J = 6.7 Hz, 3H). ^{13}C NMR (151 MHz, DMSO-d_6): δ 167.20, 158.53 (q, J = 32.7 Hz, TFA), 153.55, 142.13, 134.43, 132.54, 130.47, 128.23, 127.25, 125.63, 125.30, 124.61, 116.53 (q, J = 297.6 Hz, TFA), 115.73, 44.98, 35.33, 33.21, 32.59, 28.33, 17.40, 14.22. HRMS (ESI-MS): m/z [M + H$^+$] calcd for $C_{24}H_{31}N_6OS^+$: 451.2275; found: 451.2283. MF: $C_{24}H_{30}N_6OS{\cdot}C_4H_2F_6O_4$. MW: (450.61 + 228.05).

*1-(Amino{[(2-amino-4,5,6,7-tetrahydrobenzo[d]thiazol-6-yl)-methyl]amino}methylene)-3-(2-methyl-5-phenylpentyl)urea Dihydrotrifluoroacetate (**66**).* **66** was prepared from amine **17** (81 mg, 0.19 mmol, 1 equiv), **27** (83 mg, 0.21 mmol, 1.1 equiv), NEt_3 (66 μL, 0.48 mmol, 2.5 equiv), and $HgCl_2$ (104 mg, 0.38 mmol, 2 equiv) according to the general procedure, yielding the product as a white, foamlike, and hygroscopic solid (18 mg, 14%). R_f = 0.62 (CH_2Cl_2/MeOH 9:1). RP-HPLC: 100% (t_R = 15.2 min, k = 3.74). ^{1}H NMR (600 MHz, DMSO-d_6): δ 10.39 (br s, 1H), 9.12 (br s, 1H), 8.88 (br s, 2H), 8.54 (br s, 2H), 7.52 (br s, 1H), 7.29−7.21 (m, 2H), 7.20−7.11 (m, 3H), 3.31−3.25 (m, 2H), 3.08−3.00 (m, 1H), 2.95−2.87 (m, 1H), 2.57−2.50 (m, 2H), 2.47−2.37 (m, 1H), 2.24−2.14 (m, 1H), 2.10−2.01 (m, 1H), 1.92−1.83 (m, 1H), 1.65−1.40 (m, 4H), 1.36−1.26 (m, 1H), 1.14−1.05 (m, 1H), 0.83 (d, J = 6.7 Hz, 3H). ^{13}C NMR (151 MHz, DMSO-d_6): δ 168.85, 159.44 (q, J = 30.5 Hz, TFA), 154.38, 142.61, 135.59, 128.70, 128.66, 126.08, 117.35 (q, J = 297.5 Hz, TFA), 113.63, 45.39, 45.10, 40.50, 35.79, 33.67, 33.08, 28.79, 26.00, 25.04, 22.62, 17.87. HRMS (ESI-MS): m/z [M + H$^+$] calcd for $C_{22}H_{33}N_6OS^+$: 429.2431; found: 429.2433. MF: $C_{22}H_{32}N_6OS{\cdot}C_4H_2F_6O_4$. MW: (428.60 + 228.05).

*1-(Amino{[4-(2-amino-4-methylthiazol-5-yl)phenyl]amino}-methylene)-3-{6-[3-(amino{[4-(2-amino-4-methylthiazol-5-yl)-phenyl]amino}methylene)ureido]hexyl}urea tetrahydrotrifluoroacetate (**67**).* **67** was prepared from amine **15** (22 mg, 0.073 mmol, 2 equiv), **28** (20 mg, 0.036 mmol, 1 equiv), NEt_3 (25 μL, 0.18 mmol, 5 equiv), and $HgCl_2$ (40 mg, 0.144 mmol, 4 equiv) according to the general procedure, yielding the product as a white, foamlike, and hygroscopic solid (9.3 mg, 23%). R_f = 0.21 (CH_2Cl_2/MeOH 9:1). RP-HPLC: 98% (t_R = 10.3 min, k = 2.21). ^{1}H NMR (600 MHz, DMSO-d_6): δ 11.70−10.09 (m, 4H), 9.54−8.44 (m, 8H), 7.65 (t, J = 5.7 Hz, 2H), 7.53−7.45 (m, 4H), 7.42−7.33 (m, 4H), 3.12 (q, J = 6.6 Hz, 4H), 2.26 (s, 6H), 1.46 (t, J = 7.0 Hz, 4H), 1.34−1.25 (m, 4H). ^{13}C NMR (151 MHz, DMSO-d_6): δ 167.93 (2C), 160.05 (q, J = 33.2 Hz, TFA), 154.07 (2C), 153.96 (2C), 135.55 (2C), 133.83 (2C), 129.97 (4C), 129.92 (2C), 126.56 (4C), 117.01 (q, J = 294.0 Hz, TFA), 116.17 (2C), 39.65 (2C), 29.26 (2C), 26.31 (2C), 14.03 (2C). HRMS (ESI-MS): m/z [M + H$^+$] calcd for $C_{30}H_{39}N_{12}O_2S_2^+$: 663.2755; found: 663.2752. MF: $C_{30}H_{38}N_{12}O_2S_2{\cdot}C_8H_4F_{12}O_8$. MW: (662.84 + 456.09).

*1-(Amino{[3-(2-amino-4-methylthiazol-5-yl)phenyl]amino}-methylene)-3-{6-[3-(amino{[3-(2-amino-4-methylthiazol-5-yl)-phenyl]amino}methylene)ureido]hexyl}urea Tetrahydrotrifluoroacetate (**68**).* **68** was prepared from amine **16** (22 mg, 0.073 mmol, 2 equiv), **28** (20 mg, 0.036 mmol, 1 equiv), NEt_3 (25 μL, 0.18 mmol, 5 equiv), and $HgCl_2$ (40 mg, 0.144 mmol, 4 equiv) according to the general procedure, yielding the product as a white, foamlike, and hygroscopic solid (5.8 mg, 14%). R_f = 0.23 (CH_2Cl_2/MeOH 9:1). RP-HPLC: 98% (t_R = 10.2 min, k = 2.18). ^{1}H NMR (600 MHz, DMSO-d_6): δ 10.72 (br s, 2H), 10.26 (br s, 2H), 9.08−8.53 (m, 1H), 8.10 (br s, 3H), 7.62 (t, J = 5.7 Hz, 2H), 7.52 (t, J = 7.9 Hz, 2H), 7.39−7.35 (m, 2H), 7.33 (t, J = 2.0 Hz, 2H), 7.28−7.23 (m, 2H), 3.11 (q, J = 6.1 Hz, 4H), 2.25 (s, 6H), 1.44 (quint, J = 6.9 Hz, 5H), 1.32−1.24 (m, 4H). HRMS (ESI-MS): m/z [M + H$^+$] calcd for $C_{30}H_{39}N_{12}O_2S_2^+$: 663.2755; found: 663.2747. MF: $C_{30}H_{38}N_{12}O_2S_2{\cdot}C_8H_4F_{12}O_8$. MW: (662.84 + 456.09).

*1-(Amino{[3-(5-amino-1,3,4-thiadiazol-2-yl)propyl]amino}-methylene)-3-{6-[3-(amino{[3-(5-amino-1,3,4-thiadiazol-2-yl)-propyl]amino}methylene)ureido]hexyl}urea Tetrahydrotrifluoroacetate (**69**).* **69** was prepared from amine **11** (53.3 mg, 0.21 mmol, 2 equiv), **28** (57 mg, 0.10 mmol, 1 equiv), NEt_3 (71 μL, 0.52 mmol, 5 equiv), and $HgCl_2$ (112 mg, 0.41 mmol, 4 equiv) according to the general procedure, yielding the product as a white, foamlike, and hygroscopic solid (35 mg, 34%). RP-HPLC: 96% (t_R = 8.6 min, k = 1.68). ^{1}H NMR (600 MHz, DMSO-d_6) δ: 10.45 (br s, 2H), 9.05 (br s, 2H), 8.53 (br s, 4H), 8.06 (br s, 4H), 7.52 (br s, 2H), 3.30 (q, J = 6.7 Hz, 4H), 3.09 (q, J = 6.6 Hz, 4H), 2.87 (t, J = 7.5 Hz, 4H), 1.89 (quint, J = 7.4 Hz, 4H), 1.43 (quint, J = 6.7 Hz, 4H), 1.31−1.22 (m, 4H). ^{13}C NMR (151 MHz, DMSO-d_6): δ 169.06, 159.16 (q, J = 34.4 Hz, TFA), 157.57, 153.90, 153.71, 39.60, 38.83, 28.88, 27.21, 26.58, 25.88. HRMS (ESI-MS): m/z [M + H$^+$] calcd for $C_{20}H_{37}N_{14}O_2S_2^+$: 569.2660; found: 569.2660. MF: $C_{20}H_{36}N_{14}O_2S_2{\cdot}C_8H_4F_{12}O_8$. MW: (568.26 + 456.09).

*1-(Amino{[3-(5-amino-1,3,4-thiadiazol-2-yl)propyl]amino}-methylene)-3-{8-[3-(amino{[3-(5-amino-1,3,4-thiadiazol-2-yl)-propyl]amino}methylene)ureido]octyl}urea Tetrahydrotrifluoroacetate (**70**).* **70** was prepared from amine **11** (99 mg, 0.38 mmol, 2.2 equiv), **29** (100 mg, 0.17 mmol, 1 equiv), NEt_3 (118 μL, 0.85 mmol, 5 equiv), and $HgCl_2$ (185 mg, 0.68 mmol, 4 equiv) according to the general procedure, yielding the product as a white, foamlike, and hygroscopic solid (11.9 mg, 6.7%). RP-HPLC: 96% (t_R = 10.3 min, k = 2.21). ^{1}H NMR (600 MHz, DMSO-d_6) δ 10.26 (br s, 2H), 9.02 (br s, 2H), 8.50 (br s, 4H), 7.97 (br s, 3H), 7.49 (br s, 2H), 3.29 (q, J = 6.7 Hz, 4H), 3.07 (q, J = 6.6 Hz, 4H), 2.85 (t, J = 7.5 Hz, 4H), 1.88 (quint, J =

https://doi.org/10.1021/acs.jmedchem.1c00692
J. Med. Chem. 2021, 64, 8684−8709

7.3 Hz, 4H), 1.46−1.37 (m, 4H), 1.28−1.22 (m, 8H). ^{13}C NMR (151 MHz, DMSO-d_6) δ 168.97 (2C), 158.81 (q, J = 35.1 Hz, TFA), 157.53 (2C), 153.83 (2C), 153.64 (2C), 115.98 (q, J = 293.8 Hz, TFA), 40.06 (2C), 39.31 (2C), 28.92 (2C), 28.61 (2C), 27.20 (2C), 26.56 (2C), 26.18 (2C). HRMS (ESI-MS): m/z [M + H$^+$] calcd for $C_{22}H_{41}N_{14}O_2S_2^+$: 597.2973; found: 597.2967. MF: $C_{22}H_{40}N_{14}O_2S_2 \cdot C_8H_4F_{12}O_8$. MW: (596.78 + 456.09).

General Procedure for the Synthesis of Oxadiazole Derivatives 37 and 58. The oxadiazole heterocycle was formed according to a previously published procedure.[84] Cyanogen bromide (CNBr) is used as a reagent in this procedure, which is acutely toxic and potentially carcinogenic. It should be used only in a well-ventilated fume hood after reading the safety precautions and wearing proper lab safety equipment (gloves, safety goggles, and lab coats). Future synthetic work should consider replacements for CNBr. The respective acylhydrazine (1 equiv, for details regarding **108** and **109**, see SI) was dissolved in a mixture of H_2O/ethanol (EtOH, 1:1 or 2:3 (v/v), 1−2 mL), and $KHCO_3$ (3.2 equiv) was added. After addition of BrCN (3 M in CH_2Cl_2, 1 equiv), the reaction mixture was heated at 60 °C for 2 h. The reaction mixture was cooled to rt and stirred for an additional hour. EtOH was removed in a vacuum, and the residue was purified by preparative HPLC.

*1-(Amino{[3-(5-amino-1,3,4-oxadiazol-2-yl)propyl]amino}-methylene)-3-(hexyl)urea Dihydrotrifluoroacetate (**37**).* **37** was prepared from **108** (82 mg, 0.16 mmol, 1 equiv), $KHCO_3$ (51 mg, 0.51 mmol, 3.2 equiv), and BrCN (3 M in CH_2Cl_2, 53 μL, 0.16 mmol, 1 equiv) in H_2O/EtOH (1:1.5 mL) according to the general procedure, yielding the product as a white, foamlike, and hygroscopic solid (5.25 mg, 6.1%). RP-HPLC: 99% (t_R = 13.5 min, k = 3.21). ^{1}H NMR (600 MHz, DMSO-d_6) δ 10.03 (br s, 1H), 9.00 (br s, 1H), 8.50 (br s, 2H), 7.49 (t, J = 5.6 Hz, 1H), 6.93 (br s, 2H), 3.31 (q, J = 6.7 Hz, 2H), 3.09 (p, J = 6.4 Hz, 2H), 2.68 (t, J = 7.5 Hz, 2H), 1.87 (p, J = 7.4 Hz, 2H), 1.43 (p, J = 7.2 Hz, 2H), 1.29−1.24 (m, 6H), 0.91−0.82 (m, 3H). ^{13}C NMR (151 MHz, DMSO) δ 163.52, 158.59 (q, J = 34.5 Hz, TFA), 158.48, 153.76, 153.55, 39.61, 38.85, 30.86, 28.86, 25.86, 24.71, 22.01, 21.73, 13.88. HRMS (ESI-MS): m/z [M + H$^+$] calcd for $C_{13}H_{26}N_7O_2^+$: 312.2142; found: 312.2154. MF: $C_{13}H_{25}N_7O_2 \cdot C_4H_2F_6O_4$. MW: (311.39 + 228.05).

*1-(Amino{[3-(5-amino-1,3,4-oxadiazol-2-yl)propyl]amino}-methylene)-3-(2-methyl-3-(p-tolyl)propyl)urea Dihydrotrifluoroacetate (**58**).* **58** was prepared from **109** (22 mg, 0.038 mmol, 1 equiv), $KHCO_3$ (12.2 mg, 0.122 mmol, 3.2 equiv), and BrCN (3 M in CH_2Cl_2, 15.3 μL, 0.046 mmol, 1.2 equiv) in H_2O/EtOH (0.5 mL: 0.5 mL) according to the general procedure, yielding the product as a white, foamlike, and hygroscopic solid (13.97 mg, 61%). RP-HPLC: 100% (t_R = 15.8 min, k = 3.92). ^{1}H NMR (600 MHz, DMSO-d_6) δ 10.13 (br s, 1H), 9.02 (br s, 1H), 8.52 (br s, 2H), 7.57 (t, J = 5.8 Hz, 1H), 7.36−7.01 (m, 6H), 3.34 (q, J = 6.7 Hz, 2H), 3.14−2.90 (m, 2H), 2.71 (t, J = 7.4 Hz, 2H), 2.60 (dd, J = 13.5, 6.1 Hz, 1H), 2.36−2.30 (m, 1H), 2.28 (s, 3H), 1.95−1.83 (m, 3H), 0.81 (d, J = 6.7 Hz, 3H). ^{13}C NMR (151 MHz, DMSO) δ 163.17, 158.59 (q, J = 34.7 Hz, TFA), 158.52, 153.72, 153.68, 136.95, 134.72, 128.80, 128.77, 116.05 (q, J = 293.9 Hz, TFA), 44.64, 39.59, 39.39, 34.85, 24.65, 21.73, 20.60, 17.08. HRMS (ESI-MS): m/z [M + H$^+$] calcd for $C_{18}H_{28}N_7O_2^+$: 374.2299; found: 374.2300. MF: $C_{18}H_{27}N_7O_2 \cdot C_4H_2F_6O_4$. MW: (373.22 + 228.05).

Pharmacological Protocols: Cell Culture. Cells were maintained in 25 or 75 cm^2 flasks (Sarstedt, Nümbrecht, Germany) in a humidified atmosphere (95% air, 5% CO_2) at 37 °C. HEK293T-CRE-Luc-hD$_{2long}$R cells,[40] HEK293T NlucN-mGs/gpH$_2$R-NlucC cells,[26] HEK293T-ARRB2-H$_2$R cells,[41] HEK293T ElucN-βarr2 hD$_{2long}$R-ElucC cells[39], and HEK293T ElucN-βarr2 hD$_3$R-ElucC cells[40] were cultured as described previously.

Radioligand Competition Binding. *Histamine H_{1-4} Receptors.*[22,38] Competition binding experiments were performed with membrane preparations of Sf9 insect cells, expressing the hH$_1$R + RGS4,[85] hH$_2$R-G$_{s\alpha S}$ fusion protein,[48] hH$_3$R + G$_{\alpha i2}$ + G$_{\beta 1\gamma 2}$,[86] or the hH$_4$R + G$_{\alpha i2}$ + G$_{\beta 1\gamma 2}$.[87] General procedures for the generation of recombinant baculoviruses, the culture of Sf9 cells, and membrane preparations have been described elsewhere.[88] The competition binding experiments were performed as previously described in detail[22,38] with one minor modification: PBS (8 g NaCl, 0.2 g KCl, 1.0 g $Na_2HPO_4 \cdot 2H_2O$, 0.15 g $NaH_2PO_4 \cdot H_2O$, 0.1 g KH_2PO_4 in 1 L Millipore H_2O; pH 7.4; 4 °C) was used as washing buffer while harvesting instead of the previously used binding buffer.[22,38] [^{3}H]-Mepyramine (specific activity (spec. act.): 20.0−87 Ci/mmol) was from Hartmann analytics (Braunschweig, Germany) or Novandi Chemistry AB (Södertälje, Sweden), [^{3}H]**1** (specific activity: 25.0 Ci/mmol) and [^{3}H]N^α-methylhistamine (specific activity: 85.3 Ci/mmol) were from Hartmann analytics (Braunschweig, Germany). [^{3}H]UR-DE257[36] (specific activity: 63.0 Ci/mmol) and [^{3}H]UR-PI294[37] (specific activity: 41.8 Ci/mmol) were synthesized and characterized in our laboratories. Histamine dihydrochloride and diphenhydramine hydrochloride were from TCI Deutschland GmbH (Eschborn, Germany). Famotidine was from Alfa Aesar (Karlsruhe, Germany).

Dopamine D_{1-5} Receptors. The competition binding experiments were performed on homogenates of HEK293T-CRE-Luc-hD$_x$R (x = 1, 2long, 3 or 5) or HEK293T ElucN-βarr2 hD$_{4.4}$R-ELuc cells using [^{3}H]N-methylspiperone (hD$_{2long/3/4.4}$R, specific activity: 77 Ci/mmol, Novandi Chemistry AB) or [^{3}H]SCH23390 (hD$_{1/5}$R, specific activity: 81 Ci/mmol, Novandi Chemistry AB) using the previously published protocol.[40] Generation and cell culture of HEK293T-CRE-Luc cells, expressing the hD$_1$-, hD$_{2long}$-, hD$_3$-, or hD$_{4.4}$ receptors as well as the general procedure for the homogenate preparation have been described in the same publication.[40]

The HEK293T-CRE-Luc cell line stably expressing the hD$_5$R was generated in an analogous manner as published for the hD$_1$R, hD$_{2long}$R, hD$_3$R, or hD$_{4.4}$R.[40] In brief, 2 μg of the pIRESneo3 SP-FLAG-hD$_5$R vector (generated in an analogous manner as described for the hD$_1$R, hD$_{2long}$R, hD$_3$R, and hD$_{4.4}$R[40]) was used and selection was achieved in the presence of 600 μg/mL of G418. The preparation of cell homogenates was performed as previously described[40] with the following modification: after centrifugation (6 °C, 50 000g, 15 min) and resuspension of the remaining pellet in tris(hydroxymethyl)-aminomethane (Tris)−MgSO$_4$ buffer[40] homogenization was performed with a Potter homogenizer (10 times, ice-cooled) instead of a syringe and needle.

Competition binding experiments with hD$_1$ and hD$_5$ receptors were performed by incubating homogenates in binding buffer[40] at a final concentration of 0.3 μg (hD$_1$R) or 0.4 μg (hD$_5$R) protein/well together with [^{3}H]SCH23390 (hD$_1$R (K_d = 0.23 nM) and hD$_5$R (K_d = 0.2 nM): c = 0.4 nM) and increasing concentrations of the competing ligands (**6**, **31**, **47**, and **54**) for 120 min at room temperature. Binding studies at the hD$_{2long}$R, hD$_3$R, and hD$_{4.4}$R were performed in binding buffer[40] at a concentration of 0.3 μg (hD$_{2long}$R), 0.7 μg (hD$_3$R), or 0.5−1.0 μg (hD$_{4.4}$R) protein/well together with [^{3}H]N-methylspiperone (hD$_{2long}$R (K_d = 0.0149 nM): c = 0.05 nM; hD$_3$R (K_d = 0.0258 nM): c = 0.05 nM; hD$_{4.4}$R (K_d = 0.078 nM): c = 0.1 nM) and varying concentrations of the competing ligands (**6**, **31**, **32**, **46**, **43**, **47**, **48**, **53**, **54**, **56**, **57**, **59**, **63**, and/or **69**) for 60 min in the case of the hD$_{2long}$R and hD$_3$R and 140 min in the case of the hD$_{4.4}$R at room temperature. Nonspecific binding was determined in the presence of 2 μM (+)-butaclamol (Sigma, Taufkirchen, Germany, hD$_1$R, hD$_{2long}$R, hD$_3$R) or nemonapride (Tocris Bioscience, Bristol, U.K., hD$_{4.4}$R).

Muscarinic Acetylcholine M_{1-5} Receptors. Binding studies at human muscarinic receptors (stably expressed in CHO-hM$_x$R cells, x = 1−5) were performed using previously described radioligand competition binding assays.[78]

Binding affinities toward the human adrenoceptors α_{1A}, α_{2A}, β_1, and β_2 as well as to the human serotonin receptor 5-HT$_{1A}$ and the human opioid receptor μOR were determined as previously described.[79,80] In brief, membranes were prepared from HEK293T cells each transiently transfected with appropriate cDNAs (cDNA of α_{1A}, β_2, and 5-HT$_{1A}$ from the cDNA Resource Center, Bloomsburg, PA, for α_{2A}: a gift from the D. Yang, Chinese University of Hong Kong, Shenzhen, China, for μOR: a gift from the Ernest Gallo Clinic and Research Center, UCSF, CA, for β_1: a gift from the R. Sunahara, UCSD, CA). Receptor density (B_{max} value) and specific binding affinities (K_D value) for α_{1A} were determined as 6500 fmol/mg and 0.25 nM, respectively ([^{3}H]prazosin

https://doi.org/10.1021/acs.jmedchem.1c00692
J. Med. Chem. 2021, 64, 8684−8709

(specific activity: 84 Ci/mmol, PerkinElmer, Rodgau, Germany) at a concentration of 0.4 nM), for α_{2A}: 1800 fmol/mg and 0.60 nM, respectively ([^{3}H]RX821002 (spec. act. 52 Ci/mmol, Novandi Chemistry AB) at 0.5 nM), for β_1: 3500 fmol/mg and 0.075 nM, respectively ([^{3}H]CGP12177 (spec. act. 52 Ci/mmol, PerkinElmer) at 0.2 nM), for β_2: 2000 fmol/mg and 0.070 nM, respectively ([^{3}H]CGP12177 at 0.2 nM), for 5-HT$_{1A}$: 1100 fmol/mg and 0.080 nM, respectively ([^{3}H]WAY600135 (spec. act. 80 Ci/mmol, Biotrend, Cologne, Germany) at 0.2 nM), and μOR: 1700 fmol/mg and 0.090 nM, respectively ([^{3}H]diprenorphine (spec. act. 31 Ci/mmol, PerkinElmer) at 0.3 nM). Competition binding experiments with α_{1A} and 5-HT$_{1A}$ were performed by incubating membranes in buffer A (50 mM Tris, 5 mM $MgCl_2$, 0.1 mM ethylenediaminetetraacetic acid (EDTA), 5 μg/mL bacitracin, and 5 μg/mL soybean trypsin inhibitor at pH 7.4) at a final protein concentration of 1 μg/well and 6 μg/well together with the radioligand and varying concentrations of the competing ligands for 60 min at 37 °C. Binding at α_{2A} and μOR was performed in buffer B (50 mM Tris at pH 7.4) at a protein concentration of 10 and 6 μg/well, respectively, and for β_1 and β_2 in buffer C (25 mM *N*-(2-hydroxyethyl)piperazine-*N*′-ethanesulfonic acid (HEPES), 5 mM $MgCl_2$, 1 mM EDTA, and 0.01% bovine serum albumin (BSA) at pH 7.4) at a protein concentration of 2 and 4 μg/well, respectively. Nonspecific binding was determined in the presence of 10 μM of prazosin (α_{1A}), RX821002 (α_{2A}), CGP12177 (β_1 and β_2), WAY600135 (5-HT$_{1A}$), and naloxone (μOR). The protein concentration was established using the method of Lowry.[89] The resulting competition curves were analyzed by nonlinear regression using the algorithms implemented in PRISM 6.0 (GraphPad Software, San Diego, CA) to provide an IC_{50} value, which was subsequently transformed into the K_i value, employing the equation of Cheng and Prusoff.[49]

[^{35}S]GTPγS Binding Assay. The assay was performed on Sf9 membranes expressing the hH$_2$R-G$_{s\alpha S}$ fusion protein as previously described[22,38,48] with one minor modification: PBS (8 g NaCl, 0.2 g KCl, 1.0 g $Na_2HPO_4{\cdot}2H_2O$, 0.15 g $NaH_2PO_4{\cdot}H_2O$, 0.1 g KH_2PO_4 in 1 L Millipore H_2O; pH 7.4; 4 °C) was used as washing buffer while harvesting instead of the previously used binding buffer. [^{35}S]GTPγS was from Hartmann Analytics (Braunschweig, Germany). GTPγS and GDP were purchased from Roche (Mannheim, Germany).

Mini-G Protein Recruitment Assay. The mini-G protein recruitment assay at the hH$_2$R or gpH$_2$R was performed using HEK293T NlucN-mGs/hH$_2$R-NlucC[42] or HEK293T NlucN-mGs/gpH$_2$R-NlucC[26] cells as previously described in detail. Furimazine was from Promega (Mannheim, Germany).

***β*-Arrestin2 Recruitment Assay.** *Histamine H$_2$ Receptor.* The β-arrestin2 recruitment assay at the hH$_2$R was performed using HEK293T-ARRB2-H$_2$R[41] cells, as previously described in detail.[46]

Dopamine D$_{2long/3}$ Receptors. The β-arrestin2 recruitment assay at the hD$_{2long}$R or hD$_3$R was performed using HEK293T ElucN-βarr2 hD$_{2long}$R-ElucC or HEK293T ElucN-βarr2 hD$_3$R-ElucC cells, as previously described in detail.[40] Quinpirole was from Tocris Bioscience (Bristol, U.K.). Pierce D-luciferin was purchased as the potassium salt from Fisher Scientific GmbH (Schwerte, Germany).

Docking. *Models of the Active-State hH$_2$R and Active-State hD$_2$R.* For the receptor modeling, docking studies, and presentation of the results, Sybyl 7.3 software (Tripos Inc., St. Louis, MO) was used. Since the compounds, for which the interaction with the hH$_2$R should be analyzed, were experimentally identified as partial agonists at the hH$_2$R, an active-state model of the hH$_2$R was generated by homology modeling, using the crystal structure of the β_2 adrenergic receptor−Gs protein complex (protein databank code: 3SN6) as a template.[50] The G$\alpha\beta\gamma$-subunits (chain A, B, G), the endolysin, and the camelid antibody variable domain of the heavy chain of the heavy-chain antibody (VHH) fragment (chain N) were deleted. According to an appropriate sequence alignment between $h\beta_2$R and hH$_2$R, the homology model was generated by exchanging all amino acids of the template, being different to the corresponding amino acid of the hH$_2$R sequence using the tool "Mutate Monomers" of Sybyl, into the correct amino acid of the hH$_2$R. N-terminus and loops (tool: "Loop Search" of Sybyl) were modeled, according to procedures, as described elsewhere.[90] Briefly, the first 14 amino acids of the N-terminus of the hH$_2$R were added to the first amino acid present in the receptor-part (E30) of the 3SN6 crystal structure with a random conformation using the tool "Build Protein" of Sybyl. The amino acid sequences RNETSKGNHTTSK (part of the E2 Loop) and GDD (part of the E3-Loop) were modeled using the "Loop Search" Module. In addition, the amino acids NHISSWKAA (part of the I3-Loop) were added using the "Loop Search" Module to close the gap, which was present in the 3SN6 template, between TM5 and TM6. The C-Terminus of the hH$_2$R, starting with C^{354}, was not included in the homology model because the C-terminus was not present in the 3SN6 template. The resulting active-state model of the hH$_2$R was minimized with the Amber 7 FF99 force field.

Since the compounds, for which the interaction with the hD$_2$R should be analyzed, were also identified as partial agonists at the hD$_2$R by functional studies, an active-state model of the hD$_2$R was used. For this purpose, the crystal structure of the dopamine D$_2$ receptor−G protein complex (protein databank code: 6VMS) was used as a template.[51] The G$\alpha\beta\gamma$-subunits (chain A, B, C) and the scFv16 (chain E) were deleted. This model was refined by exchanging all amino acids of the template, which is different from the corresponding amino acid of the hD$_2$R in the correct amino acid of the hD$_2$R (tool: "Mutate Monomers" of Sybyl). The N-terminus (the first 31 amino acids) of the hD$_2$R was not added. The I3-loop (R^{227}−R^{360}), which was not present in the template structure, was not modeled. However, the gap between TM5 and TM6 was already closed in the template by connecting K^{226} with R^{361}. The resulting active-state hD$_2$R was minimized with the Amber 7 FF99 force field. Based on the model of the hD$_2$R, the receptor mutant hD$_2$R-E$^{E2.49}$V-I$^{E2.51}$S was generated, using the "Mutate Monomers" tool to exchange E$^{E2.49}$ into V and E$^{E2.51}$ into S followed by minimization as described above.

The compounds **6**, **31**, and **32**, provided with the Gasteiger−Hückel charges, were docked manually into the orthosteric binding pocket of the respective receptor, considering mutations studies, described in the literature, differences in the amino acid alignment of the hH$_2$R, hD$_2$R, and hD$_3$R (Figure S146 in the SI), and the pharmacological results of the present study. The net charge for **6**, **31**, and **32** was 1, with the positive charge being located on the carbamoylguanidine group. The resulting ligand−receptor complexes were minimized with the Amber 7 FF99 force field.

Data Processing. Compound purities were calculated as the percentage peak area of the analyzed compound by UV detection at 220 nm. Retention (capacity) factors (k) were calculated from retention times (t_R) according to $k = (t_R - t_0)/t_0$, t_0 = dead time. Data from radioligand competition binding assays (hH$_{1-4}$[38] and hD$_{2long/3}$[40] receptors), from the [^{35}S]GTPγS binding assay,[38] from the mini-G protein (hH$_2$R,[42] gpH$_2$R[26]), or β-arrestin2 (hH$_2$[41,46] and hD$_{2long/3}$[40] receptors) recruitment assays, and from the H$_2$R assay on isolated guinea pig right atrium[38] were processed, as reported previously. K_i values for the calculation of relative affinities (H$_2$R selectivity, Tables 1 and 2) were obtained by transforming the pK_i mean value to K_i ($K_i = 10^{-pK_i}$).

■ ASSOCIATED CONTENT

Supporting Information

The Supporting Information is available free of charge at https://pubs.acs.org/doi/10.1021/acs.jmedchem.1c00692.

Experimental details for the amines **8**−**17** and the guanidinylating reagents **18**−**29**; experimental details for the acylhydrazines **108** and **109**; NMR spectra for the carbamoylguanidines **30**−**70**; RP-HPLC chromatograms of compounds **30**−**70**; RP-HPLC chromatograms: chemical stability of **30**−**35**, **37**, **41**, and **57**; determination of the pK_a value; radioligand competition binding data; concentration−response curves obtained using β-arrestin2 or mini-G protein recruitment assays; investigation of β-arrestin2 and mGs recruitment at HEK293T-hH$_2$R cells for cmpds UR-CH20, UR-SB291, UR-CH22, UR-Po563, UR-MB-69, UR-SB257, UR-

https://doi.org/10.1021/acs.jmedchem.1c00692
J. Med. Chem. 2021, 64, 8684−8709

KAT527, **30**, **33**−**35**, **37**−**42**, **44**−**46**, **49**−**52**, **55**, **58**, **60**−**62**, **64**−**68**, and **70**; bias analysis, docking; synthesis and characterization of zolantidine dihydrotrifluoroacetate; estimation of the selectivity with respect to the relative receptor expression in different CNS tissues; computation prediction of the membrane permeability; and MS (ESI) data of Boc-/Trt-protected intermediates (PDF)

Molecular formula strings, $h\mathrm{H}_{1-4}\mathrm{R}$ and $h\mathrm{D}_{2\mathrm{long}/3}$ binding data, $h/gp\mathrm{H}_2\mathrm{R}$, and $h\mathrm{D}_{2\mathrm{long}/3}$ functional data binding data (CSV)

Three-dimensional (3D) coordinates of the $h\mathrm{D}_2\mathrm{R}$ in complex with **6**, obtained through molecular docking; 3D coordinates of the $h\mathrm{D}_2\mathrm{R}$ in complex with **31**, obtained through molecular docking; 3D coordinates of the $h\mathrm{D}_2\mathrm{R}$ in complex with **32**, obtained through molecular docking; 3D coordinates of $h\mathrm{D}_2\mathrm{R}$-E249V-I251S in complex with **6**, obtained through molecular docking; 3D coordinates of $h\mathrm{D}_2\mathrm{R}$-D249V-I251S in complex with **31**, obtained through molecular docking; 3D coordinates of $h\mathrm{D}_2\mathrm{R}$-E249V-I251S in complex with **32**, obtained through molecular docking; 3D coordinates of the $h\mathrm{H}_2\mathrm{R}$ in complex with **6**, obtained through molecular docking; 3D coordinates of the $h\mathrm{H}_2\mathrm{R}$ in complex with **31**, obtained through molecular docking; 3D coordinates of the $h\mathrm{H}_2\mathrm{R}$ in complex with **32**, obtained through molecular docking; 3D coordinates of $h\mathrm{H}_2\mathrm{R}$-D542S in complex with **31**, obtained through molecular docking; and 3D coordinates of $h\mathrm{H}_2\mathrm{R}$-D542S in complex with **32**, obtained through molecular docking (ZIP)

AUTHOR INFORMATION

Corresponding Authors

Steffen Pockes − *Institute of Pharmacy, University of Regensburg, D-93053 Regensburg, Germany; Department of Neurology, University of Minnesota, Minneapolis, Minnesota 55455, United States; Department of Medicinal Chemistry, Institute for Therapeutics Discovery and Development, University of Minnesota, Minneapolis, Minnesota 55414, United States;* orcid.org/0000-0002-2211-9868; Phone: (+49)941 943-4814/4825; Email: steffen.pockes@ur.de; Fax: (+49)941 943-4809

Andrea Strasser − *Institute of Pharmacy, University of Regensburg, D-93053 Regensburg, Germany;* orcid.org/0000-0002-3994-3079; Phone: (+49)941 943-4821/4694; Email: andrea.strasser@ur.de; Fax: (+49)941 943-4820

Authors

Katharina Tropmann − *Institute of Pharmacy, University of Regensburg, D-93053 Regensburg, Germany*

Merlin Bresinsky − *Institute of Pharmacy, University of Regensburg, D-93053 Regensburg, Germany*

Lisa Forster − *Institute of Pharmacy, University of Regensburg, D-93053 Regensburg, Germany*

Denise Mönnich − *Institute of Pharmacy, University of Regensburg, D-93053 Regensburg, Germany*

[⊥]**Armin Buschauer** − *Institute of Pharmacy, University of Regensburg, D-93053 Regensburg, Germany;* orcid.org/0000-0002-9709-1433

Hans-Joachim Wittmann − *Institute of Pharmacy, University of Regensburg, D-93053 Regensburg, Germany*

Harald Hübner − *Department of Chemistry and Pharmacy, Medicinal Chemistry, Friedrich-Alexander-University of Erlangen-Nürnberg, 91058 Erlangen, Germany*

Peter Gmeiner − *Department of Chemistry and Pharmacy, Medicinal Chemistry, Friedrich-Alexander-University of Erlangen-Nürnberg, 91058 Erlangen, Germany;* orcid.org/0000-0002-4127-197X

Complete contact information is available at: https://pubs.acs.org/10.1021/acs.jmedchem.1c00692

Author Contributions

M.B. and L.F. contributed equally to this work. K.T. and M.B. performed the synthesis and analytical characterization of chemical compounds. K.T. performed the investigation of the chemical stability. M.B. determined the pK_a value for the 2-aminothiadiazole. K.T. and M.B. performed radioligand competition binding experiments at $\mathrm{H}_{1\text{-}4}$Rs and analyzed the data. L.F. performed radioligand competition binding experiments at D_{1-5}Rs and analyzed the data. D.M. generated the HEK293T-CRE-Luc-$h\mathrm{D}_5\mathrm{R}$ cell line and prepared the corresponding homogenates. K.T. performed radioligand competition binding experiments at $\mathrm{M}_{1-5}\mathrm{R}$ and analyzed the data. H.H. and P.G. performed the radioligand binding studies at the human adrenoceptors α_{1A}, α_{2A}, β_1, and β_2 as well as to the human serotonin receptor 5-HT_{1A} and the human opioid receptor μOR and analyzed the data. K.T. performed the functional studies at $\mathrm{H}_2\mathrm{R}$ and analyzed the data, with the exception of guinea right atrium experiments, which were performed and analyzed by M.B. L.F. and K.T. performed and analyzed functional studies at $\mathrm{D}_{2\mathrm{long}/3}$Rs. H.-J.W. and A.S. performed molecular docking and processed the data. A.B. and A.S. initiated and planned the project. S.P. and A.S. supervised the research. K.T., S.P., and A.S. wrote the manuscript. All authors have given approval to the final version of the manuscript.

Funding

This work was funded by the Graduate Training Program (Graduiertenkolleg) GRK1910, "Medicinal chemistry of selective GPCR ligands", of the Deutsche Forschungsgemeinschaft (K.T., A.B., H.H., P.G., A.S.).

Notes

The authors declare no competing financial interest.

[⊥]Deceased, July 18, 2017.

ACKNOWLEDGMENTS

The authors are grateful to Christine Gebhardt-Braun and Kerstin Röhrl for carrying out guinea pig right atrium experiments, Brigitte Wenzl for excellent technical assistance, and Dr Max Keller for supporting the muscarinic receptor binding studies. We thank Dr Anja Kraus for the synthesis of 3-methyl-6-phenylhexanoic acid and 3-cyclohexylbutanoic acid. We also thank Claudia Honisch, Drs Sabrina Biselli and Nicole Plank for synthesis and providing the compounds UR-CH22, UR-SB257, UR-SB291, and UR-NK22. We thank Dr Johannes Felixberger for proving the HEK293T-ARRB2-$\mathrm{H}_2\mathrm{R}$ cell line and Carina Höring for providing the HEK293T NlucN-mGs/$h\mathrm{H}_2\mathrm{R}$-NlucC and the HEK293T NlucN-mGs/$gp\mathrm{H}_2\mathrm{R}$-NlucC cell lines. We thank Josef Kiermaier and Wolfgang Söllner for mass spectrometry analysis. We thank Fritz Kastner for NMR measurements.

https://doi.org/10.1021/acs.jmedchem.1c00692
J. Med. Chem. 2021, 64, 8684−8709

■ ABBREVIATIONS

5-HT_{1A}, serotonin 1A receptor; α_{1A}, adrenoreceptor α 1A; α_{2A}, adrenoreceptor α 2A; β_1, adrenoceptor β_1, adrenoceptor β_2, βarr2 or ARRB2, β-arrestin2 gene, and protein; δ, chemical shift in ppm; μOR, μ opioid receptor; AU, absorption units; BB, building block; *c*, molar concentration; $CDCl_3$, deuterated chloroform; cf., confer/conferatur; CRE-Luc, cAMP-response element driven transcriptional luciferase reporter; CH_2Cl_2, dichloromethane; CHO, Chinese hamster ovary; CNS, central nervous system; cmpd, compound; DAD, diode array detector; DMSO-d_6, deuterated DMSO; D_xR, dopamine receptor subtype x; E, extracellular loop; EI, electron ionization; Eluc, Emerald luciferase; ElucC, C-terminal Eluc fragment; ElucN, N-terminal Eluc fragment; E_{max}, maximal inducible receptor response referenced to a standard compound; Et_2O, diethyl ether; EtOAc, ethyl acetate; EtOH, ethanol; FLAG, polypeptide protein tag with sequence motif DYKDDDDK; g, gram(s) or number of times the gravitational force; G418, geneticin; $G_{\alpha i2}$, α-subunit of the G_{i2} protein that mediates the inhibition of adenylyl cyclase; $G_{\beta 1\gamma 2}$, G protein β_1- and γ_2-subunit; *gp*, guinea pig; Gs, adenylyl cyclase stimulatory G protein; $G_{s\alpha S}$, α-subunit (short splice variant) of the Gs protein that mediates stimulation of adenylyl cyclase; GTPγS, guanosine 5′-*O*-[γ-thio]phosphate; *h*, human; HEK293T, human embryonic kidney 293T cells; Het, heterocycle; H_xR, histamine receptor subtype *x*; *k*, retention (or capacity) factor (HPLC); K_a, acid dissociation constant; K_b, dissociation constant obtained from a functional assay; K_d, dissociation constant obtained from a saturation binding experiment; K_i, dissociation constant obtained from a competition binding experiment; LC, liquid chromatography; MeOD, deuterated methanol; MeCN, acetonitrile; MeOH, methanol; MF, molecular formula; mG or mini-G, engineered minimal G protein; mGs, engineered guanosine triphosphate hydrolase domain of $G\alpha_s$ subunit (long splice variant); L-DOPA, levodopa; M_xR, muscarinic receptor subtype *x*; NEt_3, triethylamine; Nluc, NanoLuc luciferase; NlucC, C-terminal Nluc fragment; NlucC, N-terminal Nluc fragment; PE, petroleum ether; pEC_{50}, negative logarithm of the half-maximum activity concentration in M; pH, potential or power of hydrogen; pK_a, negative logarithm of the K_a in M; pK_b, negative logarithm of the K_b in M; pK_i, negative logarithm of the K_i in M; *r*, rat; R, residue; RGS4, regulator of G protein signaling proteins 4; RP-HPLC, reversed-phase HPLC; Q-TOF, quadrupole time of flight; scFv16, single-chain variable fragment derived from mAb16 antibody; SEM, standard error of the mean; SF, SuperFlash; Sf9, *Spodoptera frugiperda* insect cell line; SI, Supporting Information; SP, signal peptide: subunit A of the murine type 3 receptor for 5-hydroxytryptamine; spec. act., specific activity; t_0, dead time; t_R, retention time; Tris, tris(hydroxymethyl)-aminomethane; Trt, trityl; UHD, ultrahigh definition; VHH, variable domain of heavy chain of heavy-chain antibody

■ REFERENCES

(1) Hill, S. J.; Ganellin, C. R.; Timmerman, H.; Schwartz, J. C.; Shankley, N. P.; Young, J. M.; Schunack, W.; Levi, R.; Haas, H. L. International union of pharmacology. XIII. Classification of histamine receptors. *Pharmacol. Rev.* **1997**, *49*, 253−278.

(2) Panula, P.; Chazot, P. L.; Cowart, M.; Gutzmer, R.; Leurs, R.; Liu, W. L.; Stark, H.; Thurmond, R. L.; Haas, H. L. International union of basic and clinical pharmacology. XCVIII. Histamine receptors. *Pharmacol. Rev.* **2015**, *67*, 601−655.

(3) Dove, S.; Elz, S.; Seifert, R.; Buschauer, A. Structure-activity relationships of histamine H_2 receptor ligands. *Mini-Rev. Med. Chem.* **2004**, *4*, 941−954.

(4) Traiffort, E.; Pollard, H.; Moreau, J.; Ruat, M.; Schwartz, J. C.; Martinez-Mir, M. I.; Palacios, J. M. Pharmacological characterization and autoradiographic localization of histamine H_2 receptors in human brain identified with [^{125}I]iodoaminopotentidine. *J. Neurochem.* **1992**, *59*, 290−299.

(5) Black, J. W.; Duncan, W. A. M.; Durant, G. J.; Ganellin, C. R.; Parsons, M. E. Definition and antagonism of histamine H_2-receptors. *Nature* **1972**, *236*, 385−390.

(6) Yanagisawa, I.; Hirata, Y.; Ishii, A. Studies on histamine H_2 receptor antagonists. 2. Synthesis and pharmacological activities of *N*-sulfamoyl and *N*-sulfonyl amidine derivatives. *J. Med. Chem.* **1987**, *30*, 1787−1793.

(7) Schneider, E. H.; Neumann, D.; Seifert, R. Modulation of behavior by the histaminergic system: lessons from H_1R-and H_2R-deficient mice. *Neurosci. Biobehav. Rev.* **2014**, *42*, 252−266.

(8) Deutsch, S. I.; Rosse, R. B.; Schwartz, B. L. Histamine H_2 receptor antagonists in schizophrenia. *CNS Drugs* **1997**, *8*, 276−284.

(9) Farzin, D.; Hosseini, S. H.; Shafaat, A. A randomized double blind clinical trial in famotidine adjuvant therapy in schizophrenia. *Iran. J. Med. Sci.* **2005**, *30*, 59−62.

(10) Johnston, T. H.; van der Meij, A.; Brotchie, J. M.; Fox, S. H. Effect of histamine H_2 receptor antagonism on levodopa−induced dyskinesia in the MPTP-macaque model of Parkinson's disease. *Mov. Disord.* **2010**, *25*, 1379−1390.

(11) Meskanen, K.; Ekelund, H.; Laitinen, J.; Neuvonen, P. J.; Haukka, J.; Panula, P.; Ekelund, J. A randomized clinical trial of histamine 2 receptor antagonism in treatment-resistant schizophrenia. *J. Clin. Psychopharmacol.* **2013**, *33*, 472−478.

(12) Shi, H.; Yang, X.; Zhao, H.; Zhang, S.; Zu, J.; Zhang, W.; Shen, X.; Cui, G.; Hua, F.; Yan, C. Ranitidine reduced levodopa-induced dyskinesia by remodeling neurochemical changes in hemiparkinsonian model of rats. *Neuropsychiatr. Dis. Treat.* **2015**, *11*, 1331−1337.

(13) Ahmed, M. R.; Jayakumar, M.; Ahmed, M. S.; Zamaleeva, A. I.; Tao, J.; Li, E. H.; Job, J. K.; Pittenger, C.; Ohtsu, H.; Rajadas, J. Pharmacological antagonism of histamine H_2R ameliorated L-DOPA-induced dyskinesia via normalization of GRK3 and by suppressing FosB and ERK in PD. *Neurobiol. Aging* **2019**, *81*, 177−189.

(14) Oyewumi, L. K.; Vollick, D.; Merskey, H.; Plumb, C. Famotidine as an adjunct treatment of resistant schizophrenia. *J. Psychiatry Neurosci.* **1994**, *19*, 145−150.

(15) White, J. M.; Rumbold, G. R. Behavioural effects of histamine and its antagonists: a review. *Psychopharmacology* **1988**, *95*, 1−14.

(16) Khan, N.; Saad, A.; Nurulain, S. M.; Darras, F. H.; Decker, M.; Sadek, B. The dual-acting H3 receptor antagonist and AChE inhibitor UW-MD-71 dose-dependently enhances memory retrieval and reverses dizocilpine-induced memory impairment in rats. *Behav. Brain Res.* **2016**, *297*, 155−164.

(17) Darras, F. H.; Pockes, S.; Huang, G.; Wehle, S.; Strasser, A.; Wittmann, H. J.; Nimczick, M.; Sotriffer, C. A.; Decker, M. Synthesis, biological evaluation, and computational studies of Tri- and tetracyclic nitrogen-bridgehead compounds as potent dual-acting AChE inhibitors and hH_3 receptor antagonists. *ACS Chem. Neurosci.* **2014**, *5*, 225−242.

(18) Sadek, B.; Khan, N.; Darras, F. H.; Pockes, S.; Decker, M. The dual-acting AChE inhibitor and H_3 receptor antagonist UW-MD-72 reverses amnesia induced by scopolamine or dizocilpine in passive avoidance paradigm in rats. *Physiol. Behav.* **2016**, *165*, 383−391.

(19) Ghorai, P.; Kraus, A.; Keller, M.; Götte, C.; Igel, P.; Schneider, E.; Schnell, D.; Bernhardt, G.; Dove, S.; Zabel, M.; Elz, S.; Seifert, R.; Buschauer, A. Acylguanidines as bioisosteres of guanidines: N^G-acylated imidazolylpropylguanidines, a new class of histamine H_2 receptor agonists. *J. Med. Chem.* **2008**, *51*, 7193−7204.

(20) Kraus, A.; Ghorai, P.; Birnkammer, T.; Schnell, D.; Elz, S.; Seifert, R.; Dove, S.; Bernhardt, G.; Buschauer, A. N^G-Acylated aminothiazolylpropylguanidines as potent and selective histamine H_2 receptor agonists. *ChemMedChem* **2009**, *4*, 232−240.

https://doi.org/10.1021/acs.jmedchem.1c00692
J. Med. Chem. 2021, 64, 8684−8709

(21) Ghorai, P.; Kraus, A.; Birnkammer, T.; Geyer, R.; Bernhardt, G.; Dove, S.; Seifert, R.; Elz, S.; Buschauer, A. Chiral N^G-acylated hetarylpropylguanidine-type histamine H_2 receptor agonists do not show significant stereoselectivity. *Bioorg. Med. Chem. Lett.* **2010**, *20*, 3173−3176.
(22) Kagermeier, N.; Werner, K.; Keller, M.; Baumeister, P.; Bernhardt, G.; Seifert, R.; Buschauer, A. Dimeric carbamoylguanidine-type histamine H_2 receptor ligands: a new class of potent and selective agonists. *Bioorg. Med. Chem.* **2015**, *23*, 3957−3969.
(23) Biselli, S.; Bresinsky, M.; Tropmann, K.; Forster, L.; Honisch, C.; Buschauer, A.; Bernhardt, G.; Pockes, S. Pharmacological characterization of a new series of carbamoylguanidines reveals potent agonism at the H_2R and D_3R. *Eur. J. Med. Chem.* **2021**, *214*, No. 113190.
(24) Biselli, S. Synthesis and Pharmacological Characterization of Subtype-Selective Ligands, Including Radio- and Fluorescence Labeled Ligands, for the Histamine H_2 Receptor. Ph.D. Thesis, University of Regensburg, 2020.
(25) Birnkammer, T.; Spickenreither, A.; Brunskole, I.; Lopuch, M.; Kagermeier, N.; Bernhardt, G.; Dove, S.; Seifert, R.; Elz, S.; Buschauer, A. The bivalent ligand approach leads to highly potent and selective acylguanidine-type histamine H_2 receptor agonists. *J. Med. Chem.* **2012**, *55*, 1147−1160.
(26) Tropmann, K.; Höring, C.; Plank, N.; Pockes, S. Discovery of a G protein biased radioligand for the histamine H_2 receptor with reversible binding properties. *J. Med. Chem.* **2020**, *63*, 13090−13102.
(27) DeVos, S. L.; Miller, T. M. Direct intraventricular delivery of drugs to the rodent central nervous system. *J. Visualized Exp.* **2013**, No. e50326.
(28) Mierau, J. Pramipexole: a dopamine-receptor agonist for treatment of Parkinson's disease. *Clin. Neuropharmacol.* **1995**, *18*, S195−S206.
(29) Bennett, J. P., Jr.; Piercey, M. F. Pramipexole-a new dopamine agonist for the treatment of Parkinson's disease. *J. Neurol. Sci.* **1999**, *163*, 25−31.
(30) Ganellin, C. R. In *Chemistry and Structure Activity Relationships of Drugs Acting at Histamine Receptors*; Ganellin, C. R.; Parson, M. E., Eds.; Wright PSG: Bristol, 1982; pp 10−102.
(31) Daina, A.; Michielin, O.; Zoete, V. SwissADME: a free web tool to evaluate pharmacokinetics, drug-likeness and medicinal chemistry friendliness of small molecules. *Sci. Rep.* **2017**, *7*, 42717−42717.
(32) Bastos, C. M.; Munoz, B.; Tait, B. Compounds, Compositions, and Methods for Increasing CFTR Activity. WO2015/138909, 2015; *Chem. Abstr.* 2015, 163, 438650.
(33) Geyer, R.; Kaske, M.; Baumeister, P.; Buschauer, A. Synthesis and functional characterization of imbutamine analogs as histamine H_3 and H_4 receptor ligands. *Arch. Pharm.* **2014**, *347*, 77−88.
(34) Geyer, R.; Igel, P.; Kaske, M.; Elz, S.; Buschauer, A. Synthesis, SAR and selectivity of 2-acyl- and 2-cyano-1-hetarylalkyl-guanidines at the four histamine receptor subtypes: a bioisosteric approach. *Med. Chem. Commun.* **2014**, *5*, 72−81.
(35) Kim, K. S.; Qian, L. Improved method for the preparation of guanidines. *Tetrahedron Lett.* **1993**, *34*, 7677−7680.
(36) Baumeister, P.; Erdmann, D.; Biselli, S.; Kagermeier, N.; Elz, S.; Bernhardt, G.; Buschauer, A. [^{3}H]UR-DE257: development of a tritium-labeled squaramide-type selective histamine H_2 receptor antagonist. *ChemMedChem* **2015**, *10*, 83−93.
(37) Igel, P.; Schnell, D.; Bernhardt, G.; Seifert, R.; Buschauer, A. Tritium-labeled N^1-[3-(1H-imidazol-4-yl)propyl]-N^2-propionylguanidine ([^{3}H]UR-PI294), a high-affinity histamine H_3 and H_4 receptor radioligand. *ChemMedChem* **2009**, *4*, 225−231.
(38) Pockes, S.; Wifling, D.; Keller, M.; Buschauer, A.; Elz, S. Highly potent, stable, and selective dimeric hetarylpropylguanidine-type histamine H_2 receptor agonists. *ACS Omega* **2018**, *3*, 2865−2882.
(39) Pertz, H. H.; Görnemann, T.; Schurad, B.; Seifert, R.; Straßer, A. Striking differences of action of lisuride stereoisomers at histamine H_1 receptors. *Naunyn-Schmiedeberg's Arch. Pharmacol.* **2006**, *374*, 215−222.
(40) Forster, L.; Grätz, L.; Mönnich, D.; Bernhardt, G.; Pockes, S. A split luciferase complementation assay for the quantification of β-arrestin2 recruitment to dopamine D_2-like receptors. *Int. J. Mol. Sci.* **2020**, *21*, No. 6103.
(41) Felixberger, J. Luciferase Complementation for the Determination of Arrestin Recruitment: Investigation of Histamine and NPY receptors. Ph.D. Thesis, University of Regensburg, 2014.
(42) Höring, C.; Seibel, U.; Tropmann, K.; Grätz, L.; Mönnich, D.; Pitzl, S.; Bernhardt, G.; Pockes, S.; Strasser, A. A dynamic, split-luciferase-based mini-G protein sensor to functionally characterize ligands at all four histamine receptor subtypes. *Int. J. Mol. Sci.* **2020**, *21*, No. 8440.
(43) Carpenter, B.; Tate, C. G. Engineering a minimal G protein to facilitate crystallisation of G protein-coupled receptors in their active conformation. *Protein Eng., Des. Sel.* **2016**, *29*, 583−594.
(44) Nehmé, R.; Carpenter, B.; Singhal, A.; Strege, A.; Edwards, P. C.; White, C. F.; Du, H.; Grisshammer, R.; Tate, C. G. Mini-G proteins: novel tools for studying GPCRs in their active conformation. *PLoS One* **2017**, *12*, No. e0175642.
(45) Wan, Q.; Okashah, N.; Inoue, A.; Nehmé, R.; Carpenter, B.; Tate, C. G.; Lambert, N. A. Mini G protein probes for active G protein−coupled receptors (GPCRs) in live cells. *J. Biol. Chem.* **2018**, *293*, 7466−7473.
(46) Grätz, L.; Tropmann, K.; Bresinsky, M.; Müller, C.; Bernhardt, G.; Pockes, S. NanoBRET binding assay for histamine H_2 receptor ligands using live recombinant HEK293T cells. *Sci. Rep.* **2020**, *10*, No. e13288.
(47) Xie, S.-X.; Ghorai, P.; Ye, Q.-Z.; Buschauer, A.; Seifert, R. Probing ligand-specific histamine H_1- and H_2-receptor conformations with N^G-acylated imidazolylpropylguanidines. *J. Pharmacol. Exp. Ther.* **2006**, *317*, 139−146.
(48) Kelley, M. T.; Bürckstürmmer, T.; Wenzel-Seifert, K.; Dove, S.; Buschauer, A.; Seifert, R. Distinct interaction of human and guinea pig histamine H_2-receptor with guanidine-type agonists. *Mol. Pharmacol.* **2001**, *60*, 1210−1225.
(49) Yung-Chi, C.; Prusoff, W. H. Relationship between the inhibition constant (K_i) and the concentration of inhibitor which causes 50 per cent inhibition (I_{50}) of an enzymatic reaction. *Biochem. Pharmacol.* **1973**, *22*, 3099−3108.
(50) Rasmussen, S. G. F.; DeVree, B. T.; Zou, Y.; Kruse, A. C.; Chung, K. Y.; Kobilka, T. S.; Thian, F. S.; Chae, P. S.; Pardon, E.; Calinski, D.; Mathiesen, J. M.; Shah, S. T. A.; Lyons, J. A.; Caffrey, M.; Gellman, S. H.; Steyaert, J.; Skiniotis, G.; Weis, W. I.; Sunahara, R. K.; Kobilka, B. K. Crystal structure of the β_2 adrenergic receptor−Gs protein complex. *Nature* **2011**, *477*, 549−555.
(51) Yin, J.; Chen, K.-Y. M.; Clark, M. J.; Hijazi, M.; Kumari, P.; Bai, X.-c.; Sunahara, R. K.; Barth, P.; Rosenbaum, D. M. Structure of a D_2 dopamine receptor−G-protein complex in a lipid membrane. *Nature* **2020**, *584*, 125−129.
(52) Simpson, M. M.; Ballesteros, J. A.; Chiappa, V.; Chen, J.; Suehiro, M.; Hartman, D. S.; Godel, T.; Snyder, L. A.; Sakmar, T. P.; Javitch, J. A. Dopamine D_4/D_2 receptor selectivity is determined by a divergent aromatic microdomain contained within the second, third, and seventh membrane-spanning segments. *Mol. Pharmacol.* **1999**, *56*, 1116−1126.
(53) Bruysters, M.; Jongejan, A.; Gillard, M.; van de Manakker, F.; Bakker, R. A.; Chatelain, P.; Leurs, R. Pharmacological differences between human and guinea pig histamine H_1 receptors: Asn^{84} (2.61) as key residue within an additional binding pocket in the H_1 receptor. *Mol. Pharmacol.* **2005**, *67*, 1045−1052.
(54) Straßer, A.; Striegl, B.; Wittmann, H. J.; Seifert, R. Pharmacological profile of histaprodifens at four recombinant histamine H_1 receptor species isoforms. *J. Pharmacol. Exp. Ther.* **2008**, *324*, 60−71.
(55) Michino, M.; Donthamsetti, P.; Beuming, T.; Banala, A.; Duan, L.; Roux, T.; Han, Y.; Trinquet, E.; Newman, A. H.; Javitch, J. A.; Shi, L. A single glycine in extracellular loop 1 is the critical determinant for pharmacological specificity of dopamine D_2 and D_3 receptors. *Mol. Pharmacol.* **2013**, *84*, 854−864.
(56) Vass, M.; Podlewska, S.; de Esch, I. J. P.; Bojarski, A. J.; Leurs, R.; Kooistra, A. J.; de Graaf, C. Aminergic GPCR-ligand interactions: a

https://doi.org/10.1021/acs.jmedchem.1c00692
J. Med. Chem. 2021, 64, 8684−8709

chemical and structural map of receptor mutation data. *J. Med. Chem.* **2019**, *62*, 3784−3839.
(57) Ferruz, N.; Doerr, S.; Vanase-Frawley, M. A.; Zou, Y.; Chen, X.; Marr, E. S.; Nelson, R. T.; Kormos, B. L.; Wager, T. T.; Hou, X.; Villalobos, A.; Sciabola, S.; De Fabritiis, G. Dopamine D_3 receptor antagonist reveals a cryptic pocket in aminergic GPCRs. *Sci. Rep.* **2018**, *8*, No. 897.
(58) Wang, S.; Che, T.; Levit, A.; Shoichet, B. K.; Wacker, D.; Roth, B. L. Structure of the D_2 dopamine receptor bound to the atypical antipsychotic drug risperidone. *Nature* **2018**, *555*, 269−273.
(59) Chemel, B. R.; Bonner, L. A.; Watts, V. J.; Nichols, D. E. Ligand-specific roles for transmembrane 5 serine residues in the binding and efficacy of dopamine D_1 receptor catechol agonists. *Mol. Pharmacol.* **2012**, *81*, 729−738.
(60) Fowler, J. C.; Bhattacharya, S.; Urban, J. D.; Vaidehi, N.; Mailman, R. B. Receptor conformations involved in dopamine D_{2L} receptor functional selectivity induced by selected transmembrane-5 serine mutations. *Mol. Pharmacol.* **2012**, *81*, 820−831.
(61) Woodward, R.; Coley, C.; Daniell, S.; Naylor, L. H.; Strange, P. G. Investigation of the role of conserved serine residues in the long form of the rat D_2 dopamine receptor using site-directed mutagenesis. *J. Neurochem.* **1996**, *66*, 394−402.
(62) Sartania, N.; Strange, P. G. Role of conserved serine residues in the interaction of agonists with D_3 dopamine receptors. *J. Neurochem.* **1999**, *72*, 2621−2624.
(63) Braden, M. R.; Nichols, D. E. Assessment of the roles of serines 5.43(239) and 5.46(242) for binding and potency of agonist ligands at the human serotonin 5-HT_{2A} receptor. *Mol. Pharmacol.* **2007**, *72*, 1200−1209.
(64) Pollock, N. J.; Manelli, A. M.; Hutchins, C. W.; Steffey, M. E.; MacKenzie, R. G.; Frail, D. E. Serine mutations in transmembrane V of the dopamine D_1 receptor affect ligand interactions and receptor activation. *J. Biol. Chem.* **1992**, *267*, 17780−17786.
(65) Almaula, N.; Ebersole, B. J.; Ballesteros, J. A.; Weinstein, H.; Sealfon, S. C. Contribution of a helix 5 locus to selectivity of hallucinogenic and nonhallucinogenic ligands for the human 5-hydroxytryptamine2A and 5-hydroxytryptamine2C receptors: direct and indirect effects on ligand affinity mediated by the same locus. *Mol. Pharmacol.* **1996**, *50*, 34−42.
(66) Leurs, R.; Smit, M. J.; Tensen, C. P.; Terlaak, A. M.; Timmerman, H. Site-directed mutagenesis of the histamine H_1-receptor reveals a selective interaction of asparagine[207] with subclasses of H_1-receptor agonists. *Biochem. Biophys. Res. Commun.* **1994**, *201*, 295−301.
(67) Ohta, K.; Hayashi, H.; Mizuguchi, H.; Kagamiyama, H.; Fujimoto, K.; Fukui, H. Site-directed mutagenesis of the histamine H_1 receptor: roles of aspartic acid[107], asparagine[198] and threonine[194]. *Biochem. Biophys. Res. Commun.* **1994**, *203*, 1096−1101.
(68) Jongejan, A.; Lim, H. D.; Smits, R. A.; de Esch, I. J. P.; Haaksma, E.; Leurs, R. Delineation of agonist binding to the human histamine H_4 Receptor using mutational analysis, homology modeling, and ab initio aalculations. *J. Chem. Inf. Model.* **2008**, *48*, 1455−1463.
(69) Shin, N.; Coates, E.; Murgolo, N. J.; Morse, K. L.; Bayne, M.; Strader, C. D.; Monsma, F. J., Jr. Molecular modeling and site-specific mutagenesis of the histamine-binding site of the histamine H_4 receptor. *Mol. Pharmacol.* **2002**, *62*, 38−47.
(70) Hwa, J.; Perez, D. M. The unique nature of the serine interactions for α_1-adrenergic receptor agonist binding and activation. *J. Biol. Chem.* **1996**, *271*, 6322−6327.
(71) Cho, W.; Taylor, L. P.; Mansour, A.; Akil, H. Hydrophobic residues of the D_2 dopamine receptor are important for binding and signal transduction. *J. Neurochem.* **1995**, *65*, 2105−2115.
(72) Seifert, R.; Wenzel-Seifert, K.; Burckstummer, T.; Pertz, H. H.; Schunack, W.; Dove, S.; Buschauer, A.; Elz, S. Multiple differences in agonist and antagonist pharmacology between human and guinea pig histamine H_1-receptor. *J. Pharmacol. Exp. Ther.* **2003**, *305*, 1104−1115.
(73) Wieland, K.; Laak, A. M.; Smit, M. J.; Kühne, R.; Timmerman, H.; Leurs, R. Mutational analysis of the antagonist-binding site of the histamine H_1 receptor. *J. Biol. Chem.* **1999**, *274*, 29994−30000.
(74) Lan, H.; DuRand, C. J.; Teeter, M. M.; Neve, K. A. Structural determinants of pharmacological specificity between D_1 and D_2 dopamine receptors. *Mol. Pharmacol.* **2006**, *69*, 185−194.
(75) Lundstrom, K.; Turpin, M. P.; Large, C.; Robertson, G.; Thomas, P.; Lewell, X. Q. Mapping of dopamine D_3 receptor binding site by pharmacological characterization of mutants expressed in CHO cells with the Semliki Forest virus system. *J. Recept. Signal Transduction* **1998**, *18*, 133−150.
(76) Woodward, R.; Daniell, S. J.; Strange, P. G.; Naylor, L. H. Structural studies on D_2 dopamine receptors: mutation of a histidine residue specifically affects the binding of a subgroup of substituted benzamide drugs. *J. Neurochem.* **1994**, *62*, 1664−1669.
(77) Matsui, H.; Lazareno, S.; Birdsall, N. J. Probing of the location of the allosteric site on m1 muscarinic receptors by site-directed mutagenesis. *Mol. Pharmacol.* **1995**, *47*, 88−98.
(78) Weinhart, C. G.; Wifling, D.; Schmidt, M. F.; Neu, E.; Höring, C.; Clark, T.; Gmeiner, P.; Keller, M. Dibenzodiazepinone-type muscarinic receptor antagonists conjugated to basic peptides: impact of the linker moiety and unnatural amino acids on M_2R selectivity. *Eur. J. Med. Chem.* **2021**, *213*, No. 113159.
(79) Hübner, H.; Haubmann, C.; Utz, W.; Gmeiner, P. Conjugated Enynes as Nonaromatic Catechol Bioisosteres: Synthesis, Binding Experiments, and Computational Studies of Novel Dopamine Receptor Agonists Recognizing Preferentially the D_3 Subtype. *J. Med. Chem.* **2000**, *43*, 756−762.
(80) Hellmann, J.; Drabek, M.; Yin, J.; Gunera, J.; Pröll, T.; Kraus, F.; Langmead, C. J.; Hübner, H.; Weikert, D.; Kolb, P.; Rosenbaum, D. M.; Gmeiner, P. Structure-based development of a subtype-selective orexin 1 receptor antagonist. *Proc. Natl. Acad. Sci. U.S.A.* **2020**, *117*, 18059−18067.
(81) Fulmer, G. R.; Miller, A. J. M.; Sherden, N. H.; Gottlieb, H. E.; Nudelman, A.; Stoltz, B. M.; Bercaw, J. E.; Goldberg, K. I. NMR chemical shifts of trace impurities: common laboratory solvents, organics, and gases in deuterated solvents relevant to the organometallic chemist. *Organometallics* **2010**, *29*, 2176−2179.
(82) Gottlieb, H. E.; Kotlyar, V.; Nudelman, A. NMR chemical shifts of common laboratory solvents as trace impurities. *J. Org. Chem.* **1997**, *62*, 7512−7515.
(83) Aldrich, C.; Bertozzi, C.; Georg, G. I.; L, K.; Lindsley, C.; Liotta, D.; Merz, K. M.; Schepartz, A.; Wang, S. The ecstasy and agony of assay interference compounds. *ACS Cent. Sci.* **2017**, *3*, 143−147.
(84) Bleicher, K.; Mutel, V.; Vieira, E.; Wichmann, J.; Woltering, T. J. Preparation of Carbamic Acid Derivatives and Evaluation of Their Use as Metabotropic Glutamate Receptor Ligands. WO2000/063166, 2000; *Chem. Abstr.* 2000, 133, 321633, 2000.
(85) Houston, C.; Wenzel-Seifert, K.; Bürckstümmer, T.; Seifert, R. The human histamine H_2-receptor couples more efficiently to Sf9 insect cell G_s-proteins than to insect cell G_q-proteins: limitations of Sf9 cells for the analysis of receptor/G_q-protein coupling. *J. Neurochem.* **2002**, *80*, 678−696.
(86) Schnell, D.; Strasser, A.; Seifert, R. Comparison of the pharmacological properties of human and rat histamine H_3-receptors. *Biochem. Pharmacol.* **2010**, *80*, 1437−1449.
(87) Schneider, E. H.; Schnell, D.; Papa, D.; Seifert, R. High constitutive activity and a G-protein-independent high-affinity state of the human histamine H_4-receptor. *Biochemistry* **2009**, *48*, 1424−1438.
(88) Pop, N.; Igel, P.; Brennauer, A.; Cabrele, C.; Bernhardt, G.; Seifert, R.; Buschauer, A. Functional reconstitution of human neuropeptide Y (NPY) Y_2 and Y_4 receptors in Sf9 insect cells. *J. Recept. Signal Transduction* **2011**, *31*, 271−285.
(89) Lowry, O. H.; Rosebrough, N. J.; Farr, A. L.; Randall, R. J. Protein measurement with the Folin phenol reagent. *J. Biol. Chem.* **1951**, *193*, 265−275.
(90) Wifling, D.; Löffel, K.; Nordemann, U.; Strasser, A.; Bernhardt, G.; Dove, S.; Seifert, R.; Buschauer, A. Molecular determinants for the high constitutive activity of the human histamine H_4 receptor: functional studies on orthologues and mutants. *Br. J. Pharmacol.* **2015**, *172*, 785−798.

https://doi.org/10.1021/acs.jmedchem.1c00692
J. Med. Chem. 2021, 64, 8684−8709